

How Does Ferrocene Correlate with Ferroptosis? Multiple Approaches to Explore Ferrocene-Appended GPX4 Inhibitors as Anticancer Agents

Wei Li,^{[a]#} Jing Yu,^{[a]#} Jing Wang,^{[a]#} Xuejing Fan,^{[a]#} Ximing Xu,^[b] Hui Wang,^[a] Ying Xiong,^[c] Xinyu Li,^[a] Xiaomin Zhang,^[a] Qianer Zhang,^[a] Xin Qi,^[a] Pascal Pigeon,^[d,e] Qing Gu,^[f] Julia Bruno-Colmenarez,^[g] Gérard Jaouen,^[d,e] Michael J. McGlinchey,^[g] Xue Qiu,^[a] Shu-Li You,^[f] Jing Li,^{[a]*} and Yong Wang^{[a]*}

[a] School of Medicine and Pharmacy, Key Laboratory of Marine Drugs, Chinese Ministry of Education, Ocean University of China, Qingdao 26003, Shandong, P. R. China; Laboratory for Marine Drugs and Bioproducts, Pilot National Laboratory for Marine Science and Technology, Qingdao 266200, P. R. China

E-mail: lijing_ouc@ouc.edu.cn, wangyong8866@ouc.edu.cn

[b] Marine Biomedical Research Institute of Qingdao, School of Medicine and Pharmacy, Key Laboratory of Marine Drugs, Chinese Ministry of Education, Ocean University of China, Qingdao 266003, Shandong, P. R. China

[c] School of Pharmacy, Fudan University, Shanghai, 201203, China

[d] PSL, Chimie ParisTech, 11 rue Pierre et Marie Curie, F-75005 Paris, France

[e] Sorbonne Université, UMR 8232 CNRS, IPCM, 4 place Jussieu, F-75005 Paris, France

[f] State Key Laboratory of Organometallic Chemistry, Shanghai Institute of Organic Chemistry, Chinese Academy of Sciences, 345 Lingling Lu, Shanghai 200032, P. R. China

[g] UCD School of Chemistry, University College Dublin, Belfield, Dublin 4, Ireland

These authors contributed equally.

Supplementary Figures, Schemes and Tables, P2-P27

Experimental section, P28-P49

References, P49

NMR Spectrums, P50-P67

HRMS and purity data, P68-P93

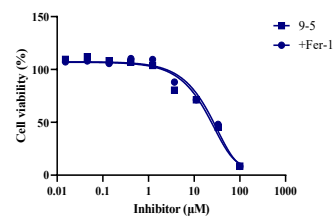
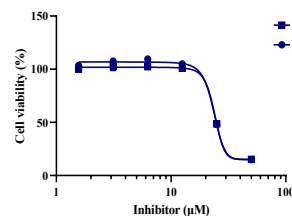
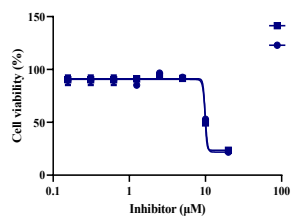
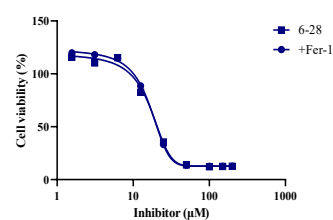
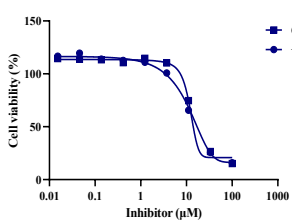
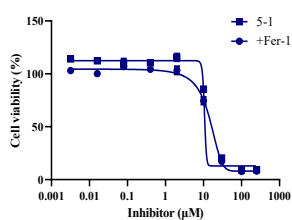
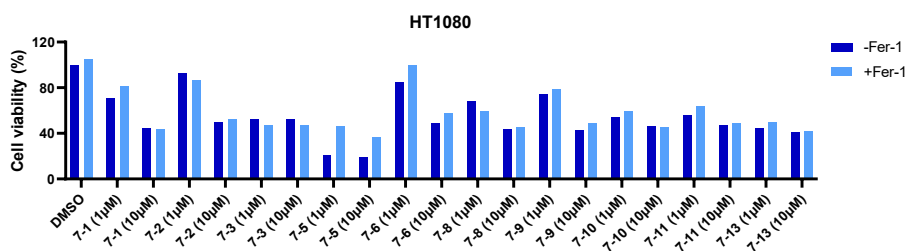
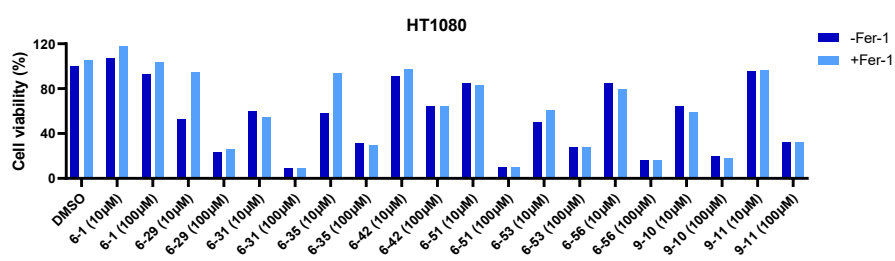
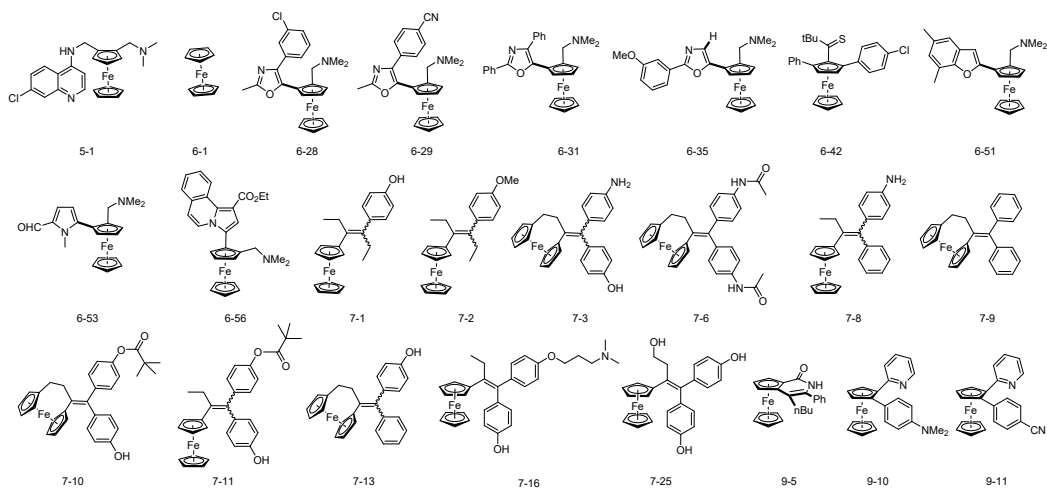
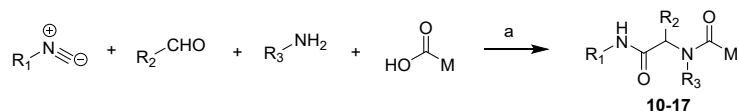
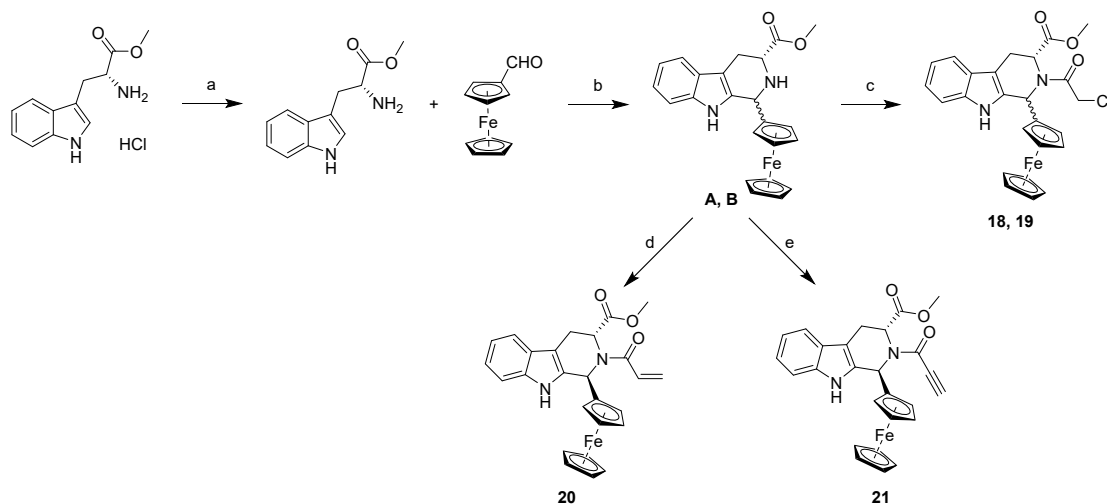


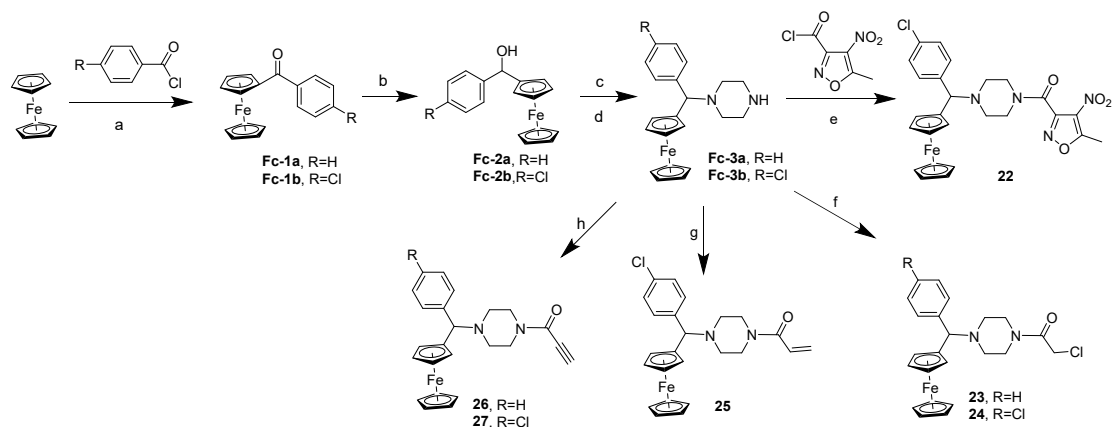
Figure S1. The represent molecules of ferrocene-based compounds libraries, and their antiproliferative activities on HT1080 cells at two concentrations (1 and 10 μM, or 10 and 100 μM) with or without fer-1 (1.5 μM), and the IC₅₀ curves of selected molecules with or without fer-1 (1.5 μM).



Scheme S2. Reagents and conditions to prepare the ferrocenyl compounds of **10-17**:
(a) MeOH, rt.



Scheme S3. Reagents and conditions to prepare the ferrocenyl compounds of **18-21**:
(a) NEt₃, DCM; (b) TFA, DCM; (c) NaHCO₃, DCM, chloroacetyl chloride; (d) NaHCO₃, DCM, acryloyl chloride; (e) HBTU, DIPEA, propionic acid, DMF.



Scheme S4. Reagents and conditions to prepare the ferrocenyl compounds of: (a) AlCl₃, DCM; (b) NaBH₄, THF-MeOH; (c) Ac₂O, pyridine; (d) Piperazine, CH₃CN; (e) Et₃N, DCM; (f) Chloroacetyl chloride, Et₃N, DCM; (g) Acryloyl chloride, Et₃N, DCM; (h) propionic acid, HBTU, DIPEA, DCM.

Table S5. Crystallographic data for compound **12**, **15** and **17**.

	15	12	17
Empirical formula	C ₂₉ H ₂₈ Cl ₂ FeN ₂ O ₃	C ₂₇ H ₂₇ ClFeN ₂ O ₂ S	C ₃₀ H ₂₇ ClFeN ₂ O ₃
Formula weight	579.28	534.86	554.83
Temperature [K]	298(2)	293(2)	293(2)
Crystal system	triclinic	monoclinic	monoclinic
Space group (number)	<i>P</i> $\bar{1}$ (2)	<i>P</i> 2 ₁ / <i>c</i> (14)	<i>C</i> 2/ <i>c</i> (15)
<i>a</i> [Å]	10.5013(3)	15.0583(4)	19.7467(5)
<i>b</i> [Å]	12.2497(4)	17.6346(5)	13.7604(3)
<i>c</i> [Å]	12.4905(4)	9.3797(3)	19.3018(5)
α [°]	60.915(2)	90	90
β [°]	76.060(2)	90.429(2)	94.242(2)
γ [°]	73.339(2)	90	90
Volume [Å ³]	1335.26(8)	2490.68(13)	5230.4(2)
<i>Z</i>	2	4	8
ρ_{calc} [gcm ⁻³]	1.441	1.426	1.409
μ [mm ⁻¹]	6.645	6.843	5.845
<i>F</i> (000)	600	1112	2304
Radiation	CuK α (λ =1.54186 Å)	CuK α (λ =1.54186 Å)	CuK α (λ =1.54186 Å)
2 θ range [°]	8.16 to 137.25 (0.83 Å)	5.87 to 137.16 (0.83 Å)	7.84 to 137.39 (0.83 Å)
Index ranges	-5 ≤ <i>h</i> ≤ 12 -14 ≤ <i>k</i> ≤ 14 -14 ≤ <i>l</i> ≤ 14	-7 ≤ <i>h</i> ≤ 18 -21 ≤ <i>k</i> ≤ 17 -10 ≤ <i>l</i> ≤ 11	-23 ≤ <i>h</i> ≤ 23 -15 ≤ <i>k</i> ≤ 4 -22 ≤ <i>l</i> ≤ 22
Reflections collected	9674	11883	16531
Independent reflections	4772 <i>R</i> _{int} = 0.0322 <i>R</i> _{sigma} = 0.0306	4468 <i>R</i> _{int} = 0.0288 <i>R</i> _{sigma} = 0.0390	4711 <i>R</i> _{int} = 0.0237 <i>R</i> _{sigma} = 0.0195
Completeness	97.9 %	98.4 %	98.2 %
Data / Restraints / Parameters	4772/73/434	4468/141/466	4711/1/443
Goodness-of-fit on <i>F</i> ²	1.047	0.944	1.082
Final <i>R</i> indexes [<i>I</i> ≥ 2 σ (<i>I</i>)]	<i>R</i> ₁ = 0.0631 <i>wR</i> ₂ = 0.1729	<i>R</i> ₁ = 0.0391 <i>wR</i> ₂ = 0.0969	<i>R</i> ₁ = 0.0402 <i>wR</i> ₂ = 0.0950
Final <i>R</i> indexes [all data]	<i>R</i> ₁ = 0.0671 <i>wR</i> ₂ = 0.1771	<i>R</i> ₁ = 0.0572 <i>wR</i> ₂ = 0.1038	<i>R</i> ₁ = 0.0513 <i>wR</i> ₂ = 0.1090
Largest peak/hole [eÅ ⁻³]	0.74/-0.50	0.36/-0.33	0.37/-0.44

Table S6. Bond lengths and angles of molecule **15**.

Atom–Atom	Length [Å]	Atom–Atom	Length [Å]
Fe1–C27	2.011(5)	C9A–H9C	0.9600
Fe1–C26	2.021(5)	C9B–H9D	0.9600
Fe1–C23	2.028(5)	C9B–H9E	0.9600
Fe1–C19	2.028(4)	C9B–H9F	0.9600
Fe1–C20	2.029(4)	C10–C11	1.523(6)
Fe1–C18	2.034(3)	C10–H10A	0.9700
Fe1–C21	2.035(4)	C10–H10B	0.9700
Fe1–C22	2.035(4)	C11–C12	1.501(6)
Fe1–C25	2.037(5)	C11–H11A	0.9700
Fe1–C24	2.043(4)	C11–H11B	0.9700
Cl1A–C5A	1.703(3)	C12–C17	1.373(7)
O2A–C6A	1.344(5)	C12–C13	1.398(7)
O2A–C9A	1.422(6)	C13–C14	1.363(8)
C3A–C4A	1.381(7)	C13–H13	0.9300
C3A–C8A	1.387(7)	C14–C15	1.371(9)
C3A–N2	1.439(5)	C14–H14	0.9300
C4A–C5A	1.381(6)	C15–C16	1.375(9)
C4A–H4A	0.9300	C15–H15	0.9300
C5A–C6A	1.419(6)	C16–C17	1.386(8)
C6A–C7A	1.379(7)	C16–H16	0.9300
C7A–C8A	1.387(7)	C17–H17	0.9300
C7A–H7A	0.9300	C18–C22	1.438(5)
C8A–H8A	0.9300	C18–C19	1.439(5)
N2–C28	1.348(5)	C19–C20	1.410(6)
N2–C3B	1.459(9)	C19–H19	0.9300
N2–C2	1.493(4)	C20–C21	1.423(6)
Cl1B–C5B	1.696(5)	C20–H20	0.9300
O2B–C6B	1.324(9)	C21–C22	1.399(6)
O2B–C9B	1.398(10)	C21–H21	0.9300
C3B–C4B	1.384(12)	C22–H22	0.9300
C3B–C8B	1.395(12)	C23–C27	1.414(8)
C4B–C5B	1.391(11)	C23–C24	1.427(8)
C4B–H4B	0.9300	C23–H23	0.9300
C5B–C6B	1.428(11)	C24–C25	1.412(9)
C6B–C7B	1.382(12)	C24–H24	0.9300
C7B–C8B	1.379(12)	C25–C26	1.386(9)
C7B–H7B	0.9300	C25–H25	0.9300
C8B–H8B	0.9300	C26–C27	1.385(9)
Cl2A–C29	1.744(4)	C26–H26	0.9300

C12B–C29	1.723(5)	C27–H27	0.9300
O1–C1	1.211(4)	C28–C29	1.520(6)
O3–C28	1.220(5)	C29–H29A	0.9700
N1–C1	1.340(5)	C29–H29B	0.9700
N1–C10	1.450(5)	C29–H29C	0.9700
N1–H1	0.84(5)	C29–H29D	0.9700
C1–C2	1.536(5)	C9A–H9A	0.9600
C2–C18	1.491(5)	C9A–H9B	0.9600
C2–H2	0.91(4)		
Atom–Atom–Atom	Angle [°]	Atom–Atom–Atom	Angle [°]
C27–Fe1–C26	40.2(3)	C4A–C5A–C6A	120.8(4)
C27–Fe1–C23	41.0(2)	C4A–C5A–Cl1A	120.3(4)
C26–Fe1–C23	68.8(3)	C6A–C5A–Cl1A	118.8(3)
C27–Fe1–C19	159.6(2)	O2A–C6A–C7A	127.2(5)
C26–Fe1–C19	159.6(2)	O2A–C6A–C5A	114.7(5)
C23–Fe1–C19	123.98(19)	C7A–C6A–C5A	118.1(4)
C27–Fe1–C20	157.9(2)	C6A–C7A–C8A	121.1(5)
C26–Fe1–C20	122.0(3)	C6A–C7A–H7A	119.5
C23–Fe1–C20	159.3(2)	C8A–C7A–H7A	119.5
C19–Fe1–C20	40.67(17)	C7A–C8A–C3A	120.1(5)
C27–Fe1–C18	122.1(2)	C7A–C8A–H8A	120.0
C26–Fe1–C18	156.2(2)	C3A–C8A–H8A	120.0
C23–Fe1–C18	108.27(18)	C28–N2–C3A	120.9(3)
C19–Fe1–C18	41.50(14)	C28–N2–C3B	123.0(4)
C20–Fe1–C18	69.28(16)	C28–N2–C2	118.9(3)
C27–Fe1–C21	121.5(2)	C3A–N2–C2	119.9(3)
C26–Fe1–C21	105.0(2)	C3B–N2–C2	116.7(4)
C23–Fe1–C21	158.8(2)	C6B–O2B–C9B	120.2(10)
C19–Fe1–C21	68.60(17)	C4B–C3B–C8B	115.9(10)
C20–Fe1–C21	41.00(18)	C4B–C3B–N2	128.1(14)
C18–Fe1–C21	68.77(16)	C8B–C3B–N2	116.0(13)
C27–Fe1–C22	106.20(18)	C3B–C4B–C5B	123.7(13)
C26–Fe1–C22	119.2(2)	C3B–C4B–H4B	118.1
C23–Fe1–C22	123.76(19)	C5B–C4B–H4B	118.1
C19–Fe1–C22	69.25(15)	C4B–C5B–C6B	120.6(11)
C20–Fe1–C22	68.82(17)	C4B–C5B–Cl1B	123.0(11)
C18–Fe1–C22	41.38(14)	C6B–C5B–Cl1B	116.5(11)
C21–Fe1–C22	40.21(17)	O2B–C6B–C7B	127.6(16)
C27–Fe1–C25	67.2(3)	O2B–C6B–C5B	118.4(14)
C26–Fe1–C25	39.9(3)	C7B–C6B–C5B	114.0(9)
C23–Fe1–C25	68.4(3)	C8B–C7B–C6B	125.4(14)

C19–Fe1–C25	125.3(2)	C8B–C7B–H7B	117.3
C20–Fe1–C25	107.6(2)	C6B–C7B–H7B	117.3
C18–Fe1–C25	162.9(2)	C7B–C8B–C3B	120.4(13)
C21–Fe1–C25	120.6(2)	C7B–C8B–H8B	119.8
C22–Fe1–C25	154.6(2)	C3B–C8B–H8B	119.8
C27–Fe1–C24	68.2(2)	C1–N1–C10	123.5(3)
C26–Fe1–C24	68.2(2)	C1–N1–H1	119(3)
C23–Fe1–C24	41.1(2)	C10–N1–H1	117(3)
C19–Fe1–C24	109.71(18)	O1–C1–N1	123.8(3)
C20–Fe1–C24	122.8(2)	O1–C1–C2	123.0(3)
C18–Fe1–C24	126.0(2)	N1–C1–C2	113.2(3)
C21–Fe1–C24	157.2(2)	C18–C2–N2	111.8(3)
C22–Fe1–C24	162.2(2)	C18–C2–C1	114.5(3)
C25–Fe1–C24	40.5(3)	N2–C2–C1	108.7(3)
C6A–O2A–C9A	116.4(5)	C18–C2–H2	104(2)
C4A–C3A–C8A	120.2(4)	N2–C2–H2	105(2)
C4A–C3A–N2	121.7(5)	C1–C2–H2	112(2)
C8A–C3A–N2	118.1(5)	O2A–C9A–H9A	109.5
C3A–C4A–C5A	119.7(5)	O2A–C9A–H9B	109.5
C3A–C4A–H4A	120.1	H9A–C9A–H9B	109.5
C5A–C4A–H4A	120.1	O2A–C9A–H9C	109.5
H9B–C9A–H9C	109.5	H9A–C9A–H9C	109.5
O2B–C9B–H9D	109.5	Fe1–C20–H20	126.2
O2B–C9B–H9E	109.5	C22–C21–C20	108.9(3)
H9D–C9B–H9E	109.5	C22–C21–Fe1	69.9(2)
O2B–C9B–H9F	109.5	C20–C21–Fe1	69.3(2)
H9D–C9B–H9F	109.5	C22–C21–H21	125.5
H9E–C9B–H9F	109.5	C20–C21–H21	125.5
N1–C10–C11	111.4(3)	Fe1–C21–H21	126.8
N1–C10–H10A	109.3	C21–C22–C18	108.2(3)
C11–C10–H10A	109.3	C21–C22–Fe1	69.9(2)
N1–C10–H10B	109.3	C18–C22–Fe1	69.26(19)
C11–C10–H10B	109.3	C21–C22–H22	125.9
H10A–C10–H10B	108.0	C18–C22–H22	125.9
C12–C11–C10	112.5(3)	Fe1–C22–H22	126.5
C12–C11–H11A	109.1	C27–C23–C24	106.3(5)
C10–C11–H11A	109.1	C27–C23–Fe1	68.9(3)
C12–C11–H11B	109.1	C24–C23–Fe1	70.1(3)
C10–C11–H11B	109.1	C27–C23–H23	126.8
H11A–C11–H11B	107.8	C24–C23–H23	126.8
C17–C12–C13	118.0(5)	Fe1–C23–H23	125.8

C17-C12-C11	120.9(4)	C25-C24-C23	107.1(5)
C13-C12-C11	121.1(4)	C25-C24-Fe1	69.5(3)
C14-C13-C12	121.2(5)	C23-C24-Fe1	68.9(2)
C14-C13-H13	119.4	C25-C24-H24	126.4
C12-C13-H13	119.4	C23-C24-H24	126.4
C13-C14-C15	120.5(5)	Fe1-C24-H24	126.7
C13-C14-H14	119.7	C26-C25-C24	109.1(6)
C15-C14-H14	119.7	C26-C25-Fe1	69.4(3)
C14-C15-C16	119.3(6)	C24-C25-Fe1	70.0(3)
C14-C15-H15	120.3	C26-C25-H25	125.4
C16-C15-H15	120.3	C24-C25-H25	125.4
C15-C16-C17	120.4(6)	Fe1-C25-H25	126.7
C15-C16-H16	119.8	C27-C26-C25	107.9(6)
C17-C16-H16	119.8	C27-C26-Fe1	69.5(3)
C12-C17-C16	120.7(5)	C25-C26-Fe1	70.6(3)
C12-C17-H17	119.7	C27-C26-H26	126.1
C16-C17-H17	119.7	C25-C26-H26	126.1
C22-C18-C19	106.7(3)	Fe1-C26-H26	125.4
C22-C18-C2	129.4(3)	C26-C27-C23	109.6(5)
C19-C18-C2	123.8(3)	C26-C27-Fe1	70.3(3)
C22-C18-Fe1	69.4(2)	C23-C27-Fe1	70.1(3)
C19-C18-Fe1	69.0(2)	C26-C27-H27	125.2
C2-C18-Fe1	128.2(2)	C23-C27-H27	125.2
C20-C19-C18	108.3(3)	Fe1-C27-H27	125.9
C20-C19-Fe1	69.7(2)	O3-C28-N2	123.6(4)
C18-C19-Fe1	69.5(2)	O3-C28-C29	123.8(4)
C20-C19-H19	125.8	N2-C28-C29	112.6(3)
C18-C19-H19	125.8	C28-C29-Cl2B	114.2(5)
Fe1-C19-H19	126.6	C28-C29-Cl2A	108.6(4)
C19-C20-C21	107.8(4)	C28-C29-H29A	110.0
C19-C20-Fe1	69.6(2)	Cl2A-C29-H29A	110.0
C21-C20-Fe1	69.7(3)	C28-C29-H29B	110.0
C19-C20-H20	126.1	Cl2A-C29-H29B	110.0
C21-C20-H20	126.1	H29A-C29-H29B	108.4
Cl2B-C29-H29D	108.7	C28-C29-H29C	108.7
H29C-C29-H29D	107.6	C28-C29-H29D	108.7
Cl2B-C29-H29C	108.7		

Table S7. Bond lengths and angles of molecule **12**.

Atom–Atom	Length [Å]	Atom–Atom	Length [Å]
Fe1–C26B	1.98(3)	C6B–H6D	0.9700
Fe1–C23A	1.985(16)	C7B–C8B	1.363(7)
Fe1–C27A	2.025(10)	C7B–C12B	1.363(7)
Fe1–C18	2.026(2)	C8B–C9B	1.371(7)
Fe1–C22	2.029(3)	C8B–H8B	0.9300
Fe1–C19	2.029(3)	C9B–C10B	1.359(7)
Fe1–C24A	2.033(10)	C9B–H9B	0.9300
Fe1–C20	2.034(3)	C10B–C11B	1.361(7)
Fe1–C25A	2.044(15)	C10B–H10B	0.9300
Fe1–C21	2.045(4)	C11B–C12B	1.370(7)
Fe1–C27B	2.057(18)	C11B–H11B	0.9300
Fe1–C26A	2.070(8)	C12B–H12B	0.9300
C11–C4	1.761(3)	C13–C14	1.407(4)
S1–C16	1.685(4)	C14–C15	1.404(4)
S1–C13	1.721(3)	C14–H14	0.9300
O1–C1	1.212(3)	C15–C16	1.344(6)
O2–C3	1.228(3)	C15–H15	0.9300
N2–C3	1.345(3)	C16–H16	0.9300
N2–C17	1.478(3)	C17–C18	1.499(3)
N2–C2	1.486(3)	C17–H17A	1.00(3)
C2–C13	1.495(3)	C17–H17B	0.94(3)
C2–C1	1.548(3)	C18–C22	1.411(4)
C2–H2	0.98(2)	C18–C19	1.419(4)
C3–C4	1.521(4)	C19–C20	1.412(4)
C4–H4A	0.92(3)	C19–H19	0.91(3)
C4–H4B	0.97(3)	C20–C21	1.402(5)
C1–N1	1.325(3)	C20–H20	0.96(4)
N1–C5A	1.451(5)	C21–C22	1.417(5)
N1–C5B	1.477(7)	C21–H21	0.99(4)
N1–H1	0.844(10)	C22–H22	0.85(4)
C5A–C6A	1.525(4)	C23A–C24A	1.389(8)
C5A–H5A	0.9700	C23A–C27A	1.400(8)
C5A–H5B	0.9700	C23A–H23A	0.9300
C6A–C7A	1.505(6)	C24A–C25A	1.410(9)
C6A–H6A	0.9700	C24A–H24A	0.9300
C6A–H6B	0.9700	C25A–C26A	1.410(10)
C7A–C8A	1.361(6)	C25A–H25A	0.9300
C7A–C12A	1.363(6)	C26A–C27A	1.410(9)
C8A–C9A	1.376(6)	C26A–H26A	0.9300

C8A–H8A	0.9300	C27A–H27A	0.9300
C9A–C10A	1.356(6)	C23B–C24B	1.397(9)
C9A–H9A	0.9300	C23B–C27B	1.400(9)
C10A–C11A	1.358(7)	C23B–H23B	0.9300
C10A–H10A	0.9300	C24B–C25B	1.411(10)
C11A–C12A	1.371(6)	C24B–H24B	0.9300
C11A–H11A	0.9300	C25B–C26B	1.405(11)
C12A–H12A	0.9300	C25B–H25B	0.9300
C5B–C6B	1.530(5)	C26B–C27B	1.409(10)
C5B–H5C	0.9700	C26B–H26B	0.9300
C5B–H5D	0.9700	C27B–H27B	0.9300
C6B–C7B	1.506(8)	C6B–H6C	0.9700
Atom–Atom–Atom	Angle [°]		
C23A–Fe1–C27A	40.9(3)	C22–C18–C19	107.2(3)
C26B–Fe1–C18	175.0(7)	C22–C18–C17	128.0(3)
C23A–Fe1–C18	106.4(3)	C19–C18–C17	124.8(3)
C27A–Fe1–C18	120.7(3)	C22–C18–Fe1	69.75(17)
C26B–Fe1–C22	142.0(8)	C19–C18–Fe1	69.65(15)
C23A–Fe1–C22	118.9(3)	C17–C18–Fe1	123.69(18)
C27A–Fe1–C22	103.2(3)	C20–C19–C18	108.3(3)
C18–Fe1–C22	40.72(12)	C20–C19–Fe1	69.85(18)
C26B–Fe1–C19	141.0(9)	C18–C19–Fe1	69.38(15)
C23A–Fe1–C19	125.8(4)	C20–C19–H19	127.6(19)
C27A–Fe1–C19	159.7(3)	C18–C19–H19	124(2)
C18–Fe1–C19	40.97(11)	Fe1–C19–H19	124.9(18)
C22–Fe1–C19	68.27(14)	C21–C20–C19	108.2(3)
C23A–Fe1–C24A	40.4(3)	C21–C20–Fe1	70.3(2)
C27A–Fe1–C24A	67.7(3)	C19–C20–Fe1	69.48(17)
C18–Fe1–C24A	124.3(5)	C21–C20–H20	129(2)
C22–Fe1–C24A	156.9(4)	C19–C20–H20	122(2)
C19–Fe1–C24A	112.7(4)	Fe1–C20–H20	122(2)
C26B–Fe1–C20	115.6(8)	C20–C21–C22	107.8(3)
C23A–Fe1–C20	163.8(4)	C20–C21–Fe1	69.5(2)
C27A–Fe1–C20	155.0(3)	C22–C21–Fe1	69.0(2)
C18–Fe1–C20	68.82(11)	C20–C21–H21	127(2)
C22–Fe1–C20	68.20(15)	C22–C21–H21	125(2)
C19–Fe1–C20	40.67(12)	Fe1–C21–H21	123(2)
C24A–Fe1–C20	128.7(3)	C18–C22–C21	108.6(3)
C23A–Fe1–C25A	68.4(4)	C18–C22–Fe1	69.53(17)
C27A–Fe1–C25A	67.6(4)	C21–C22–Fe1	70.3(2)
C18–Fe1–C25A	161.6(6)	C18–C22–H22	128(3)

C22-Fe1-C25A	157.5(6)	C21-C22-H22	123(3)
C19-Fe1-C25A	126.9(5)	Fe1-C22-H22	119(3)
C24A-Fe1-C25A	40.5(3)	C24A-C23A-C27A	108.3(6)
C20-Fe1-C25A	111.0(4)	C24A-C23A-Fe1	71.7(6)
C26B-Fe1-C21	116.1(8)	C27A-C23A-Fe1	71.1(7)
C23A-Fe1-C21	154.0(4)	C24A-C23A-H23A	125.9
C27A-Fe1-C21	118.2(3)	C27A-C23A-H23A	125.9
C18-Fe1-C21	68.64(12)	Fe1-C23A-H23A	123.0
C22-Fe1-C21	40.70(14)	C23A-C24A-C25A	108.0(7)
C19-Fe1-C21	68.06(15)	C23A-C24A-Fe1	67.9(8)
C24A-Fe1-C21	162.4(4)	C25A-C24A-Fe1	70.2(7)
C20-Fe1-C21	40.22(16)	C23A-C24A-H24A	126.0
C25A-Fe1-C21	123.9(5)	C25A-C24A-H24A	126.0
C26B-Fe1-C27B	40.8(5)	Fe1-C24A-H24A	127.4
C18-Fe1-C27B	135.9(7)	C26A-C25A-C24A	108.2(8)
C22-Fe1-C27B	117.7(8)	C26A-C25A-Fe1	70.9(7)
C19-Fe1-C27B	167.5(6)	C24A-C25A-Fe1	69.4(6)
C20-Fe1-C27B	150.6(6)	C26A-C25A-H25A	125.9
C21-Fe1-C27B	124.0(6)	C24A-C25A-H25A	125.9
C23A-Fe1-C26A	68.4(4)	Fe1-C25A-H25A	125.4
C27A-Fe1-C26A	40.3(2)	C27A-C26A-C25A	106.9(8)
C18-Fe1-C26A	156.2(5)	C27A-C26A-Fe1	68.2(5)
C22-Fe1-C26A	119.8(5)	C25A-C26A-Fe1	69.0(8)
C19-Fe1-C26A	160.0(4)	C27A-C26A-H26A	126.6
C24A-Fe1-C26A	67.7(4)	C25A-C26A-H26A	126.6
C20-Fe1-C26A	122.3(3)	Fe1-C26A-H26A	127.8
C25A-Fe1-C26A	40.1(3)	C23A-C27A-C26A	108.5(7)
C21-Fe1-C26A	105.3(4)	C23A-C27A-Fe1	68.0(7)
C16-S1-C13	92.19(18)	C26A-C27A-Fe1	71.6(5)
C3-N2-C17	123.0(2)	C23A-C27A-H27A	125.7
C3-N2-C2	114.47(19)	C26A-C27A-H27A	125.7
C17-N2-C2	122.0(2)	Fe1-C27A-H27A	126.2
N2-C2-C13	114.8(2)	C24B-C23B-C27B	108.5(8)
N2-C2-C1	109.2(2)	C24B-C23B-Fe1	69.9(12)
C13-C2-C1	109.6(2)	C27B-C23B-Fe1	68.5(11)
N2-C2-H2	105.4(14)	C24B-C23B-H23B	125.8
C13-C2-H2	107.0(14)	C27B-C23B-H23B	125.8
C1-C2-H2	110.8(14)	Fe1-C23B-H23B	127.4
O2-C3-N2	121.8(2)	C23B-C24B-C25B	107.4(9)
O2-C3-C4	122.0(2)	C23B-C24B-Fe1	71.2(12)
N2-C3-C4	116.2(2)	C25B-C24B-Fe1	71.0(15)

C3-C4-C11	111.46(18)	C23B-C24B-H24B	126.3
C3-C4-H4A	111.8(18)	C25B-C24B-H24B	126.3
C11-C4-H4A	107.7(18)	Fe1-C24B-H24B	123.2
C3-C4-H4B	107.5(15)	C26B-C25B-C24B	108.1(10)
C11-C4-H4B	107.5(15)	C26B-C25B-Fe1	65(2)
H4A-C4-H4B	111(2)	C24B-C25B-Fe1	69.7(14)
O1-C1-N1	124.7(2)	C26B-C25B-H25B	126.0
O1-C1-C2	121.3(2)	C24B-C25B-H25B	126.0
N1-C1-C2	113.9(2)	Fe1-C25B-H25B	130.7
C1-N1-C5A	126.4(6)	C25B-C26B-C27B	107.2(10)
C1-N1-C5B	117.0(8)	C25B-C26B-Fe1	75(2)
C1-N1-H1	120.5(17)	C27B-C26B-Fe1	72.4(14)
C5A-N1-H1	113.0(18)	C25B-C26B-H26B	126.4
C5B-N1-H1	122.1(18)	C27B-C26B-H26B	126.4
N1-C5A-C6A	109.8(6)	Fe1-C26B-H26B	118.5
N1-C5A-H5A	109.7	C23B-C27B-C26B	108.0(8)
C6A-C5A-H5A	109.7	C23B-C27B-Fe1	72.2(12)
N1-C5A-H5B	109.7	C26B-C27B-Fe1	66.8(16)
C6A-C5A-H5B	109.7	C23B-C27B-H27B	126.0
H5A-C5A-H5B	108.2	C26B-C27B-H27B	126.0
C7A-C6A-C5A	114.3(5)	Fe1-C27B-H27B	126.5
C7A-C6A-H6A	108.7	C14-C13-C2	129.6(2)
C5A-C6A-H6A	108.7	C14-C13-S1	110.7(2)
C7A-C6A-H6B	108.7	C2-C13-S1	119.6(2)
C5A-C6A-H6B	108.7	C15-C14-C13	110.4(3)
H6A-C6A-H6B	107.6	C15-C14-H14	124.8
C8A-C7A-C12A	116.2(7)	C13-C14-H14	124.8
C8A-C7A-C6A	125.3(7)	C16-C15-C14	114.6(3)
C12A-C7A-C6A	118.4(7)	C16-C15-H15	122.7
C7A-C8A-C9A	122.3(8)	C14-C15-H15	122.7
C7A-C8A-H8A	118.9	C15-C16-S1	112.1(3)
C9A-C8A-H8A	118.9	C15-C16-H16	123.9
C10A-C9A-C8A	119.6(8)	S1-C16-H16	123.9
C10A-C9A-H9A	120.2	N2-C17-C18	114.6(2)
C8A-C9A-H9A	120.2	N2-C17-H17A	108.7(15)
C9A-C10A-C11A	119.7(7)	C18-C17-H17A	110.7(15)
C9A-C10A-H10A	120.2	N2-C17-H17B	107.6(18)
C11A-C10A-H10A	120.2	C18-C17-H17B	108.5(18)
C10A-C11A-C12A	119.2(8)	H17A-C17-H17B	106(2)
C10A-C11A-H11A	120.4	C8B-C7B-C12B	116.8(8)
C12A-C11A-H11A	120.4	C8B-C7B-C6B	123.6(9)

C7A-C12A-C11A	122.7(8)	C12B-C7B-C6B	119.6(9)
C7A-C12A-H12A	118.7	C7B-C8B-C9B	122.5(9)
C11A-C12A-H12A	118.7	C7B-C8B-H8B	118.8
N1-C5B-C6B	107.9(8)	C9B-C8B-H8B	118.8
N1-C5B-H5C	110.1	C10B-C9B-C8B	119.2(10)
C6B-C5B-H5C	110.1	C10B-C9B-H9B	120.4
N1-C5B-H5D	110.1	C8B-C9B-H9B	120.4
C6B-C5B-H5D	110.1	C9B-C10B-C11B	119.8(10)
H5C-C5B-H5D	108.4	C9B-C10B-H10B	120.1
C7B-C6B-C5B	114.1(8)	C11B-C10B-H10B	120.1
C7B-C6B-H6C	108.7	C10B-C11B-C12B	119.7(9)
C5B-C6B-H6C	108.7	C10B-C11B-H11B	120.1
C7B-C6B-H6D	108.7	C12B-C11B-H11B	120.1
C5B-C6B-H6D	108.7	C7B-C12B-C11B	121.9(9)
H6C-C6B-H6D	107.6	C7B-C12B-H12B	119.1
		C11B-C12B-H12B	119.1

Table S8. Bond lengths and angles of molecule 17.

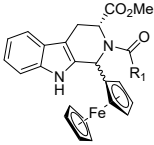
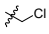
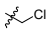
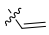
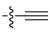
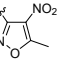
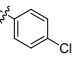
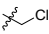
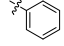
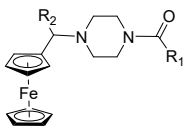
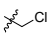
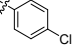
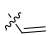
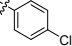
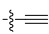
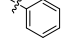
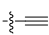
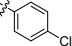
Atom–Atom	Length [Å]	Atom–Atom	Length [Å]
Fe1–C5	2.015(4)	C16–C17	1.383(5)
Fe1–C1	2.018(4)	C16–H16	0.97(4)
Fe1–C4	2.029(4)	C17–C18	1.355(6)
Fe1–C2	2.037(3)	C17–H17	0.96(4)
Fe1–C7	2.038(3)	C18–C19	1.359(6)
Fe1–C9	2.039(3)	C18–H18	1.03(5)
Fe1–C10	2.040(3)	C19–C20	1.392(5)
Fe1–C6	2.041(3)	C19–H19	1.00(5)
Fe1–C8	2.042(3)	C20–H20	0.94(4)
Fe1–C3	2.045(3)	C21–C22	1.456(4)
Cl1–C26	1.738(3)	C22–C23	1.172(5)
O1–C12	1.215(3)	C23–H23	0.90(5)
O2–C21	1.224(3)	C24–C29	1.374(4)
O3–C27	1.353(3)	C24–C25	1.386(4)
O3–C30	1.414(4)	C25–C26	1.384(4)
N1–C12	1.331(4)	C25–H25	0.97(4)
N1–C13	1.466(4)	C26–C27	1.386(4)
N1–H1A	0.85(3)	C27–C28	1.387(4)
N2–C21	1.349(3)	C28–C29	1.391(4)
N2–C24	1.438(3)	C28–H28	0.95(4)
N2–C11	1.487(3)	C29–H29	1.02(4)
C1–C2	1.379(5)	C30–H30A	0.91(4)
C1–C5	1.386(6)	C30–H30B	0.96(4)
C1–H1	0.85(4)	C30–H30C	1.02(5)
C2–C3	1.382(5)	C8–H8	0.96(4)
C2–H2	0.93(4)	C9–C10	1.412(5)
C3–C4	1.387(6)	C9–H9	0.92(4)
C3–H3	0.93(4)	C10–H10	0.92(3)
C4–C5	1.397(7)	C11–C12	1.542(4)
C4–H4	0.85(5)	C11–H11	0.97(3)
C5–H5	0.909(19)	C13–C14	1.474(5)
C6–C7	1.421(4)	C13–H13A	0.95(5)
C6–C10	1.427(4)	C13–H13B	0.99(5)
C6–C11	1.500(4)	C14–C15	1.511(4)
C7–C8	1.411(4)	C14–H14A	1.06(5)
C7–H7	0.95(3)	C14–H14B	0.97(5)
C8–C9	1.402(5)	C15–C20	1.372(5)
C15–C16	1.389(5)		
Atom–Atom–Atom	Angle [°]	Atom–Atom–Atom	Angle [°]

C5-Fe1-C1	40.21(18)	C5-Fe1-C10	111.11(15)
C5-Fe1-C4	40.4(2)	C1-Fe1-C10	137.12(15)
C1-Fe1-C4	67.71(18)	C4-Fe1-C10	113.36(16)
C5-Fe1-C2	66.93(17)	C2-Fe1-C10	176.78(14)
C1-Fe1-C2	39.77(16)	C7-Fe1-C10	68.38(12)
C4-Fe1-C2	67.00(17)	C9-Fe1-C10	40.51(13)
C5-Fe1-C7	144.00(18)	C5-Fe1-C6	114.20(14)
C1-Fe1-C7	114.47(15)	C1-Fe1-C6	111.40(13)
C4-Fe1-C7	175.06(19)	C4-Fe1-C6	143.41(17)
C2-Fe1-C7	111.55(14)	C2-Fe1-C6	136.97(13)
C5-Fe1-C9	136.32(19)	C7-Fe1-C6	40.79(10)
C1-Fe1-C9	176.40(18)	C9-Fe1-C6	68.44(12)
C4-Fe1-C9	110.13(17)	C10-Fe1-C6	40.95(11)
C2-Fe1-C9	142.66(15)	C5-Fe1-C8	175.3(2)
C7-Fe1-C9	67.92(13)	C1-Fe1-C8	143.36(17)
C4-Fe1-C8	135.23(19)	C27-O3-C30	117.6(3)
C2-Fe1-C8	114.11(15)	C12-N1-C13	121.8(3)
C7-Fe1-C8	40.45(13)	C12-N1-H1A	117(2)
C9-Fe1-C8	40.17(14)	C13-N1-H1A	121(2)
C10-Fe1-C8	68.07(13)	C21-N2-C24	120.5(2)
C6-Fe1-C8	68.43(12)	C21-N2-C11	117.0(2)
C5-Fe1-C3	66.99(17)	C24-N2-C11	122.4(2)
C1-Fe1-C3	66.92(15)	C2-C1-C5	107.8(4)
C4-Fe1-C3	39.80(18)	C2-C1-Fe1	70.9(2)
C2-Fe1-C3	39.56(16)	C5-C1-Fe1	69.8(2)
C7-Fe1-C3	136.17(16)	C2-C1-H1	123(3)
C9-Fe1-C3	113.47(15)	C5-C1-H1	130(3)
C10-Fe1-C3	142.62(15)	Fe1-C1-H1	125(3)
C6-Fe1-C3	176.12(16)	C1-C2-C3	108.5(4)
C8-Fe1-C3	110.65(15)	C1-C2-Fe1	69.4(2)
C3-C2-H2	126(3)	C3-C2-Fe1	70.6(2)
Fe1-C2-H2	122(3)	C1-C2-H2	125(3)
C2-C3-C4	108.3(4)	C29-C24-N2	120.5(2)
C2-C3-Fe1	69.9(2)	O1-C12-C11	121.2(2)
C4-C3-Fe1	69.5(2)	N1-C12-C11	114.8(3)
C2-C3-H3	120(3)	N1-C13-C14	110.8(3)
C4-C3-H3	131(3)	N1-C13-H13A	107(3)
Fe1-C3-H3	121(3)	C14-C13-H13A	110(3)
C3-C4-C5	107.2(4)	N1-C13-H13B	109(3)
C3-C4-Fe1	70.7(2)	C14-C13-H13B	111(3)
C5-C4-Fe1	69.2(2)	H13A-C13-H13B	109(4)

C3-C4-H4	124(4)	C13-C14-C15	115.8(3)
C5-C4-H4	128(4)	C13-C14-H14A	106(3)
Fe1-C4-H4	120(4)	C15-C14-H14A	112(3)
C1-C5-C4	108.2(4)	C13-C14-H14B	100(3)
C1-C5-Fe1	70.0(2)	C15-C14-H14B	114(3)
C4-C5-Fe1	70.4(2)	H14A-C14-H14B	108(4)
C1-C5-H5	131(3)	C20-C15-C16	118.2(3)
C4-C5-H5	121(3)	C20-C15-C14	119.3(3)
Fe1-C5-H5	123(3)	C16-C15-C14	122.5(3)
C7-C6-C10	107.1(3)	C17-C16-C15	120.3(4)
C7-C6-C11	125.0(2)	C17-C16-H16	117(2)
C10-C6-C11	127.8(2)	C15-C16-H16	123(2)
C7-C6-Fe1	69.52(15)	C18-C17-C16	120.7(4)
C10-C6-Fe1	69.50(15)	C18-C17-H17	122(3)
C11-C6-Fe1	128.21(18)	C16-C17-H17	118(3)
C8-C7-C6	108.3(3)	C17-C18-C19	120.0(4)
C8-C7-Fe1	69.93(18)	C17-C18-H18	122(3)
C6-C7-Fe1	69.69(15)	C19-C18-H18	118(3)
C8-C7-H7	129(2)	C18-C19-C20	120.1(4)
C6-C7-H7	123(2)	C18-C19-H19	123(3)
Fe1-C7-H7	126(2)	C20-C19-H19	116(3)
C9-C8-C7	108.2(3)	C15-C20-C19	120.7(4)
C9-C8-Fe1	69.78(19)	C15-C20-H20	117(2)
C7-C8-Fe1	69.62(17)	C19-C20-H20	122(2)
C9-C8-H8	129(2)	O2-C21-N2	123.1(2)
C7-C8-H8	123(2)	O2-C21-C22	121.4(3)
Fe1-C8-H8	128(2)	N2-C21-C22	115.5(2)
C8-C9-C10	108.6(3)	C23-C22-C21	176.2(4)
C8-C9-Fe1	70.05(19)	C22-C23-H23	176(3)
C10-C9-Fe1	69.79(17)	C29-C24-C25	120.1(3)
C8-C9-H9	126(2)	C10-C9-H9	125(2)
Fe1-C9-H9	123(2)	C25-C24-N2	119.2(2)
C9-C10-C6	107.8(3)	C26-C25-C24	119.2(3)
C9-C10-Fe1	69.71(18)	C26-C25-H25	121(2)
C6-C10-Fe1	69.55(15)	C24-C25-H25	119(2)
C9-C10-H10	125(2)	C25-C26-C27	121.6(3)
C6-C10-H10	127(2)	C25-C26-C11	119.1(2)
Fe1-C10-H10	126(2)	C27-C26-C11	119.3(2)
N2-C11-C6	110.9(2)	O3-C27-C26	116.6(3)
N2-C11-C12	108.7(2)	O3-C27-C28	125.1(3)
C6-C11-C12	112.4(2)	C26-C27-C28	118.3(3)

N2-C11-H11	105.4(15)	C27-C28-C29	120.5(3)
C6-C11-H11	108.9(14)	C27-C28-H28	121(2)
C12-C11-H11	110.3(14)	C29-C28-H28	118(2)
O1-C12-N1	124.0(3)	C24-C29-C28	120.2(3)
C28-C29-H29	120.5(19)	C24-C29-H29	119.1(19)
O3-C30-H30A	107(2)	H30A-C30-H30B	109(3)
O3-C30-H30B	113(3)	O3-C30-H30C	112(3)
H30B-C30-H30C	103(3)	H30A-C30-H30C	114(3)

Table S9. Antitumor activities and ferroptosis selectivity of target compounds towards HT1080 cells.

Comp.	R ₁	R ₂	HT1080, IC ₅₀ (μM) ^a		Selectivity ^b	
			-fer-1	+fer-1		
	18^c		--	1.100±0.127	1.021±0.149	0.9
	19^d		--	1.430±0.253	1.201±0.154	0.8
	20^c		--	13.350±0.330	15.920±0.275	1.2
	21^c		--	0.041±0.014	1.499±0.267	36.6
22			> 10	> 30	--	
23			4.237±0.334	4.603±0.212	1.1	
	24			2.736±0.217	3.115±0.439	1.1
	25			> 10	> 30	--
	26			6.602±0.138	7.583±0.184	1.1
	27			2.935±0.112	4.733±0.201	1.6
RSL3				0.024±0.006	3.704±1.358	154.3

(a) Values are expressed as the mean of three independent experiments ± SD; (b) Selectivity: HT1080 IC₅₀ with fer-1/ HT1080 IC₅₀ without fer-1; (c) (1*S*, 3*R*)-diastereomer; (d) (1*R*, 3*R*)-diastereomer.

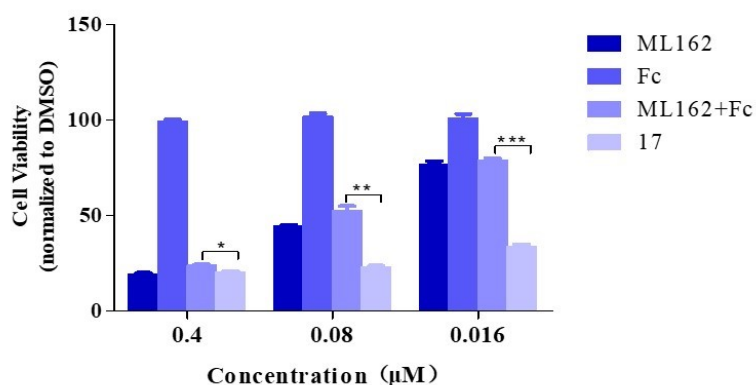


Figure S10. Cell viability of HT1080 cells treated with ML162 (0.4, 0.08, 0.016 µM), Ferrocene (Fc, 0.4, 0.08, 0.016 µM), **17** (0.4, 0.08, 0.016 µM), ML162 (0.4, 0.08, 0.016 µM) + Fc (0.4, 0.08, 0.016 µM) for 72 h. Data are shown as the mean ± SD (n = 3).

	ML162		17	
	0.5 h	1 h	0.5 h	1 h
Cellular uptake (pmol/mg prot)	19.71 ± 1.12	26.38 ± 1.53	35.40 ± 2.75	94.70 ± 9.60
Relative cellular uptake (%) ^a	0.21 ± 0.02	0.30 ± 0.03	1.12 ± 0.15	3.18 ± 1.46

^aRelative cellular uptake = cellular amount of substance/the initial amount of substance*100%, n=3

Figure S11. The cellular uptake of ML162 and **17** on HT1080 cells by the way of LC-MS/MS method, with the concentration of 2 µM.

Table S12. The EC₅₀ values of different cell death inhibitor to rescue the antitumor activities of ML162 and **17** on OS-RC2 cells with the concentration of 0.1 μM.

Death manner	Inhibitors	IC ₅₀ ±SD (μM) ^a	
		ML162	17
Apoptosis	Z-VAD-FMK	>100	>100
Necrosis	Nec-1	>100	>100
Autophagy	Wortmannin	>100	>100
Ferroptosis	Fer-1	0.48±0.02	0.89±0.08
	DFO	2.50±0.07	9.98±0.05

(a) Values are expressed as the mean of three independent experiments ± SD.

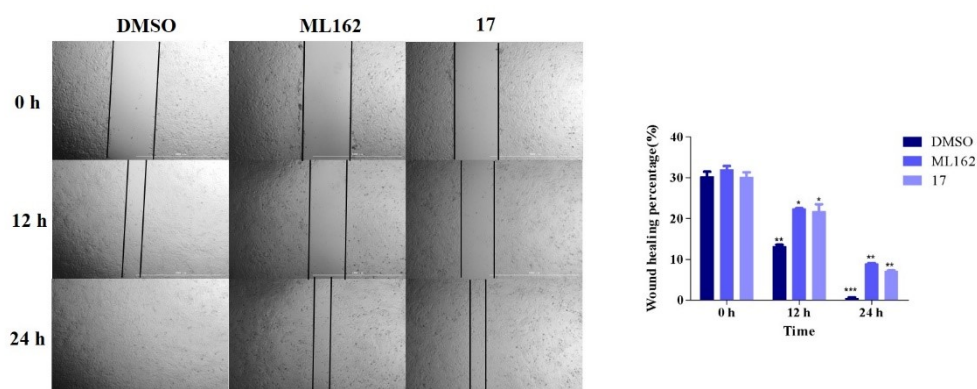


Figure S13. Wound-healing assays were used to detect the migration of 4T1 cells after treatment of ML162, **17** (0.5 μM), the migrated ratio was calculated. Data are shown as the mean ± SD (n = 6).

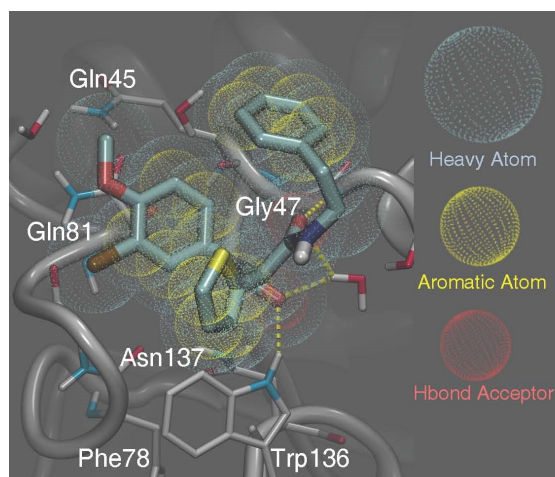


Figure S14. The template for molecular docking. The model of the template is composed of heavy atoms, aromatic atoms and hydrogen bond receptors, which is generated by Watvina docking program using score_only and genph4 mode. The heavy atoms (cyan) contributes the shape similarity, while aromatic atoms (yellow), hydrogen bond acceptors (red) are for pharmacophore model.

Table S15. Statistics of RNA-Seq for the control and the 17-treated groups.

Sample	Total Reads	Mapped Reads
Control-1	71303282	61727181(86.57%)
Control-2	80514212	70173048(87.16%)
Control-3	77114278	65857973(85.4%)
17-1	79761924	67679985(84.85%)
17-2	78019778	64314182(82.43%)
17-3	76383880	64828259(84.87%)

Table S16. The source information of the genes used for Venn diagrams to show overlap with up-regulated DEGs.

Ferroptosis driver	<p>RPL8 、 IREB2 、 ATP5MC3 、 CS 、 EMC2 、 ACSF2 、 NOX1 、 CYBB 、 NOX3 、 NOX4 、 NOX5 、 DUOX1 、 DUOX2 、 G6PD 、 PGD 、 VDAC2 、 PIK3CA 、 FLT3 、 SCP2 、 TP53 、 ACSL4 、 LPCAT3 、 NRAS 、 KRAS 、 HRAS 、 TF 、 TFRC 、 TFR2 、 SLC38A1 、 SLC1A5 、 GLS2 、 GOT1 、 CARS1 、 TP53 、 ALOX5 、 KEAP1 、 HMOX1 、 TP53 、 TP53 、 GLS2 、 ATG5 、 ATG7 、 NCOA4 、 TF 、 ALOX5 、 ALOX12 、 ALOX12B 、 ALOX15 、 ALOX15B 、 ALOXE3 、 PHKG2 、 TFRC 、 ACO1 、 IREB2 、 SLC38A1 、 GLS2 、 G6PDX 、 ULK1 、 ATG3 、 ATG4D 、 ATG5 、 BECN1 、 MAP1LC3A 、 GABARAPL2 、 GABARAPL1 、 ATG16L1 、 WIPI1 、 WIPI2 、 SNX4 、 ATG13 、 ULK2 、 NCOA4 、 ACSL4 、 TP53 、 SAT1 、 ALOX15 、 ACSL4 、 LPCAT3 、 ALOX15 、 ACSL4 、 KEAP1 、 EGFR 、 NOX4 、 MAPK3 、 MAPK1 、 BID 、 ACSL4 、 ZEB1 、 KEAP1 、 DPP4 、 ALOX15 、 ALOX12 、 CDKN2A 、 PEBP1 、 SOCS1 、 CDO1 、 MYB 、 HMOX1 、 MAPK8 、 MAPK9 、 MAPK1 、 MAPK3 、 SLC1A5 、 CHAC1 、 MAPK14 、 LINC00472 、 NOX4 、 GOT1 、 BECN1 、 PRKAA2 、 PRKAA1 、 ELAVL1 、 BAP1 、 TP53 、 ABCC1 、 ACSL4 、 MIR6852 、 ACVR1B 、 TGFBR1 、 BAP1 、 EPAS1 、 HILPDA 、 HIF1A 、 ALOX12 、 ACSL4 、 HMOX1 、 FNG 、 ANO6 、 LPIN1 、 HMGB1 、 TNFAIP3 、 TLR4 、 NOX4 、 ATF3 、 ATM 、 YY1AP1 、 EGLN2 、 MIOX 、 TFAFAZZIN 、 MTDH 、 IDH1 、 SIRT1 、 TFAFAZZIN 、 BECN1 、 FBXW7 、 PANX1 、 DNAJB6 、 BACH1 、 ACSL4 、 LONP1 、 CD82 、 IL1B 、 CTSB 、 POR 、 CYB5R1 、 ELOVL5 、 FADS1 、 ALOX12 、 FBXW7 、 PTEN 、 NR1D1 、 NR1D2 、 TBK1 、 IL6 、 USP7 、 miR-182-5p 、 miR-378a-3p 、 CTSB 、 ACSL4 、 ATF4 、 BECN1 、 AQP3 、 AQP5 、 AQP8 、 LINC00618 、 IREB2 、 MT1DP 、 ACSL4 、 PEX10 、 KEAP1 、 AGPAT3 、 PEX12 、 CHP1 、 GPAT4 、 BRPF1 、 OSBPL9 、 INTS2 、 MMD 、 CYP4F8 、 MLLT1 、 TTPA 、 GRIA3 、 EPT1 、 POM121L12 、 LIG3 、 AEBP2 、 AGPS 、 CDCA3 、 PEX2 、 LPCAT3 、 PEX6 、 TIMM9 、 DCAF7 、 LCE2C 、 FAR1 、 PHF21A 、 SMAD7 、 LYRM1 、 AMN 、 PEX3 、 MTCH1 、 ZEB1 、 SIRT1 、 ACADSB 、 PVT1 、 hsa_circ_0008367 、 SLC39A14 、 NCOA4 、 MAP3K11 、 GSK3B 、 MAPK8 、 BRD7 、 TP53 、 SLC25A28 、 ACSL4 、 MFN2 、 ACSL4 、 SLC11A2 、 ZFAS1 、 SLC38A1 、 TSC1 、 PEBP1 、 TGFB1 、 SNCA 、 SIRT3 、 PRKAA2 、 TFRC 、 CGAS 、 STING1 、 HDHC3 、 MIR761 、 MDM2 、 MDM4 、 ALOX15 、 POR 、 MIR214 、 DLD 、 LONP1 、 ACSL4 、 BACH1 、 DNAJB6 、 WWTR1 、 SIRT1 、 ATM 、 PRKCA 、 LGMN 、 ACSL4 、 TP53 、 IFNG 、 SMPD1 、 MYCN 、 SLC11A2 、 IFNA1 、 IFNA2 、 IFNA4 、 IFNA5 、 IFNA6 、 IFNA7 、 IFNA8 、 IFNA10 、 IFNA13 、 IFNA14 、 IFNA16 、 IFNA17 、 IFNA21 、 SMG9 、 NR1D1 、 ACSL4 、 PPARG 、 TLR4 、 IL6 、 MIR335 、 ATF3 、 HMOX1 、 HMGB1 、 EPAS1 、 SNX5 、 PAQR3 、 MICU1 、 NOX4 、 TOR2A 、 MIR375 、 MAP3K14 、 SIRT3 、 CircKDM4C 、 MIR324 、 QSOX1 、 MIB2 、 CLTRN 、 KLF2 、 MIR5096 、 TFRC 、 HOTAIR 、 H19 、 FOXO4 、 ELAVL1 、 YTHDC2 、 DDR2 、 SLC39A7 、</p>
---------------------------	---

TRIM46、ACSL1、KDM5A、TRIM21、HMOX1、DPEP1、CYGB、IDO1、GSTZ1、TP53、ACO1、GJA1、IREB2、SLC7A11、PGRMC1、CIRBP、FAR1、circPSEN1、USP11、STING1、YAP1、HMOX1、MIR135B、TRIM26、YAP1、NDRG1、MIR302A、ASMTL-AS1、ZFAS1、FADS2、PIEZO1、LIFR、PTPN6、MIR15A、EGR1、ADAM23、ARHGEF26-AS1、ACSL4、CPEB1、COX4I2、lncRNA AABR07017145.1、TIMP1、MIR15A、KDM6B、NCOA4、GSK3B、IFNG、METTL14、CHAC1、MIB1、KDM5C、ACSL4、MEG3、CCDC6、ATF3、IREB2、CFL1、ALOXE3、MIR539、KMT2D

DEGs
(Upregulated)

PCDHGB3、KRT5、BORCS7-ASMT、KRT81、TNNI2、KRT14、IER5L-AS1、RP9P、PDXDC2P、ZBTB46-AS2、KRT6A、CICP14、LINC02076、HK3、IGSF9、NHSL2、KRT8P39、FAM95A、SNX18P25、TENM3-AS1、SAMDM3、CFHR5、ACTN3、RPL13AP20、GPR142、LAMA5AS1、ACTA1、PIK3R5、ICAM4、DRP2、KRT17、MYH2、MPZ、KCNC4、SLC6A17、PLA2G4B、ACTC1、PTX3、CSF2、BTBD17、SRRM3、HMGB1P37、HLA-DOA、PLAC8、FAM81A、ATP2A1、ST6GALNAC6、MIR9-3HG、VGF、MFAP4、TIAM1、H4C15、CRIP3、MMP15、LRFN3、RPL3P4、ACOT4、INO80B-WBP1、NRGN、TMEFF2、RAB4B-EGLN2、EGFR-AS1、RASA4CP、KIF19、GIMD1、DES、MRC2、DOCK2、RNASEK-C17orf49、ELN-AS1、ANKRD2、RDM1、CXCL8、NRXN3、AEBP1、TTBK1、SMG1P5、TNFRSF9、NPBWR1、MYH4、C1orf116、PLXNB3、LOXL3、PCDHGB6、CREB3L1、FOLR1、HSPA1A、PREX1、PCDHGA6、LDLR、NUP210、DENND2D、C15orf48、MYH11、FOSL1、PIF1、RPL10P16、KREMEN2、DLK2、COL1A1、RTN4RL1、PEX6、SFRP1、C1QTNF3-AMACR、CCL2、FDXR、TUBBP1、IFI6、HRH2、SLC17A3、ADAMTSL5、CDC20、TPM2、APLP1、FBLN1、RAD54L、ITGB3、SLC16A12、HYAL3、DISP2、DOC2B、ARPIN-AP3S2、PHLDA2、EIF3CL、RECQL4、MAPK8IP2、SLC51B、CTSE、ITGB6、TNF、NPTXR、CILP、GFRA2、IL4I1、KCTD1、TMEM125、LRRN4、CAMK2N2、PHF19、GDF15、TIMP2、C8G、LINC01843、AKR1B1、CARMIL2、FRMD3、STK32B、CABP1、KRT80、FLNA、CORO1A、NFASC、TRAF1、CDKN1A、IQGAP3、IER3、DNM1P47、WDR62、TMEM179、SLCO4A1、SLC6A19、VDR、MARVELD1、CPLANE2、SERPINH1、GNB1L、SLC2A6、F3、THBS4、PRKAR1B、LGALS1、CXCL1c、CENPM、HYAL1、LINC02904、HSD17B1、HSPA1B、JOSD2、CNDP1、CYBB、DLG4、POC1A、SEMA7A、LIF、MAGED4B、PIK3R2、ELFN2、KCNJ15、BIRC5、CAPN6、LAMB3、ICAM1、POLQ、BANP、PTGS1、OAS1、ACHE、HAO2、ACTG1P14、TENM3、SMTN、AURKB、FBLN5、TGFB3L、EHD3、NAPA-AS1、IKBKE、THTPA、OASL、TSPAN4、ACTG2、WDR54、MMP24、TINAGL1、SLC6A18、RBP5、MRM1、CCDC61、COL1A2、ABCC10、PGLYRP2、MYEOV、ACTA2、G0S2、TACC3、HMGCS2、RCCD1、SOWAHB、UHRF1、GPT、COG4、SLC38A3、

SYT9 、 ARMC6 、 COL3A1 、 BGN 、 CDCA3 、 HLA-DPA1 、 PTK7 、 PYCR1 、
NFKB2 、 EMX1 、 FKBP4 、 CCNB1 、 TRIM16 、 SLC1A4 、 SMIM1 、 THBS2 、
IL6 、 MAP3K12 、 DUSP1 、 SERF1A 、 TEDC1 、 STYXL1 、 SPC24 、 MYBL2 、
SLC22A18AS 、 MESP1 、 CHTF18 、 TM4SF5 、 H2AC6 、 NMNAT1 、 WDR4 、
HOGA1 、 ETV5 、 SPRED3 、 UBASH3B 、 SLC9A3 、 GPR153 、 C1QTNF1 、
ALDH4A1 、 APEH 、 GCNT3 、 LIN7B 、 CKMT1A 、 COL7A1 、 TP53 、 MMP2 、
IFI30 、 URB1

Ferroptosis driver CYBB 、 TP53 、 CDCA3 、 PEX6 、 IL6
and DEGs (up)

Table S17. The source information of the genes used for Venn diagrams to show overlap with down-regulated DEGs.

Ferroptosis suppressor	<p>SLC7A11、GPX4、AKR1C1、AKR1C2、AKR1C3、GPX4、RB1、 HSPB1、HSF1、SLC7A11、GPX4、GCLC、SLC7A11、NFE2L2、 SQSTM1、NQO1、HMOX1、FTH1、MUC1、SLC3A2、MT1G、 NFE2L2、SLC40A1、SLC7A11、GPX4、SLC7A11、CISD1、SLC7A11、 FANCD2、GPX4、NFE2L2、FTMT、HSPA5、ATF4、SLC7A11、 GPX4、GPX4、HMOX1、ATF4、NFE2L2、TP53、SLC7A11、HELLS、 SCD、FADS2、SRC、STAT3、NFE2L2、PML、MTOR、NFS1、TP63、 SLC7A11、TP53、CDKN1A、MIR137、SLC40A1、GPX4、GPX4、 ENPP2、VDAC2、FH、CISD2、SLC40A1、MIR9-1、MIR9-2、MIR9-3、 CBS、NFE2L2、SQSTM1、GPX4、ISCU、FTH1、ACSL3、OTUB1、 CD44、LINC00336、STAT3、BRD4、PRDX6、MIR17、SCD、SESN2、 NF2、ARNTL、HIF1A、JUN、CA9、HSPA5、TMBIM4、HSPA5、 PLIN2、MIR212、Fer1HCH、AIFM2、AIFM2、LAMP2、ZFP36、 GPX4、PROM2、CHMP5、CHMP6、AKR1C1、AKR1C2、AKR1C3、 CBS、NFE2L2、CAV1、GCH1、SIRT3、DAZAP1、PIR、GCLC、FTL、 HCAR1、SLC16A1、RRM2、SCD、NR4A1、PIK3CA、RPTOR、 SREBF1、SREBF2、FZD7、NFE2L2、NFE2L2、P4HB、NT5DC2、 BCAT2、HSF1、PLA2G6、MIR424、PARK7、FXN、SUV39H1、ATF2、 CDKN1A、FTH1、NFE2L2、STAT3、ACOT1、NFE2L2、ALDH3A2、 NFE2L2、STK11、FNDC5、CircIL4R、CDH1、NFE2L2、MIR214、 NEDD4L、SQSTM1、TF、FTMT、BRD2、BRD3、BRD4、BRDT、 SCD、SLC7A11、DECR1、NFE2L2、GPX4、SLC7A11、NFE2L2、 GLRX5、GPX4、NCOA3、NR5A2、GPX4、MTOR、PANX2、RHEBP1、 TFAP2A、CP、SLC7A11、ARF6、GDF15、ABHD12、PPP1R13L、 TFAM、KDM3B、RNF113A、PARK7、AHCY、FXN、circ-TTBK2、 MIR522、IDH2、PPARA、NOS2、SIAH2、RELA、PRKAA2、VDR、 NEDD4、FXN、AIFM2、PRDX1、AR、CBS、NFE2L2、CHMP5、 CHMP6、HMOX1、ZFP36、LAMP2、MTF1、COPZ1、NUPR1、USP35、 HSF1、PROM2、PLA2G6、HIF1A、NEAT1、RRM2、SLC7A11、 FTMT、PARP1、PARP2、PARP3、PARP4、PARP6、PARP8、PARP9、 PARP10、PARP11、PARP12、PARP14、PARP15、PARP16、PDSS2、 TXN、SENP1、PLA2G6、OIP5-AS1、MIR190A、FGF21、CREB1、 CREB3、CREB5、FTMT、GOT1、TFRC、GPX4、MIR130B、BEX1、 ASAH2、SCD、FABP4、AKT1S1、MLST8、MTOR、RPTOR、CDH1、 SIRT1、TYRO3、SIRT6、TMSB4X、TMSB4Y、KIF20A、ECH1、 circRHOT1、ETV4、MEG8、VCP、circ_0007142、ENPP2、RBMS1、 KDM4A、CBS、MGST1、circKIF4A、miR-7-5p、PRDX6、 circ_0067934、MPC1、CHMP1A、CAMKK2、SOX2、SRSF9、PROK2、</p>
-------------------------------	---

MIR4443、SIRT2、circRNA1615、MIR27A、MIR670、MEF2C、NF2、
CDH1、HSPB1、EZH2、PEDS1、SMPD1、ADAMTS13、CDC25A、
G6PD、SRSF9、CAV1、CircFNDC3B、PPARD、CISD2、ENO3、
SESN2、LCN2、MARCHF5、TRIB2、DHODH、SLC7A11、MIR545、
OTUB1、PDK4、CircPVT1、MIR9-3HG、ADIPOQ、circDTL、GPX4、
mmu_circRNA_0000309、IL6、PTPN18、FTH1、FTH1、FTL、LCN2、
ABCC5、CISD3、MS4A15、LCN2、FURIN、circRHBG、GALNT14、
KLHDC3、LINC01833、circGFRA1、MAPKAP1、MLST8、MTOR、
PRR5、RICTOR、GSTM1、TERT、circ0097009、TMEM161B-DT、
circEPSTI1、MIR18A、RARRES2、USP11

DEGs
(downregulated)

ATG14、VSIG1、MTUS1、CDC42EP3、SLFN5、ZNF138、C2orf69、
ZFAS1、C17orf78、ZNF84、EEA1、CARF、PLEKHA1、RB1CC1、
MAP4K5、DNAJB14、FOXA1、ZNF654、ANTXR1、CEP4、
RAB11FIP2、RAD54B、PTGS2、PGM2L1、NUDT12、BAG4、MBNL2、
MBIP、NOTCH2NLB、BBOF1、BRIP1、CRYZ、C9orf72、TOPORS、
DOP1A、APC、DHX36、ZNF260、UPF3B、TRIM13、MMP7、
ZBTB10、FAM204A、BCHE、ZNF644、HAUS6、CDH13、PER2、
TENT5A、RMDN2、ZNF33B、RAD17、ZNF487、CCDC138、CCDC82、
RASSF6、ZNF322、INPP4B、ODR4、FOXN2、ALB、JAK2、
ANKRD36、LYST、DYNLT3、ZMYM2、SIX4、FHL1、PBLD、MEIS2、
UACA、C12orf29、GCFC2、PDZD8、TMEM117、FABP7、BACH1、
ZNF35、TRIM2、DEPDC7、SERPINA3、ZFAND1、CLK4、BCL2L15、
ZC3H6、ANKRD12、ETAA1、SHLD2、TUBD1、RWDD4、THAP5、
ZNF141、NTM、RNF217、CD177、MAGI2、RPL36A-HNRNP2、
TWF1、UFL1、TIPARP、SAMD12、YOD1、MOB1B、RNF43、VAV3、
PSD3、LINC02274、MYH8、SGO2、ING2、PHF3、OFD1、PALMD、
ABCA1、UPF2、FGG、PIBF1、TCEAL1、NSRP1、SYNJ1、ST6GAL1、
AKAP9、SP3、FBXL3、SUZ12、HPGD、GRAMD1C、NUPR1、
ZNF595、ZNF227、MEF2C、MIER3、HSDL2-AS1、ZBED5、
MTND2P28、CRP、SNHG26、RIF1、TRIM23、ZFP14、ZNF277、
RBBP8、SLIT2、HAUS3、FAM200A、CEP126THAP6、SIM1、
LYSMD3、HOXA1、ZNF529-AS1、PGGT1B、ESCO1、GCC2、NR1D2、
LINC00997、MT-TA、RPAP3、ZNF197、PTPRR、CCPG1、ARID4A、
CEACAM19、LIFR、ZHX1、KANTR、SAMD9、ARID3C、ZUP1、
ZNF182、ZNF449、KBTBD11-AS1、USP53、DMBT1、CXADR、
WDR75、MBLAC2、LRIF1、PLEKHS1、CP、TSHZ2、RICTOR、
TRIM36、ZNF112、ARL6、CCDC121、CYSLTR2、CCDC112、SSPN、
KLF4、SOCS4、FBXO30、PDGFD、KLKB1、YPEL1、FAM214A、
MTERF2、ABCG1、ZNF678、TGFB1、RO60、CNTRL、BAZ2B、
OBI1、RAB33B、CCDC68、ZNF267、SKIL、LINC01608、ATAD5、

RESF1、H19、ZNF33A、ZNF155、MN1、PLIN1、CASP1、
MPHOSPH10、AP1AR、ATP8A1、MTMR7、PLCE1、RPGR、ICA1L、
BTNL8、MUC1、BCLAF、KRT223P、ZNF92、PPP2R3A、MAP1LC3C、
PAPPA、CHD1、OR2A7、RPS6KA5、CENPC、RND3、ZNF235、LOX、
ZNF566、ZNF547、RGS2、NARF-AS2、SYS1-DBNDD2、ZNF25、
SEMA6D、DSCAML1、TMEM74B、EFHC2、ZNF624、VASH2、
TRIB2、C1orf21、TPPP、LRRCC、GRM4、FMO5、ZNF184、PCDHB4、
N4BP2、ZC2HC1A、ID4、OR2A4、C21orf91、AFF2、SGMS1-AS1、
RBAK、FSTL5、SLC16A7、CFHR3、UGT1A4、MT-TQ、FXYD1、
SERPINB9P1、FSD1L、AFM、FANCB、MT-TN、ZNF337-AS1、EPO、
CTAGE15、TIGD7、ZNF420、ARHGDIB、EMX2OS、C21orf62、
ZNF10、RAB27B、RGPD5、MUC17、ALKAL2、TNNT3、SERPINA7、
ULK4P1、FAM228B、RAB31、ITIH4、ARG2、AKAP5、RPL21P75、
ZNF354A、ADGRG2、ZFP69、APOB、LTF、SBK2、RAPGEF5、
PWWP3B、DDIT4L、ZNF711、ARPC4-TTLL3、ODF3L1、ZNF254、
AQP9、CTAGE9、HERC2P3、ZNF567、ZDHHC11B、RGS4、SUGT1P4-
STRA6LP-CCDC180、F5、TAF5、RPL41P1、C6、NHIP、ZNF441、
ARSD-AS1、HP、GAB3、NPL、ANGPTL3、ZNF396、MT1F、PRR5-
ARHGAP8、ZNF300、ADH4、LRRC66、CELF4、PTGER4、NPBWR2、
GBP5、CENPS-CORT、LDLRAD2、IGFL2-AS1、PSD2、DNM1P35、
LSP1、NAALADL2、LINC01825、BTNL3、FLJ12825、TMEFF1、
CHRNA10、PFN4、TBC1D3D、APPBP2-DT、RALGPS2-AS1、NEDD8-
MDP1、GREB1、CCDC113、GC、SYCP3、HMGB3P32、GUCY2C、
RNA5S1、SBDSP1、DPP9-AS1、RASGRF1、UNC80、SCHLAP1、
MIR137HG、CT55、LINC00598、PCDHGA8、MICOS10-NBL1、RCC2-
AS1、SORD2P、ZNF474、RNA5S14

**Ferroptosis suppressor
and DEGs (down)** CP、NUPR1、MEF2C、TRIB2、RICTOR

Experimental Section

Chemical Synthesis

General Synthetic Methods. All reagents and solvents were obtained from commercial suppliers Aladdin, Bidepharm and Leyan, which can be used directly without purification unless otherwise mentioned. THF was obtained by distillation from sodium/benzophenone. Thin layer chromatography (TLC) was performed on silica gel 60 GF₂₅₄. Column chromatography was performed on silica gel Merck 60 (40-63 μm). All NMR experiments (¹H, ¹³C, 2D-) were carried out on Bruker 300 and 400 NMR spectrometers. Mass spectrometry was performed with a Nermag R 10-10C spectrometer. HRMS measurements were performed on a Thermo Fischer LTQ-Orbitrap XL apparatus equipped with an electrospray source. HPLC was employed to confirm the purity of compounds to be >95%: detection at 254 nm, flow rate = 1.0 mL/min, mobile A: methyl alcohol, mobile B: water, gradient elution conditions are as follows: 20% A from 0 to 1.0 min, 20-100% A from 1.0 to 10.0 min, 100% A from 10.0 to 13.0 min, 100-20% A from 13.0 to 13.5 min, and 20% A from 13.5 to 15.0 min.

Synthesis of ML162-Fc analogs

2-Chloro-N-ferrocenyl-N-(2-oxo-2-(phenethylamino)-1-(thiophen-2-yl)ethyl)acetamide (10)

2-Thiophene carboxaldehyde (0.058 g, 0.50 mmol) was dissolved in MeOH (3 mL) and aminoferrocene (0.100 g, 0.50 mmol) was added. The mixture was stirred for 30 minutes and 2-chloroacetic acid (0.054 g, 0.57 mmol) and 2-phenethyl isocyanide (0.075 g, 0.57 mmol) were added. After stirring at room temperature for 48 hours, the solvents were evaporated. The crude material was purified by column chromatography over silica gel (petroleum ether/ethyl acetate: 100/0 to 0/100) to afford 0.020 g (0.04 mmol, 8% yield) of **10** as a red solid. ¹H NMR (400 MHz, Acetone-d₆) δ 7.44 (d, J = 5.2 Hz, 1H), 7.32 – 7.21 (m, 6H), 7.18 (d, J = 7.0 Hz, 1H), 7.00 (t, J = 4.4 Hz, 1H), 6.23 (s, 1H), 4.58 (s, 1H), 4.33 (s, 1H), 4.26 (d, J = 5.1 Hz, 6H), 4.23 (s, 1H), 4.05 (d, J =

21.4 Hz, 2H), 3.55 – 3.50 (m, 1H), 3.41 (dt, $J = 13.2, 6.7$ Hz, 1H), 2.79 (s, 2H). ^{13}C NMR (101 MHz, Acetone- d_6) δ 205.46, 167.38, 166.58, 139.69, 138.93, 128.93, 128.56, 128.51, 127.13, 126.23, 126.07, 103.40, 70.29, 69.65, 66.49, 66.16, 65.88, 65.31, 42.40, 41.25, 35.52. HRMS (ESI) m/z : $[\text{M}+\text{Na}]^+$: $\text{C}_{26}\text{H}_{25}\text{ClFeN}_2\text{O}_2\text{S}+\text{Na}$, calculated 543.0675; found 543.0584. Purity : 96.30%.

2-Chloro-N-ferrocenylmethyl-N-(2-oxo-2-(phenethylamino)-1-(thiophen-2-yl)ethyl) acetamide (11)

2-Thiophene carboxaldehyde (0.029 g, 0.26 mmol) was dissolved in MeOH (1.5 mL) and ferrocene-methylamine (0.055 g, 0.26 mmol) was added. The mixture was stirred for 30 minutes and 2-chloroacetic acid (0.024 g, 0.26 mmol) and 2-phenethyl isocyanide (0.034 g, 0.26 mmol) were added. After stirring at room temperature for 40 hours, the solvents were evaporated. The crude material was purified by column chromatography over silica gel (petroleum ether/ethyl acetate: 100/0 to 0/100) to afford 0.046g (0.09 mmol, 34% yield) of **11** as a red solid. ^1H NMR (400 MHz, Acetone- d_6) δ 7.52 (d, $J = 4.5$ Hz, 1H), 7.30 – 7.26 (m, 2H), 7.21 (d, $J = 6.7$ Hz, 4H), 7.12 (s, 1H), 7.06 (s, 1H), 6.10 (s, 1H), 4.61 (s, 1H), 4.49 (d, $J = 15.7$ Hz, 1H), 4.33 (s, 2H), 4.23 (s, 1H), 4.08 (s, 7H), 4.00 (s, 1H), 3.69 (s, 1H), 3.45 (d, $J = 24.8$ Hz, 2H), 2.84 (s, 2H). ^{13}C NMR (101 MHz, Acetone- d_6) δ 166.46, 139.39, 137.18, 128.87, 128.44, 127.33, 126.60, 126.24, 108.69, 68.80, 67.67, 60.66, 57.36, 45.54, 42.59, 41.34, 35.12. HRMS (ESI) m/z : $[\text{M}+\text{Na}]^+$: $\text{C}_{27}\text{H}_{27}\text{ClFeN}_2\text{O}_2\text{S}+\text{Na}$, calculated 557.0831; found 557.0730. Purity : 95.52%.

2-Chloro-N-(3-chloro-4-methoxyphenyl)-N-(2-oxo-2-(ferrocenylethylamino)-1-(thiophen-2-yl)ethyl) acetamide (12)

2-Thiophene carboxaldehyde (0.125 g, 1.11 mmol) was dissolved in MeOH (4 mL) and 3-chloro-4-methoxyaniline (0.221 g, 1.11 mmol) was added. The mixture was stirred for 15 minutes and 2-chloroacetic acid (0.088 g, 0.93 mmol) and Ferrocene-ethylisonitrile (0.222 g, 0.93 mmol) were added. After stirring at room temperature for 7 hours, the solvents were evaporated. The crude material was purified by column

chromatography over silica gel (hexanes/ethyl acetate: 100/0 to 0/100) to afford 0.136 g (0.23 mmol, 24% yield) of **12** as a red solid. ¹H NMR (400 MHz, Acetone-d₆) δ 7.51 (s, 1H), 7.36 (d, J = 4.9 Hz, 1H), 7.06 – 6.92 (m, 3H), 6.89 – 6.86 (m, 1H), 6.32 (s, 1H), 4.12 (s, 5H), 4.03 (d, J = 4.9 Hz, 4H), 3.98 – 3.96 (m, 2H), 3.87 (s, 3H), 3.40 (dq, J = 13.3, 6.8 Hz, 2H), 3.03 (s, 2H). ¹³C NMR (101 MHz, Acetone-d₆) δ 168.54, 165.95, 155.27, 136.19, 132.34, 131.43, 130.77, 130.09, 127.86, 126.42, 121.43, 111.84, 86.02, 68.51, 68.23, 67.31, 59.79, 55.87, 42.73, 40.70. HRMS (ESI) m/z: [M]⁺: C₂₇H₂₆Cl₂FeN₂O₃S, calculated 584.0391; found 584.0396. Purity : 98.06%.

2-Chloro-N-(3-chloro-4-methoxyphenyl)-N-(2-oxo-2-(ferrocenylmethylamino)-1-(thiophen-2-yl)ethyl) acetamide (13)

2-Thiophene carboxaldehyde (0.125 g, 1.12 mmol) was dissolved in MeOH (3 mL) and 3-chloro-4-methoxyaniline (0.176 g, 1.12 mmol) was added. The mixture was stirred for 30 minutes and 2-chloroacetic acid (0.088 g, 0.93 mmol) and ferrocene-ethylisonitrile (0.222 g, 0.93 mmol) were added. After stirring at room temperature for 21 hours, the solvents were evaporated. The crude material was purified by column chromatography over silica gel (hexanes/ethyl acetate: 100/0 to 0/100) to afford 0.045 g (0.08 mmol, 8% yield) of **13** as a brown solid. ¹H NMR (400 MHz, Chloroform-d) δ 7.40 – 7.29 (m, 2H), 7.05 – 6.92 (m, 3H), 6.83 (dt, J = 13.5, 7.0 Hz, 1H), 6.21 – 6.16 (m, 1H), 6.05 (s, 1H), 4.15 (dd, J = 4.7, 1.9 Hz, 3H), 4.10 (t, J = 2.0 Hz, 3H), 4.02 (s, 5H), 3.90 (s, 3H), 3.87 (s, 2H). ¹³C NMR (101 MHz, Acetone-d₆) δ 168.27, 166.03, 155.29, 136.19, 131.65, 130.69, 130.19, 128.02, 126.44, 111.70, 85.79, 68.45, 67.70, 67.53, 60.09, 55.86, 42.19, 39.11. HRMS (ESI) m/z: [M]⁺: C₂₆H₂₄Cl₂FeN₂O₃S, calculated 570.0234; found 570.0235. Purity : 97.98%.

2-Chloro-N-(3-chloro-4-methoxyphenyl)-N-(2-oxo-2-(ferrocenylamino)-1-(thiophen-2-yl)ethyl) acetamide (14)

2-Thiophene carboxaldehyde (0.088 g, 0.78 mmol) was dissolved in MeOH (2 mL) and 3-chloro-4-methoxyaniline (0.123 g, 0.78 mmol) was added. The mixture was stirred for 30 minutes and 2-chloroacetic acid (0.062 g, 0.65 mmol) and ferrocene-isonitrile

(0.138 g, 0.65 mmol) were added. After stirring at room temperature for 20 hours, the solvents were evaporated. The crude material was purified by column chromatography over silica gel (hexanes/ethyl acetate: 100/0 to 0/100) to afford 0.057 g (0.10 mmol, 16% yield) of **14** as a brown solid. ¹H NMR (400 MHz, Acetone-d₆) δ 8.88 (s, 1H), 7.38 (d, J = 4.8 Hz, 1H), 7.13 – 6.86 (m, 5H), 6.30 (s, 1H), 4.78 (d, J = 30.1 Hz, 2H), 4.17 (s, 5H), 4.00 (d, J = 11.9 Hz, 4H), 3.88 (s, 3H). ¹³C NMR (101 MHz, Acetone-D₆) δ 205.94, 167.15, 166.09, 155.27, 142.82, 135.39, 131.22, 130.31, 128.63, 126.58, 121.40, 111.80, 95.31, 68.96, 64.07, 61.01, 60.58, 60.13, 55.85, 42.64. HRMS (ESI) m/z: [M]⁺: C₂₅H₂₂Cl₂FeN₂O₃S, calculated 556.0078; found 556.0085. Purity : 97.18%.

2-Chloro-N-(3-chloro-4-methoxyphenyl)-N-(2-oxo-2-(phenethylamino)-1-(ferrocenyl-2-yl)ethyl)acetamide (15)

Ferrocenecarboxaldehyde (0.196 g, 0.91 mmol) was dissolved in MeOH (3 mL) and 3-chloro-4-methoxyaniline (0.144 g, 0.91 mmol) was added. The mixture was stirred for 30 minutes and 2-chloroacetic acid (0.072 g, 0.76 mmol) and 2-phenethyl isocyanide (0.100 g, 0.76 mmol) were added. After stirring at room temperature for 21 hours, the solvents were evaporated. The crude material was purified by column chromatography over silica gel (petroleum ether/ethyl acetate: 100/0 to 0/100) to afford 0.3535g (0.61 mmol, 80% yield) of **15** as a red solid. ¹H NMR (400 MHz, Acetone-d₆) δ 7.60 (s, 1H), 7.31 (s, 2H), 7.30 (s, 1H), 7.29 (d, J = 0.9 Hz, 1H), 7.20 (dt, J = 6.2, 2.8 Hz, 1H), 6.88 (s, 2H), 5.85 (s, 1H), 4.17 – 4.15 (m, 1H), 4.10 (s, 6H), 4.01 (dt, J = 2.6, 1.3 Hz, 1H), 3.95 (q, J = 2.3 Hz, 1H), 3.83 (d, J = 4.6 Hz, 5H), 3.67 (ddd, J = 13.2, 6.6, 1.5 Hz, 1H), 3.56 – 3.50 (m, 1H), 2.93 (q, J = 7.5, 7.1 Hz, 2H). ¹³C NMR (101 MHz, Acetone-D₆) δ 205.27, 168.35, 165.44, 155.02, 139.66, 132.36, 131.14, 130.73, 128.96, 128.50, 126.30, 81.21, 69.99, 69.75, 68.87, 68.15, 59.83, 55.75, 42.68, 40.93, 35.75. HRMS (ESI) m/z: [M+H]⁺: C₂₉H₂₈Cl₂FeN₂O₃+H, calculated 579.0826; found 579.0901. Purity : 95.27%.

2-Alkenyl-N-(3-chloro-4-methoxyphenyl)-N-(2-oxo-2-(phenethylamino)-1-(ferrocenyl-2-yl)ethyl)acetamide (16)

Ferrocenecarboxaldehyde (0.587 g, 2.74 mmol) was dissolved in MeOH (3 mL) and 3-chloro-4-methoxyaniline (0.36 g, 2.29 mmol) was added. The mixture was stirred for 30 minutes and acrylic acid (0.165 g, 2.29 mmol) and 2-phenethyl isocyanide (0.300 g, 2.29 mmol) were added. After stirring at room temperature for 24 hours, the solvents were evaporated. The crude material was purified by column chromatography over silica gel (petroleum ether/ethyl acetate: 100/0 to 0/100) to afford 0.830 g (1.49 mmol, 65% yield) of **16** as a brown solid. ¹H NMR (400 MHz, Acetone-d₆) δ 7.72 (s, 1H), 7.36 – 7.26 (m, 5H), 7.20 (t, J = 6.9 Hz, 1H), 6.90 (s, 1H), 6.25 (dd, J = 16.8, 2.4 Hz, 1H), 5.99 (s, 1H), 5.85 (dd, J = 16.7, 10.2 Hz, 1H), 5.52 (dd, J = 10.3, 2.4 Hz, 1H), 4.18 (s, 1H), 4.11 (d, J = 5.8 Hz, 7H), 3.97 (s, 1H), 3.85 (s, 3H), 3.70 – 3.54 (m, 2H), 2.94 (dt, J = 12.4, 6.0 Hz, 2H). ¹³C NMR (101 MHz, Acetone-d₆) δ 206.47, 169.50, 165.85, 154.65, 141.00, 132.24, 132.00, 130.74, 129.09, 128.94, 128.51, 127.25, 126.25, 111.34, 81.62, 70.67, 69.75, 68.84, 68.08, 59.22, 55.75, 40.92, 35.73. HRMS (ESI) m/z: [M+H]⁺: C₃₀H₂₉ClFeN₂O₃+H, calculated 557.1216; found 557.1294. Purity : 99.72%.

2-Alkynyl-N-(3-chloro-4-methoxyphenyl)-N-(2-oxo-2-(phenethylamino)-1-(ferrocenyl-2-yl)ethyl)acetamide (17)

Ferrocenecarboxaldehyde (0.392 g, 1.83 mmol) was dissolved in MeOH (2 mL) and 3-chloro-4-methoxyaniline (0.240 g, 1.83 mmol) was added. The mixture was stirred for 30 minutes and propiolic acid (0.107 g, 1.53 mmol) and 2-phenethyl isocyanide (0.200 g, 1.53 mmol) were added. After stirring at room temperature for 24 hours, the solvents were evaporated. The crude material was purified by column chromatography over silica gel (petroleum ether/ethyl acetate: 100/0 to 0/100) to afford 0.522 g (0.94 mmol, 61% yield) of **17** as a brown solid. ¹H NMR (400 MHz, Acetone-d₆) δ 7.68 (s, 1H), 7.32 (d, J = 6.4 Hz, 4H), 7.25 – 7.16 (m, 2H), 7.01 (d, J = 6.4 Hz, 1H), 6.90 (d, J = 8.8 Hz, 1H), 5.85 (s, 1H), 4.21 (s, 1H), 4.14 (s, 6H), 4.07 (s, 1H), 3.99 (s, 1H), 3.85 (s, 3H), 3.73 – 3.64 (m, 1H), 3.60 (s, 1H), 3.55 (dd, J = 12.6, 7.3 Hz, 1H), 2.95 (q, J = 6.6 Hz, 2H). ¹³C NMR (101 MHz, Acetone-d₆) δ 168.03, 154.93, 152.70, 139.59, 132.48, 131.82, 131.01, 128.94, 128.54, 126.30, 120.48, 111.00, 81.50, 80.93, 76.47, 69.92,

69.72, 68.91, 68.31, 68.20, 59.46, 55.71, 41.04, 35.68. HRMS (ESI) m/z: [M]⁺: C₃₀H₂₇ClFeN₂O₃, calculated 554.1060; found 554.1063. Purity : 96.50%.

Synthesis of RSL3-Fc analogs

A general protocol for the Pictet-Spengler and acylation reactions and amide condensation reaction are described: to a suspension of 1.2 equivalents of the corresponding S or R tryptophan methyl ester hydrochloride in CH₂Cl₂ was added 1.3 equivalents of NEt₃ at room temperature. The mixture was stirred for 1 hour and then filtered. The filtrate was concentrated to give the required product, tryptophan methyl ester as clear oil, which was dried under vacuum for 10 minutes. Tryptophan methyl ester was dissolved in anhydrous dichloromethane. Corresponding aldehydes (1.0 equivalent) and 0.1 equivalent TFA were added to the reaction mixture and the solution was refluxed for one hour. Then 3 equivalents of TFA were added to the solution, and the reaction was allowed to stir under reflux overnight. The reaction mixture was cooled to room temperature and quenched with 30% NaOH. The organic phase was separated, washed with brine and dried with Na₂SO₄ and then concentrated to give the crude product. The compound was purified by column chromatography on silica gel eluting to give two separate diastereomers.

For **18-20**, The corresponding RSL3-Fc intermediate (one of the stereoisomers) was dissolved in anhydrous CH₂Cl₂ and 1.1 equivalents of sodium bicarbonate was added. To this were added 1.0 equivalents of chloroacetyl chloride or acryloyl chloride dropwise at 0°C. The reaction was followed by TLC until all the starting material was completely consumed. The reaction was filtered and the filtrate was extracted, washed with brine, dried with Na₂SO₄ and concentrated. The compound was purified by silica gel chromatography with a mixture of petroleum ether /ethyl acetate as the eluent. A similar protocol was used to obtain the chloroacetamide derivative for the other diastereomers or acrylamide derivative.

For **21**, the corresponding (1S, 3R)-RSL3-Fc intermediate was dissolved in anhydrous DMF, then 1.5 equivalents of HBTU and 1.0 equivalents of DIPEA were added to this

solution. The reaction was followed by TLC until all the starting material was completely consumed. The reaction was filtered and the filtrate was extracted, washed with brine, dried with Na₂SO₄ and concentrated. The compound was purified by silica gel chromatography with a mixture of petroleum ether /ethyl acetate as the eluent.

(1S, 3R)-1-ferrocenyl-2,3,4,9-tetrahydro-1H-pyridino [3,4-b] indole-3-carboxylic acid methyl ester (A)

Yellow solid in a yield 18.1%. ¹H NMR (400 MHz, Acetone-*d*₆) δ 9.51 (s, 1H), 7.43 (d, *J* = 7.5 Hz, 1H), 7.27 (d, *J* = 7.8 Hz, 1H), 7.06 – 6.92 (m, 2H), 5.20 (s, 1H), 4.43 (dd, *J* = 2.5, 1.3 Hz, 1H), 4.40 – 4.34 (m, 1H), 4.26 (s, 5H), 4.22 – 4.15 (m, 2H), 4.14 – 4.08 (m, 1H), 3.72 (s, 3H), 3.07 (d, *J* = 5.5 Hz, 2H).

(1S, 3R)-2-(2-chloroacetyl)-1-ferrocenyl-2,3,4,9-tetrahydro-1H-pyridino [3,4-b] indole-3-carboxylic acid methyl ester (18)

Yellow solid in a yield 33.0%. ¹H NMR (400 MHz, Acetone-*d*₆) δ 10.07 (s, 1H), 7.55 (d, *J* = 8.4 Hz, 1H), 7.44 (s, 1H), 7.14 (t, *J* = 7.4 Hz, 1H), 7.06 (t, *J* = 7.5 Hz, 1H), 6.26 (s, 1H), 4.66 (s, 1H), 4.54 (s, 1H), 4.44 (s, 2H), 4.36 – 4.23 (m, 2H), 4.13 (s, 6H), 3.70 (s, 3H), 3.23 (s, 1H), 3.04 (s, 1H). ¹³C NMR (101 MHz, Acetone-*d*₆) δ 169.53, 166.25, 136.80, 134.00, 126.48, 121.79, 119.31, 118.12, 111.44, 107.41, 88.17, 68.93, 68.46, 67.73, 67.03, 54.70, 53.99, 51.30, 41.72, 22.08. HRMS (ESI, C₂₅H₂₄ClFeN₂O₃: [M]⁺) calcd: 491.0819, found: 491.0831. Purity : 96.41%.

(1R, 3R)-1-ferrocenyl-2,3,4,9-tetrahydro-1H-pyridino [3,4-b] indole-3-carboxylic acid methyl ester (B)

Yellow solid in a yield 17.6%. ¹H NMR (400 MHz, Acetone-*d*₆) δ 9.43 (s, 1H), 7.43 (dd, *J* = 6.8, 1.9 Hz, 1H), 7.28 – 7.21 (m, 1H), 7.05 – 6.93 (m, 2H), 5.00 (s, 1H), 4.51 (dq, *J* = 2.4, 1.1 Hz, 1H), 4.32 – 4.26 (m, 6H), 4.24 (td, *J* = 2.4, 1.3 Hz, 1H), 4.14 (td, *J* = 2.3, 1.1 Hz, 1H), 3.95 (dd, *J* = 11.3, 3.9 Hz, 1H), 3.85 (d, *J* = 0.8 Hz, 3H), 3.14 – 2.98 (m, 2H).

(1R, 3R)-2-(2-chloroacetyl)-1-ferrocenyl-2,3,4,9-tetrahydro-1H-pyridino [3,4-b] indole-3-carboxylic acid methyl ester (19)

Yellow solid in a yield 17.6%. ¹H NMR (400 MHz, Acetone-*d*₆) δ 9.28 (s, 1H), 7.55 (dd, *J* = 8.1, 3.2 Hz, 2H), 7.21 – 7.13 (m, 1H), 7.08 (t, *J* = 7.5 Hz, 1H), 6.88 (s, 1H), 5.09 (d, *J* = 7.0 Hz, 1H), 4.72 (d, *J* = 13.3 Hz, 1H), 4.59 (dt, *J* = 2.6, 1.4 Hz, 1H), 4.37 (s, 6H), 4.20 (q, *J* = 2.2 Hz, 1H), 4.05 (dd, *J* = 4.3, 2.7 Hz, 1H), 3.56 – 3.43 (m, 2H), 3.17 – 3.11 (m, 1H), 3.09 (s, 3H). ¹³C NMR (101 MHz, Acetone) δ 169.90, 166.39, 136.62, 130.22, 126.57, 121.83, 119.21, 117.98, 111.58, 106.45, 87.72, 69.36, 69.02, 68.79, 68.52, 68.40, 68.38, 66.30, 52.58, 51.56, 48.71, 42.57, 31.75, 30.80, 22.44, 21.10. HRMS (ESI, C₂₅H₂₄ClFeN₂O₃: [M]⁺) calcd: 491.0819, found: 491.0813. Purity : 95.14%.

(1S, 3R)-2-(2-acryloyl)-1-ferrocenyl-2,3,4,9-tetrahydro-1H-pyrido[3,4-b]indole-3-carboxylic acid methyl ester (20)

Yellow solid in a yield 64.2%. ¹H NMR (400 MHz, Acetone-*d*₆) δ 10.03 (s, 1H), 7.51 (ddt, *J* = 7.8, 1.4, 0.8 Hz, 1H), 7.39 (d, *J* = 8.0 Hz, 1H), 7.09 (ddd, *J* = 8.2, 7.1, 1.3 Hz, 1H), 7.02 (ddd, *J* = 8.0, 7.1, 1.1 Hz, 1H), 6.78 (dd, *J* = 16.8, 10.5 Hz, 1H), 6.30 – 6.11 (m, 2H), 5.71 (d, *J* = 10.5 Hz, 1H), 4.59 (s, 1H), 4.53 (dd, *J* = 10.9, 4.3 Hz, 1H), 4.38 (s, 1H), 4.22 (s, 1H), 4.19 – 4.14 (m, 1H), 4.09 (s, 5H), 3.69 (d, *J* = 3.2 Hz, 3H), 3.31 – 3.19 (m, 1H), 3.06 – 2.97 (m, 1H). ¹³C NMR (101 MHz, Acetone-*d*₆) δ 169.91, 166.38, 136.78, 128.76, 127.93, 126.47, 121.70, 120.88, 119.24, 118.11, 111.35, 88.74, 68.85, 68.45, 68.30, 67.62, 66.99, 66.70, 54.07, 51.20, 22.19. HRMS (ESI, C₂₆H₂₅FeN₂O₃: [M]⁺) calcd: 469.1209, found: 469.1220. found 469.1220. Purity : 98.61%.

(1S, 3R)-2-(2-propioloyl)-1-ferrocenyl-2,3,4,9-tetrahydro-1H-pyrido[3,4-b]indole-3-carboxylic acid methyl ester (21)

Yellow solid in a yield 10.2%. ¹H NMR (400 MHz, Chloroform-*d*) δ 8.06 (s, 1H), 7.54 (d, *J* = 7.7 Hz, 1H), 7.41 (d, *J* = 8.1 Hz, 1H), 7.22 (s, 1H), 7.17 (t, *J* = 7.5 Hz, 1H), 6.67 (s, 1H), 4.61 (s, 1H), 4.38 – 4.25 (m, 5H), 4.24 – 4.15 (m, 2H), 4.04 (d, *J* = 5.1 Hz, 1H), 3.75 (s, 3H), 3.55 (s, 1H), 3.29 (s, 2H), 3.09 – 3.00 (m, 1H). ¹³C NMR (101 MHz, CDCl₃) δ 169.45, 152.33, 136.17, 131.74, 126.43, 122.72, 120.21, 118.66, 111.09, 109.45, 86.28, 79.78, 75.67, 69.48, 68.99, 68.10, 67.84, 67.49, 56.47, 53.52, 52.41,

22.55. HRMS (ESI, C₂₆H₂₃FeN₂O₃: [M]⁺) calcd: 467.1053, found: 467.1063. Purity : 98.42%.

Synthesis of ML210-Fc analogs

(phenyl)(ferrocenyl)methanone/(4-chlorophenyl)(ferrocenyl)methanone (Fc-1a/1b)

Ferrocene (5 g, 26.9 mmol, 1.1 eq.) was dissolved in dry dichloromethane. Aluminum trichloride (3.58 g, 26.9 mmol, 1.1eq.) was added in small portions. Then 4-chlorobenzoyl chloride or Benzoyl chloride (22.4 mmol, 1eq.) was added dropwise. The stirring was continued overnight and then the solution was carefully poured into water. The aqueous layer was extracted with dichloromethane and the combined organic layers were washed with water, dried over MgSO₄ and concentrated under reduced pressure. The crude mixture was separated on a silica gel column with petroleum ether/ethyl acetate (4.8 g, 71%). ¹H NMR (400 MHz, Acetone-*d*₆) δ 8.00 – 7.89 (m, 2H), 7.57–7.51 (m, 2H), 4.89–4.80 (m, 2H), 4.69–4.59 (m, 2H), 4.22 (s, 5H).

(phenyl)(ferrocenyl)methanol/(4-chlorophenyl)(ferrocenyl)methanol (Fc-2a/2b)

Compound **Fc-1a/1b** (0.416 mmol, 1 eq.) was dissolved in methanol/tetrahydrofuran 1:1 (4 mL) and cooled to 0 °C. Sodium borohydride (0.016 g, 0.426 mmol, 1 eq.) was added in one portion, and the mixture was stirred for 30 minutes. After TLC showed complete conversion, the mixture was neutralized with acetic acid and concentrated. Dichloromethane was added, and the solution was washed with water, dried on sodium sulfate and concentrated to afford yellow solid (97%), which was carried to the next step without further purification. ¹H NMR (400 MHz, Acetone-*d*₆) δ 7.40 (d, *J* = 7.6 Hz, 2H), 7.27 (t, *J* = 7.5 Hz, 2H), 7.18 (t, *J* = 7.3 Hz, 1H), 4.26 (s, 1H), 4.14 (s, 5H), 4.08 (t, *J* = 2.1 Hz, 1H), 4.05 (d, *J* = 2.0 Hz, 2H), 2.79 (s, 1H).

1-((phenyl)(ferrocenyl)methyl)piperazine/1-((4-chlorophenyl)(ferrocenyl)methyl)piperazine (Fc-3a/3b)

A mixture of Compound **Fc-2a/2b** (0.405 mmol 1 eq.), acetic anhydride (0.75 mL) and pyridine (0.83 mL) was stirred overnight at RT. Volatile parts were evaporated under reduced pressure. A rest was dissolved in CH₃CN (5 mL), piperazine (0.349 g, 4.048 mmol 10 eq) was added and mixture was refluxed overnight. Acetonitrile was evaporated. The mixture was dissolved in ethyl acetate and washed three times with water to remove the excess piperazine. The organic phase was dried over sodium sulfate, filtered, and concentrated. The crude mixture was purified by chromatography (DCM:MeOH:Et₃N = 20:1:0.5) to afford the pure compound as orange solid (29%). ¹H NMR (400 MHz, Chloroform-d) δ 7.51–7.46 (m, 2H), 7.39 (t, *J* = 7.5 Hz, 2H), 7.34–7.29 (m, 1H), 4.17–4.07 (m, 4H), 3.90 (s, 1H), 3.71 (s, 5H), 2.87 (d, *J* = 6.1 Hz, 4H), 2.35 (s, 4H).

(4-((phenyl)(ferrocenyl)methyl)piperazin-1-yl)(5-methyl-4-nitroisoxazol-3-yl)methanone (22)

A solution of 1-((4-chlorophenyl)(ferrocenyl)methyl)piperazine (61.48 mg, 0.156 mmol, 1 eq.) and triethylamine (28.2 μL, 0.202 mmol, 1.3 eq.) in dry DCM (5 mL) was cooled in an ice bath. 5-Methyl-4-nitroisoxazole-3-carbonyl chloride (9) (35.5 μL, 0.187 mmol, 1.2 eq.) was added dropwise and the reaction was stirred overnight at rt. The crude mixture was purified on silica gel with petroleum ether/ethyl acetate to afford the final product as yellow solid (37.6 mg, 44%). ¹H NMR (400 MHz, Acetone-*d*₆) δ 7.68 – 7.55 (m, 2H), 7.55 – 7.34 (m, 2H), 5.62 (s, 1H), 4.27 (dt, *J* = 2.6, 1.4 Hz, 1H), 4.18 (dd, *J* = 2.5, 1.4 Hz, 1H), 4.16 – 4.12 (m, 2H), 4.08 (dt, *J* = 2.7, 1.3 Hz, 1H), 3.79 (s, 5H), 3.72 – 3.53 (m, 2H), 3.27 (td, *J* = 5.9, 3.8 Hz, 2H), 2.37 (t, *J* = 5.2 Hz, 2H), 2.29 – 2.11 (m, 2H). ¹³C NMR (101 MHz, Acetone-*d*₆) δ 172.87, 156.36, 153.48, 141.87, 132.25, 130.47, 128.09, 88.66, 70.53, 69.46, 68.75, 67.21, 66.88, 51.62, 50.94, 46.58, 41.93, 14.21. HRMS (ESI, C₂₆H₂₅ClFeN₄O₄: [M]⁺) calcd: 548.0914, found: 548.0912. Purity: 97.03%.

2-chloro-1-(4-((4-chlorophenyl)(phenyl)methyl)piperazin-1-yl)ethan-1-one (23)

As described previously, compound **23** was obtained as yellow solid (24.1 mg, 39%). ¹H NMR (400 MHz, Acetone-*d*₆) δ 7.57 (d, *J* = 7.6 Hz, 2H), 7.43 (t, *J* = 7.5 Hz, 2H), 7.33 (t, *J* = 7.3 Hz, 1H), 4.26 (d, *J* = 2.4 Hz, 1H), 4.19 (s, 2H), 4.17 (d, *J* = 3.1 Hz, 1H), 4.14 (p, *J* = 2.5, 2.0 Hz, 2H), 4.07 (s, 1H), 3.76 (s, 5H), 3.42 (d, *J* = 5.8 Hz, 4H), 2.37 – 2.19 (m, 4H). ¹³C NMR (400 MHz, Acetone-*d*₆) δ 165.20, 144.16, 129.88, 129.13, 129.08, 128.21, 127.52, 90.60, 71.61, 69.75, 69.58, 68.45, 67.65, 53.28, 52.56, 46.59, 42.85. HRMS (ESI, C₂₃H₂₆FeN₂O: [M]⁺) calcd: 437.1078, found: 437.1066. Purity: 96.68%.

2-chloro-1-(4-((4-chlorophenyl)(ferrocenyl)methyl)piperazin-1-yl)ethan-1-one (24)

As described previously, compound **24** was obtained as yellow solid (46 mg, 68%). ¹H NMR (400 MHz, Acetone-*d*₆) δ 7.61 (d, *J* = 8.4 Hz, 2H), 7.49 – 7.44 (m, 2H), 4.27 (dt, *J* = 2.6, 1.4 Hz, 1H), 4.19 (s, 3H), 4.16 (dq, *J* = 2.5, 1.2 Hz, 1H), 4.13 (s, 1H), 4.11 – 4.06 (m, 1H), 3.80 (s, 5H), 3.43 (t, *J* = 5.9 Hz, 4H), 2.34 – 2.19 (m, 4H). ¹³C NMR (400 MHz, Acetone-*d*₆) δ 164.37, 141.85, 132.22, 130.52, 128.09, 88.76, 70.51, 69.58, 68.76, 68.69, 67.28, 66.88, 51.71, 51.17, 46.03, 41.96, 41.25. HRMS (ESI, C₂₃H₂₅ClFeN₂O: [M]⁺) calcd: 470.0610, found: 470.0617. Purity: 96.92%.

1-(4-((4-chlorophenyl)(ferrocenyl)methyl)piperazin-1-yl)prop-2-en-1-one (25)

As described previously, compound **25** was obtained as yellow solid (35.65 mg, 51%). ¹H NMR (400 MHz, Acetone-*d*₆) δ 7.64 – 7.58 (m, 2H), 7.49 – 7.43 (m, 2H), 6.68 (dd, *J* = 16.7, 10.5 Hz, 1H), 6.12 (dd, *J* = 16.7, 2.5 Hz, 1H), 5.59 (dd, *J* = 10.5, 2.5 Hz, 1H), 4.27 (dt, *J* = 2.7, 1.4 Hz, 1H), 4.22 – 4.14 (m, 2H), 4.14 – 4.07 (m, 2H), 3.80 (s, 5H), 3.48 (s, 4H), 2.32 – 2.18 (m, 4H). ¹³C NMR (400 MHz, Acetone-*d*₆) δ 164.14, 141.82, 132.22, 130.52, 128.07, 126.51, 88.82, 70.65, 69.66, 68.86, 67.38, 66.95, 52.09, 51.39, 45.48, 41.74, 29.77, 29.57. HRMS (ESI, C₂₄H₂₆ClFeN₂O: [M]⁺) calcd: 448.1010, found: 448.1007. Purity: 95.61%.

1-(4-((phenyl)(ferrocenyl)methyl)piperazin-1-yl)prop-2-yn-1-one (26)

Propiolic acid (79 mg, 1.12 mmol, 1.2 eq.) was dissolved in dry DCM (5 mL). HBTU (450 mg, 1.40 mmol, 1.5 eq.), DIPEA (244 μ L, 1.40 mmol, 1.5 eq.), and compound **Fc-3a/3b** (300 mg, 0.93 mmol, 1 eq.) were added and the reaction was stirred at rt for 2 h. The reaction was washed with water and the organic layer was collected and concentrated under reduced pressure. The crude mixture was purified on silica gel with petroleum ether/ethyl acetate to afford the final product as yellow solid (141 mg, 41%). ^1H NMR (400 MHz, Acetone- d_6) δ 7.57 (d, J = 7.5 Hz, 2H), 7.43 (t, J = 7.6 Hz, 2H), 7.32 (dd, J = 13.8, 6.5 Hz, 1H), 4.30 – 4.25 (m, 1H), 4.17 (s, 1H), 4.13 (dt, J = 4.3, 1.9 Hz, 2H), 4.10 (s, 1H), 3.83 (s, 1H), 3.76 (s, 4H), 3.73 – 3.59 (m, 2H), 3.44 (dd, J = 6.2, 4.1 Hz, 2H), 2.73 (s, 1H), 2.37 – 2.27 (m, 2H), 2.25 (ddd, J = 8.2, 5.8, 3.6 Hz, 2H). ^{13}C NMR (400 MHz, Acetone- d_6) δ 151.77, 143.64, 129.57, 128.78, 128.59, 127.95, 90.13, 80.42, 76.32, 71.28, 71.13, 69.45, 69.28, 68.17, 67.41, 52.61, 51.80, 47.56, 41.98. HRMS (ESI, $\text{C}_{24}\text{H}_{24}\text{FeN}_2\text{O}$: $[\text{M}]^+$) calcd: 412.1233, found: 412.1237. Purity: 95.93%.

1-(4-((4-chlorophenyl)(ferrocenyl)methyl)piperazin-1-yl)prop-2-yn-1-one (27)

As described previously, compound **27** was obtained as yellow solid (134.15 mg, 35%). ^1H NMR (400 MHz, Acetone- d_6) δ 7.61 (d, J = 8.3 Hz, 2H), 7.46 (d, J = 8.1 Hz, 2H), 4.28 (s, 1H), 4.24 – 4.12 (m, 3H), 4.09 (s, 1H), 3.86 (s, 1H), 3.80 (s, 4H), 3.71 – 3.56 (m, 2H), 3.44 (t, J = 5.1 Hz, 2H), 2.73 (s, 1H), 2.30 (dt, J = 9.8, 5.2 Hz, 2H), 2.24 (q, J = 5.1 Hz, 2H). ^{13}C NMR (101 MHz, Acetone- d_6) δ 151.97, 142.62, 133.15, 131.42, 129.01, 89.50, 80.79, 76.43, 71.44, 70.39, 69.67, 68.19, 67.83, 52.65, 51.85, 47.68, 42.11, 38.84. HRMS (ESI, $\text{C}_{24}\text{H}_{24}\text{ClFeN}_2\text{O}$: $[\text{M}]^+$) calcd: 447.0921, found: 447.0933. Purity: 96.08%.

X-ray crystal structure determinations for 12, 15 and 17. A single crystal of each compound was selected, mounted onto a cryoloop and transferred into a cold nitrogen gas stream. Intensity data were collected with a Bruker Kappa-APEXII diffractometer using graphite-monochromated Mo- $\text{K}\alpha$ radiation (λ = 0.71073 Å). Data collection was performed with the Bruker APEXII suite. Unit-cell parameters determination, integration and data reduction were carried out with SAINT program. SADABS was

used for scaling and absorption corrections. The structures were solved with SHELXT-2014 and refined by full-matrix least-squares methods with SHELXL-2014 using the WinGX suite¹ or Olex2 software package². All non-hydrogen atoms were refined anisotropically. The structures were deposited at the Cambridge Crystallographic Data Centre with numbers CCDC 2310688-2310690 and can be obtained free of charge via www.ccdc.cam.ac.uk.

Molecular Docking

The structure of GPX4 complex with ML162 was obtained from RCSB PDB database (PDBID 6HKQ). The residue SEC46 was mutated to CYS by swappaa command within UCSF Chimera³. Covalent bond between CYS46 and ML162 was remodeled by Chimera structure editing plugin. Then the structure was prepared by DockPrep flow, including keeping conformation with the highest occupancy, adding hydrogens with unspecified method. Further optimization of hydrogen bond network was performed a modified optimize tool in Openbabel using MMFF94s force field (<https://github.com/biocheming/openbabel>). Receptor structure was extracted by selecting protein contents. The structures of ferrocene derivatives was built with Avogadro⁴. The initial conformation was relaxed with UFF force field, then minimized by xtb program with gfn2 parameter of GFN-xTB⁵. All the structures of receptor and ligands were converted to pdbqt format by rdkit2pdbqt.py script (<https://github.com/biocheming/watvina/blob/main/pywatvina/watvina/rdkit2pdbqt.py>), which was originally extracted from Open Drug Discovery Toolkit(ODDT) and further optimized by our group, in terms of ROOT definition and atomic typing.

The pocket of GPX4 is rather shallow and we tried the template based docking by watvina (<https://github.com/biocheming/watvina/>). According the atomic type and contribution to interaction, we generate a template containing heavy atoms, aromatic atoms and hydrogen bond receptors (using --score_only --genph4 mode in watvina). Using genetic algorithm for global searching and BFGS for local refinement in watvina, the conformation with highest template score of docked ferrocene derivatives were

aligned to the template. The covalent bonds between ligands and protein was manually modeled with Chimera. Finally, the pocket with ligand was minimized by xtb program using GFNFF forcefield⁶. The representation was made by VMD software⁷.

In Vitro and In Vivo Biological Evaluation

ROS monitoring by fluorescence spectroscopy. 2',7'-Dichlorofluorescein diacetate (DCFH-DA; 4.9 mg) was dissolved in DMF (100 μ L) and added with aqueous NaOH (0.1 M, 900 μ L). The resulting mixture was incubated for 30 min at 22 °C in the dark to obtain a stock solution of DCFH (10 mM). This solution was diluted by containing 3-(N-morpholino) propanesulfonic acid buffer (MOPS, 100 mM, pH 7.4), N,N,N',N'-ethylenediaminetetraacetic acid (EDTA, 10 mM), glutathione (GSH, 5 mM), and H₂O₂ (10 mM) to acquire the final solution of DCFH (10 μ M). Monitoring of the fluorescence ($\lambda_{\text{ex}} = 501$ nm, $\lambda_{\text{em}} = 529$ nm, Bandwidth (nm) = 0.4, Source Light Path: Xenon Lamp, Detector Light Path: Visible PMT-980) of this solution was started. After the intensity is stable, compounds (10 μ L, final concentration 0.1 mM) were added and the fluorescence monitoring was continued for the 225 mins. Meanwhile, monitoring generation of reactive oxygen species in the presence of control compounds in cell free settings.

Cell Culture. Human renal cell carcinoma OS-RC-2, human fibrosarcoma cells HT1080, human normal liver cells L02, mouse breast cancer cells 4T1, MCF-10A were obtained from the Shanghai Institute of Biochemistry and Cell Biology, CAS (Shanghai, China). OS-RC-2, 4T1 and L02 cells were cultured in RPMI1640 (KGM31800-500, KeyGen, China) supplemented with 10% fetal bovine serum (FBS) (Gibco), HT1080, MCF-10A cells were cultured in DMEM (KGM12800-500, KeyGen, CHN) supplemented with 10% fetal bovine serum (FBS) (Duanli, CHN). All the cells were cultured in a humid atmosphere of 5% CO₂.

Determination of Antiproliferative Activity. The antiproliferative activity of all compounds was evaluated against the OS-RC-2, HT1080, 4T1, MCF-10A, and L02 cell lines by using an MTT assay in vitro. Stock solutions (50 mM) of the compounds to be

tested were prepared in DMSO and were kept at -20 °C in the dark. The cells were seeded in 96-well plates at a density of 3000–5000 cells/well and cultured at 37 °C. After 24 h, different concentrations of the tested compounds were added into the corresponding wells, RSL3 or ML162 was taken as the positive group compound, and the cells were cultured at 37 °C for another 72 h. When the cell viability was determined by the MTT assay, MTT (5 mg/mL, 10% of the volume of the culture medium) was added and incubated for 4 h. After the suspension was removed, DMSO (100 µL) was added to dissolve the formazan. The absorption value was determined by a microplate reader; the detection wavelength was 570 nm, and the reference wavelength was 630 nm. The GraphPad Prism 6 was used for nonlinear regression analysis to calculate the IC₅₀ value. All experiments were repeated at least three separate times.

Cellular Uptake Measurement. HT1080 cells (2.0×10^5 cells) were seeded in a 6-well culture plate and grown in DMEM medium in 5% CO₂ at 37 °C for 24 h. After washing with PBS three times, the cells were incubated with 2 µM of ML162 or **17** in PBS for 0.5 h or 1 h at 37 °C. Cells incubated with PBS only were used as a negative control. The incubation is stopped by washing the cells with PBS twice. All cells were detached from the plates by exposing them to trypsin–EDTA solution (C0201, Beyotime, China) for 3 min. Detached cells were collected into a new tube and washed with 1 mL PBS three times to remove any compounds attached to the cell surface. After being resuspended with PBS (100 µL), 10 µL of the cell suspension was taken to determine the protein concentration with the enhanced BCA protein assay kit (P0010, Beyotime, China). After centrifugation at 12,000 rpm at 4 °C for 15 min, the remaining cells were extracted with methanol (300 µL), frozen with liquid nitrogen and immediately thawed at 25 °C three times, and lysed by ultrasonic cell crusher (Scientz-IID, Xinzhi, China) (150 W, 3 min). The cell lysate was centrifuged at 12,000 rpm for 20 min at 4 °C, and the supernatant was harvested and stored at -80 °C. The concentrations of ML162 or **17** in these were measured using the LC–MS/MS method.

LC-MS/MS instrument (Thermo Fisher Scientific, Waltham, MA, USA) consisted of a DIODEX UltiMate 3000 UHPLC system and TSQ Quantiva triple quadrupole mass spectrometer with Xcalibur 2.2 software for data acquisition and analysis. ML162 or **17** and internal standard (IS, L2) were chromatographed by injection of a 5 μ L sample into an Eclipse Plus C18 column (3.5 μ m, 2.1 \times 50 mm, Agilent, Santa Clara, CA, USA) at 35 $^{\circ}$ C. A gradient elution was performed with the mobile phase consisted of solvent A (0.1% formic acid in water) and solvent B (0.1% formic acid in acetonitrile) at a flow rate of 0.2 mL/min. A H-ESI source was used in the positive ion mode. The optimized ion spray voltage, ion transfer tube temperature and vaporizer temperature were set at 3500 V, 325 $^{\circ}$ C and 275 $^{\circ}$ C, respectively. The sheath gas and aux gas were nitrogen delivered at 35 arb and 10 arb, respectively. The collision gas (argon) pressure was 2.0 mTorr. Quantification was performed using the selective reaction monitoring (SRM) transition m/z 477.1 \rightarrow 120.1 (collision energy: 23.0 V) for ML162, m/z 554.1 \rightarrow 433.0 (collision energy: 20.3 V) for **17**, and m/z 578.0 \rightarrow 457.0 (collision energy: 20.1 V) for IS. The concentrations in the samples were normalized by the total protein concentration. Relative cellular uptake amount of the compounds was presented as cellular amount of substance /the initial amount of substance*100%.

Cell Death Manner Assay. Z-VAD-FMK (Selleck), Necrostatin-1 (Selleck), Wortmannin (Selleck), deferoxamine (TargetMol), ferrostatin-1 (TargetMol), L-Glutathione (Selleck), and N-acetyl-L-cysteine (Selleck) were purchased. OS-RC-2 cells were seeded in 96-well plates at a density of 5000 cells/well and cultured at 37 $^{\circ}$ C. After 24 h, different concentrations of ML162 or **17** were added. Following that, Z-AD-FMK (10 μ M), Necrostatin-1 (10 μ M), Wortmannin (30 mM), deferoxamine (30 μ M), and ferrostatin-1 (2 μ M) were added and incubated with ML162 or **17**. After 72 h, MTT (5 mg/mL, 10% of the volume of the culture medium) was added and incubated at 37 $^{\circ}$ C for 4 h. Then the supernatant was moved, and DMSO (100 μ L) was added to dissolve the formazan. Absorbance was measured at 570 nm using the microplate reader. All experiments were repeated at least three separate times.

Intracellular GPX4 Activity Detection. OS-RC-2 cells were incubated in six-well plates at a density of 5×10^5 for 24 h. Afterward, cells were exposed to different chemical compounds (1.0 μM) for 4 h. Then, cells were washed with phosphate-buffered saline (PBS) and add 130 μL IP lysis solution at 0 $^\circ\text{C}$ for 50 minutes, collected into 1.5 mL EP, cells were centrifuged at 12,000 rpm at 4 $^\circ\text{C}$ for 20 min. The supernatant was used to detect GPX4 activity. The GPX4 activity was accessed according to the product protocol of the GPX4 activity assay kit (Beyotime Biotechnology, China).

MDA Assay. OS-RC-2 cells were seeded into a culture dish with a diameter of 10 cm at a density of 3×10^6 cells/dish for 24 h. The medium containing ML162 (1 μM), **17** (0.5, 1, 2 μM) were added and incubated for 4 h. Then, cells were washed with phosphate-buffered saline (PBS) and add IP lysis solution at 0 $^\circ\text{C}$ for 50 minutes, collected into 1.5 mL EP, cells were centrifuged at 12,000 rpm at 4 $^\circ\text{C}$ for 20 min, the supernatant was taken, and the MDA content was determined according to the instructions of the Lipid Peroxidation MDA Assay Kit (S0131M, Beyotime Biotechnology, China).

Intracellular ROS Measurement. DCFH-DA dye was applied to measure the level of ROS by FCM and CLSM. In detail, cells were incubated in 6-well plates (3×10^5 /well) for 24 h. Then, the culture medium was replaced with a fresh medium containing ML162 and **17** (0.5 μM) with and without fer-1 (1.5 μM). After incubation for 4 h, the medium was removed, and the cells were washed with PBS, then DCFH-DA (S0033S, Beyotime, China) diluted with serum-free medium with a final concentration of 10 $\mu\text{mol/L}$ was added and stained for 0.5 h away from light. Finally, cells were harvested and analyzed by FCM (Miltenyi, MACSQuant Analyzer 16). For CLSM imaging, the exponentially growing OS-RC-2 cells were seeded into confocal laser culture dishes at a density of 1×10^4 per dish for 24 h. Same processing method as FCM, and then the cells were collected and observed by CLSM (Carl Zeiss, Germany).

Intracellular LPO Measurement. C11-BODIPY581/591 dye was applied to measure the level of LPO by FCM and CLSM. In detail, cells were incubated in 6-well plates (3×10^5 /well) for 24 h. Then, the culture medium was replaced with a fresh medium containing ML162 and **17** (0.5 μ M) with and without fer-1 (1.5 μ M). After incubation for 4 h, the medium was removed, and the cells were washed with PBS, then C11 BODIPY581/591 (RM02821, ABclonal) diluted with serum-free medium with a final concentration of 1 μ mol/L was added and stained for 0.5 h away from light. Finally, cells were harvested and analyzed by FCM. For CLSM imaging, The exponentially growing OS-RC-2 cells were seeded into confocal laser culture dishes at a density of 1×10^4 per dish for 24 h. Same processing method as FCM, and then the cells were collected and observed by CLSM.

Fe²⁺ Intensity Assay. Exponentially growing OS-RC-2 cells were seeded into confocal laser culture dishes (1×10^4 /cells/dishes) for 24 h. Then, the medium containing ML162 and **17** (0.5 μ M) was added and incubated for 4 h. The medium was discarded and washed with cold PBS buffer. Then, FerroOrange (F374, DOJINDO, Japan), a ferric ion probe diluted in serum-free medium to a final concentration of 1 μ mol/L, was incubated at 37 °C for 0.5 h away from light. Imaging observations were then made directly under CLSM (Carl Zeiss, Germany).

Western Blotting. OS-RC-2 cells were seeded in 6-well plates (5×10^5 /well) for 24 h and treated with **17** (0.01, 0.1, 0.5, 1, 2 μ M) for 3 h or **17** (0.001, 0.005, 0.01, 0.05, 0.1 μ M) for 24 h, respectively. After the cells of different groups were digested by trypsin (T1300, Solarbio) and collected, the lysis solution containing 1% PMSF was added, and then the cells were lysed on ice for 1 h and subsequently centrifuged at 4 °C at 12,000 rpm for 20 min to collect the supernatant (the total cell protein). The protein concentration was determined according to the Enhanced BCA Protein Assay Kit (P0010, Beyotime, China). Then, SDS-PAGE Sample Loading Buffer (P0015, Beyotime, China) was added and heated in a 100 °C water bath for 15 min for protein denaturation. Protein samples were taken from each group, separated by 10 or 12%

SDS-PAGE gels (FD341, FD346, FdbioScience, China), and transferred to a PVDF membrane. The PVDF membrane was blocked with 5% skim milk at room temperature for 2 h, washed with TBST, incubated with the primary antibody at 4 °C for 12–15 h, washed with TBST, and then incubated with the secondary antibody at room temperature for 2 h. Ultimately, Membranes were imaged with Imaging Systems. The relative protein level was normalized to β -tubulin. Western Blotting Substrate (Thermo Fisher Scientific Inc.) and densitometry analysis was performed using ImageJ software (Image-Pro Plus 6.0; National Institutes of Health).

CETSA Assay. OS-RC-2 cells were seeded in 6-well plates (5×10^5 /well) for 24 h. Fresh medium containing 0.1% DMSO, ML162 or **17** ($5 \mu\text{M}$) was added and co-incubated for 4 h. The medium was moved, the cells were digested with trypsin–EDTA solution (C0201, Beyotime, China), and cells were collected. After being resuspended with PBS (1 mL) containing 1% PMSF, the cell suspension was divided into 10 equal parts of 100 μL each. The 10 parts were heated at 30, 34, 37, 40, 45.2, 48.8, 54, 57, 60 °C for 3 min and cooled at room temperature for 3 min. The cells were further broken by freezing with liquid nitrogen and thawing three times at 25 °C immediately. Vortices were needed for each time of freezing and thawing. The cell lysate was centrifuged at 12,000 rpm for 20 min at 4 °C, and the supernatant was harvested. The GPX4 protein content was determined by Western blotting.

Wound-healing assay. A P10 pipette tip was used to scrape the cells in 96-well plates to produce wounds. Medium containing only 1% FBS was used to culture the cells to exclude the effect of cell proliferation. After the cells were treated with **15** and **17** ($0.5 \mu\text{M}$), the wound area was photographed at 0 h, 12 h, and 24 h. An inverted microscope (Olympus BX51, Japan) was used to take the image and representative boundaries of the wound were drawn with lines.

Transwell assay. Transwell chambers and polycarbonate membranes coated with Matrigel (R&D, USA) were used to perform the Transwell assay. The cells treated with different concentrations of **17** (0, 0.5, 2 μM) were seeded in the upper chamber with

200 μ l of medium with 5% FBS, and 500 μ l of medium with 20% FBS was added into the lower chamber as a chemoattractant. After incubation of the cells in an incubator at 37 °C for 12 h and fixation with 4% paraformaldehyde, 0.1% crystal violet was used to stain the cells on the lower side of the Transwell chamber. An inverted microscope (Olympus BX51, Japan) was used to take the image and record the cell number. Invasion rate (%) = (the number of invading cells in compound **17** group /the number of invading cells in DMSO group) \times 100%.

Antitumor Effect Evaluation *In Vivo*. The OS-RC-2 tumor model was constructed to evaluate the antitumor activity of **17**. Briefly, male BALB/c-nude mice (Beijing Vital River Laboratory Animal Technology Co., Ltd., Beijing, China), 4 weeks of age and 14-16 g of weight, were used. Cells xenograft tumor model was performed, and 2×10^6 OS-RC-2 cells were seeded into subcutaneous fat of the right limb of the mice. Animals were examined every 3 days to assess general health conditions and evaluate tumor growth by measuring tumor size. Tumor volume was calculated using the following formula: $V = (\text{width}^2 \times \text{height})/2$.

When the tumor volume reached 40 mm³, the mice were intraperitoneal injected with vehicle (10% DMSO, 40% PEG-300, 5% Tween-80, 45% saline), ML162 (20 mg/kg), **17** (10, 20 mg/kg) once every three days. When the tumor volume of control group reached about 1000 mm³, the tumors tissues and major organs were excised and weighted. The inhibition rate of tumor growth calculated as follows: inhibition rate (%) = (weight of control group tumor- weight of ML162/**17** group tumor)/weight of control group tumor \times 100%. The organs including the heart, liver, spleen, lung, and kidney were harvested and fixed with 4% paraformaldehyde, which were embedded in paraffin and sectioned. Different tissues that include heart, liver, spleen, lung, kidney and tumor were histologically examined by the hematoxylin and eosin (H&E) staining.

Immunohistochemical analysis. After fixing with 4% paraformaldehyde and paraffin embedding, the tumor tissues were sectioned. Thereafter, routine dewaxing and rehydration procedures were performed. For antigen retrieval, the slides were heated in

citrate buffer (pH 6.0) at 98 °C for 30 min and allowed to cool naturally. After endogenous peroxidase inactivation and nonspecific antigen blocking, the sections were incubated with primary antibodies, GPX4 (1:50, zenbio, 381958), overnight at 4°C. The negative control sections were incubated with phosphate-buffered saline (PBS) instead of a primary antibody. The slides were rinsed with PBS and incubated with horseradish peroxidase (HRP)-labeled secondary antibody for 30 min at 25 °C. The slides were then developed with DAB color developing solution for 1 min after washing with PBS. After counterstaining with hematoxylin for 3 min, the sections were dehydrated and mounted. Images were acquired using a microscope (Nikon DS-U3, Japan), the tan area indicates positive expression.

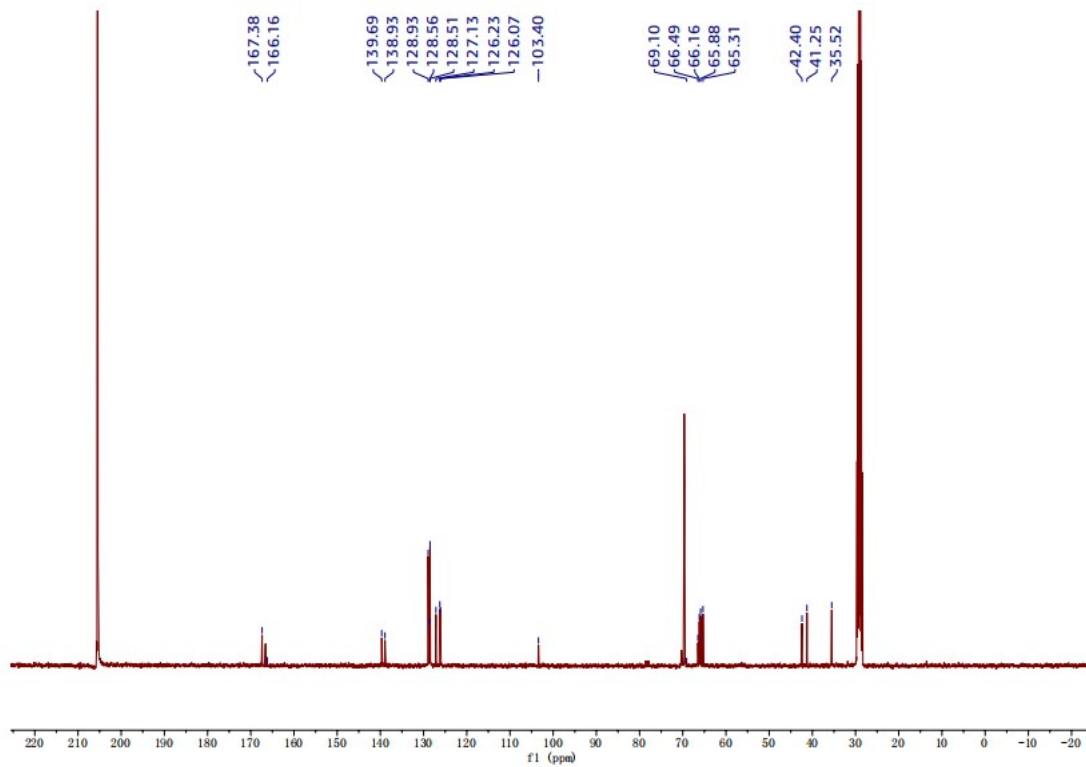
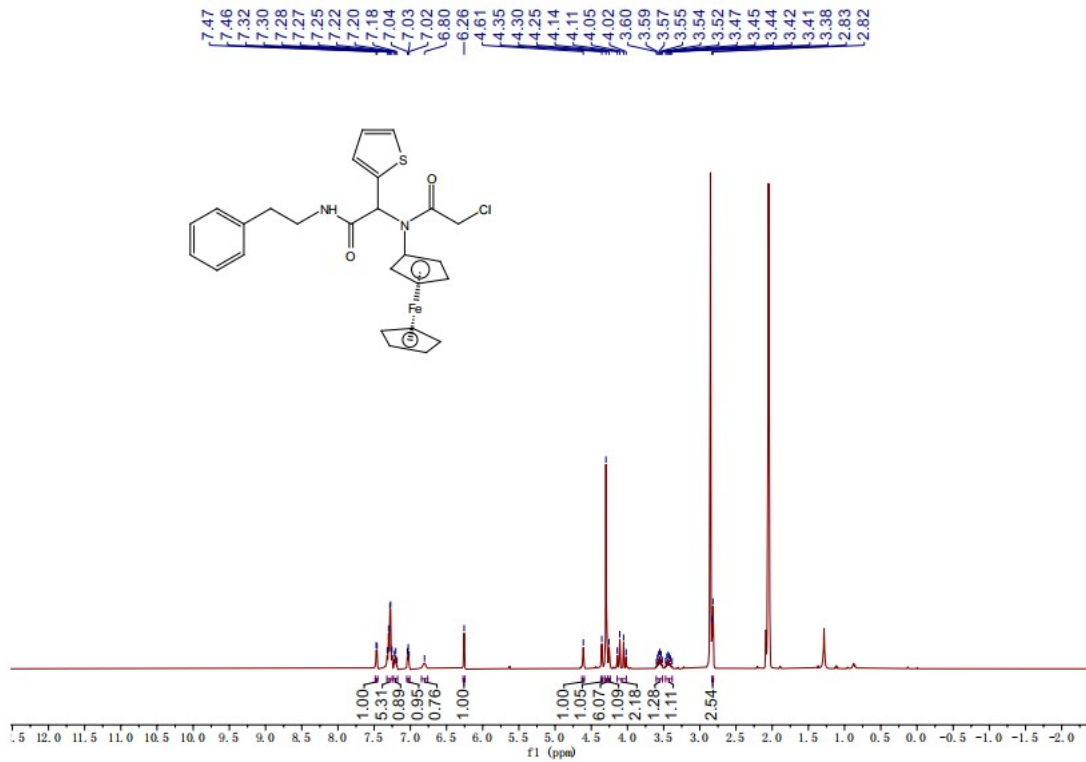
GO and KEGG functional annotation. For the annotation and visualization of differentially expressed genes related to tumorigenesis and development, the Metascape database (www.metascape.org) was utilized. Gene Ontology (GO) analysis and Kyoto Encyclopedia of Gene Genomes (KEGG) pathway analysis were performed to uncover the biological functions and signaling pathways involved. Statistical significance was determined with criteria of minimum overlap ≥ 3 and p-value ≤ 0.01 .

GSVA (Gene Set Variance Analysis). Gene Set Variation Analysis (GSVA) is a non-parametric and unsupervised method employed to evaluate gene set enrichment in transcriptomes. GSVA facilitates the transformation of gene-level changes into pathway-level changes by comprehensively scoring gene sets of interest, thereby discerning the biological functions of the samples. In this study, we will retrieve gene collections from the Molecular Signatures Database and employ the GSVA algorithm to comprehensively score each gene collection, aiming to assess potential changes in the biological functions of distinct samples.

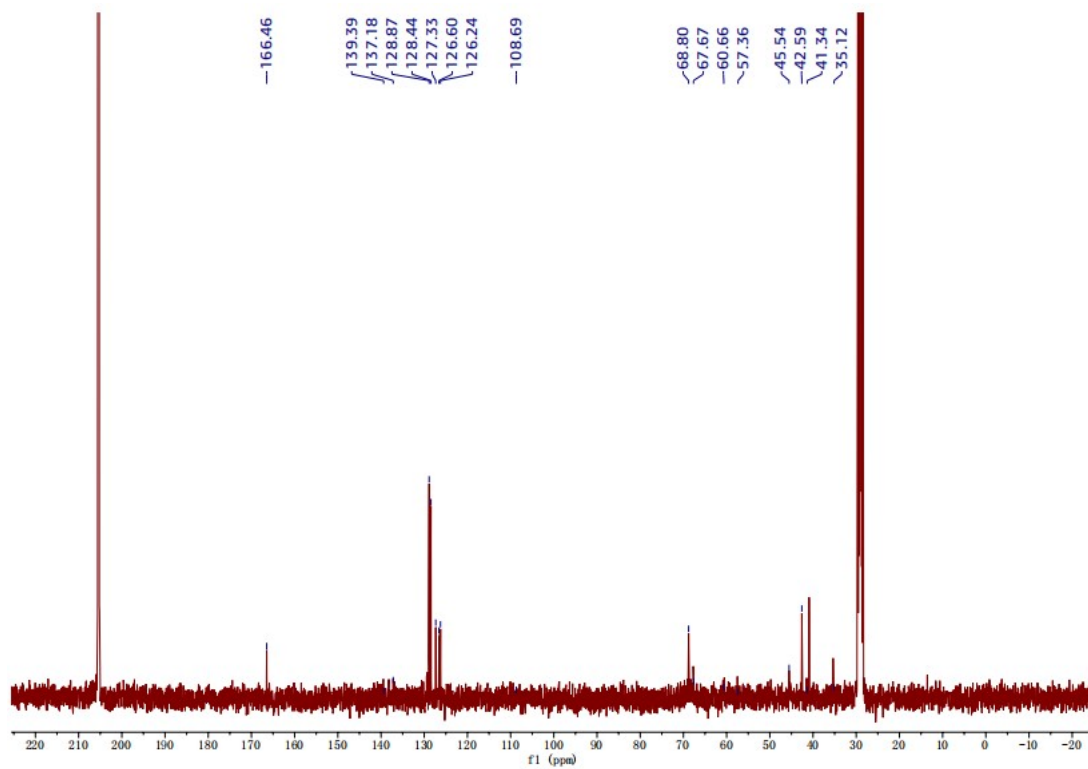
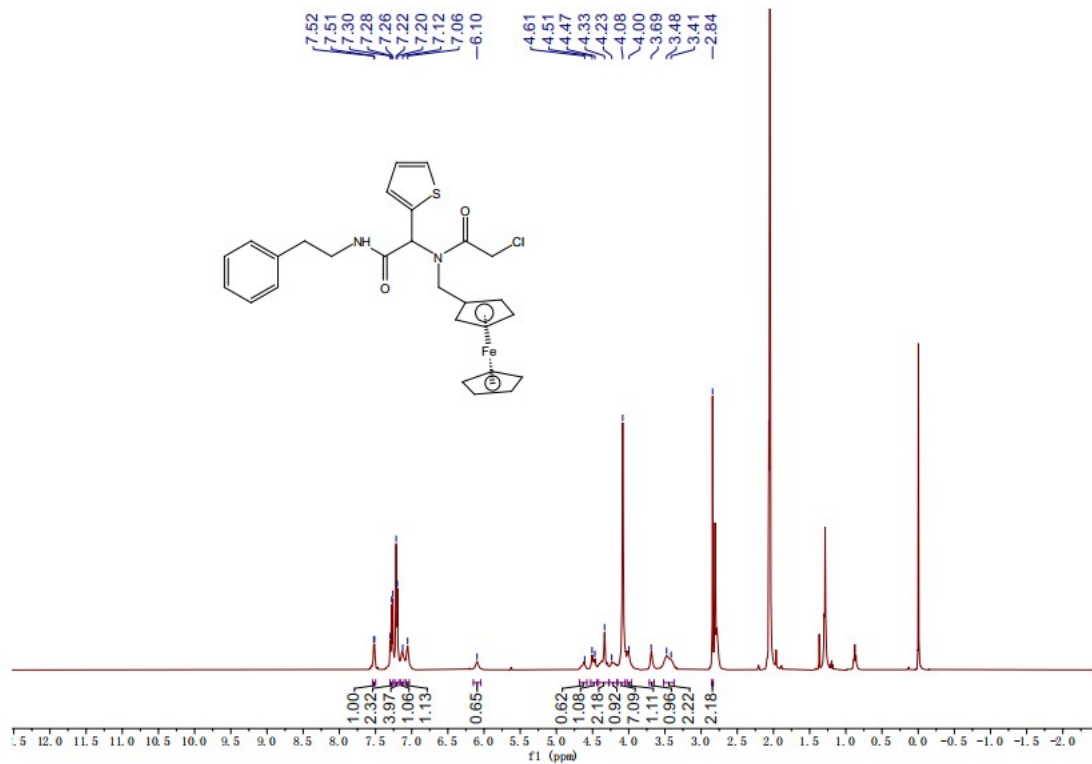
Statistical Analysis. Data were presented as mean \pm SD (represented by error bars) for all *in vitro* experiments. All the experiments had three replicates (n = 3). *In vivo* antitumor Student's t-test was used for comparing the two groups, and significant differences were indicated using *P < 0.05, **P < 0.01, ***P < 0.001 and ****P < 0.0001. Statistical analysis was performed with GraphPad Prism 8.0.1.

References

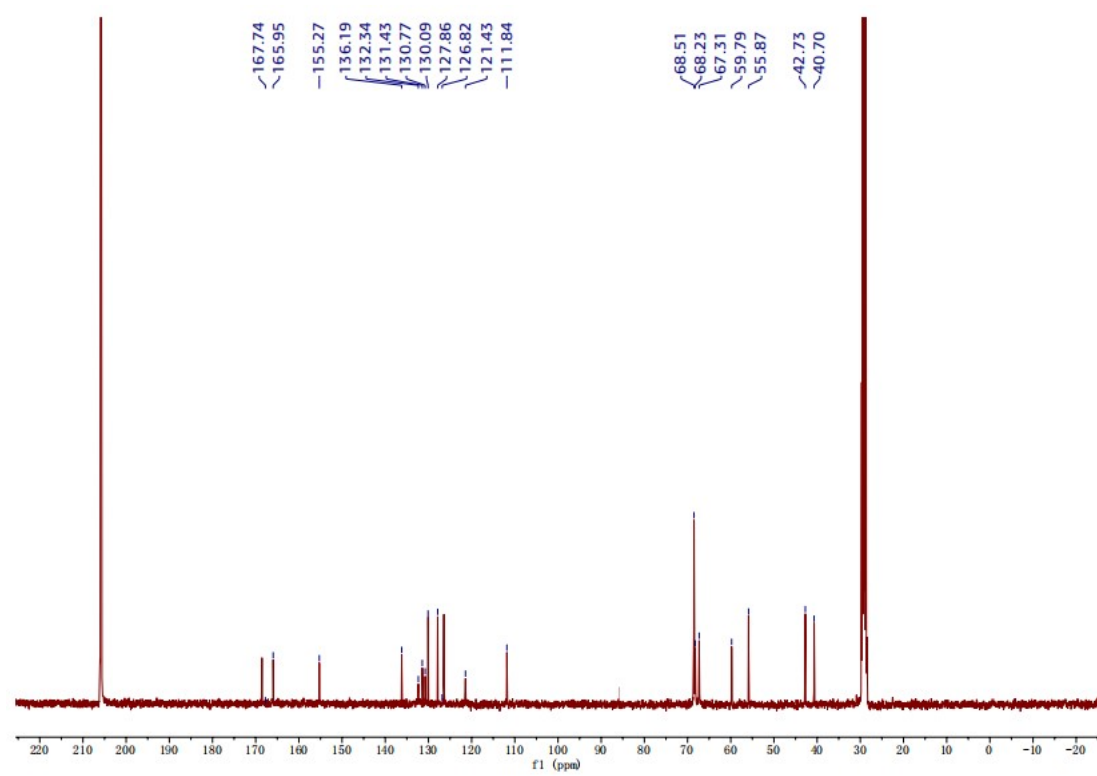
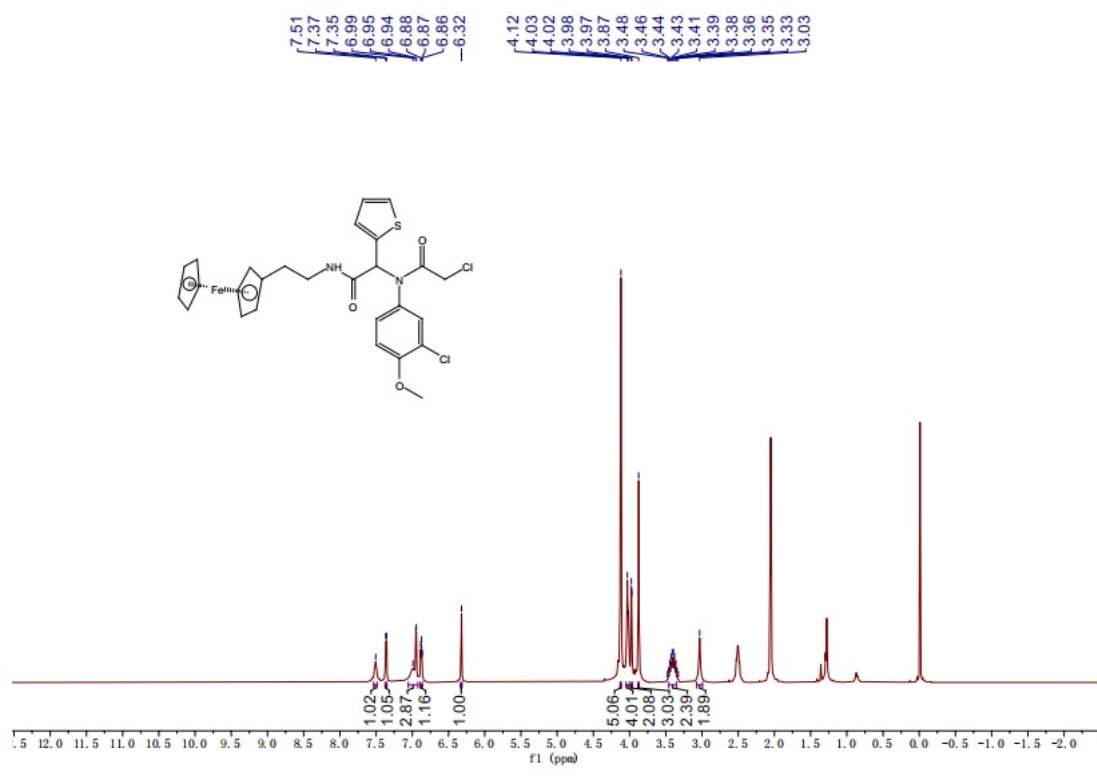
- (1) Blessing R. H., *Acta Cryst. A* **1995**, *51*, 33.
- (2) Betteridge P. W., Carruthers J. R., Cooper R. I., Prout K., Watkin D. J., *J. Appl. Crystallogr.* **2003**, *36*, 1487.
- (3) Pettersen E. F., Goddard T. D., Huang C. C., Couch G. S., Greenblatt D. M., Meng E. C., Ferrin T. E., *J Comput Chem.* **2004**, *25*, 1605-1612.
- (4) Avogadro: an open-source molecular builder and visualization tool. Version 1.XX.
<http://avogadro.cc/>
- (5) Bannwarth C., Ehlert S., Grimme, S., *J. Chem. Theory Comput.* **2019**, *15*, 1652–1671.
- (6) Spicher S., Grimme S., *Angew. Chem. Int. Ed.* **2020**, *59*, 15665-15673.
- (7) Humphrey W., Dalke A., Schulten K., *J. Molec., Graphics* **1996**, *14*, 33-38.



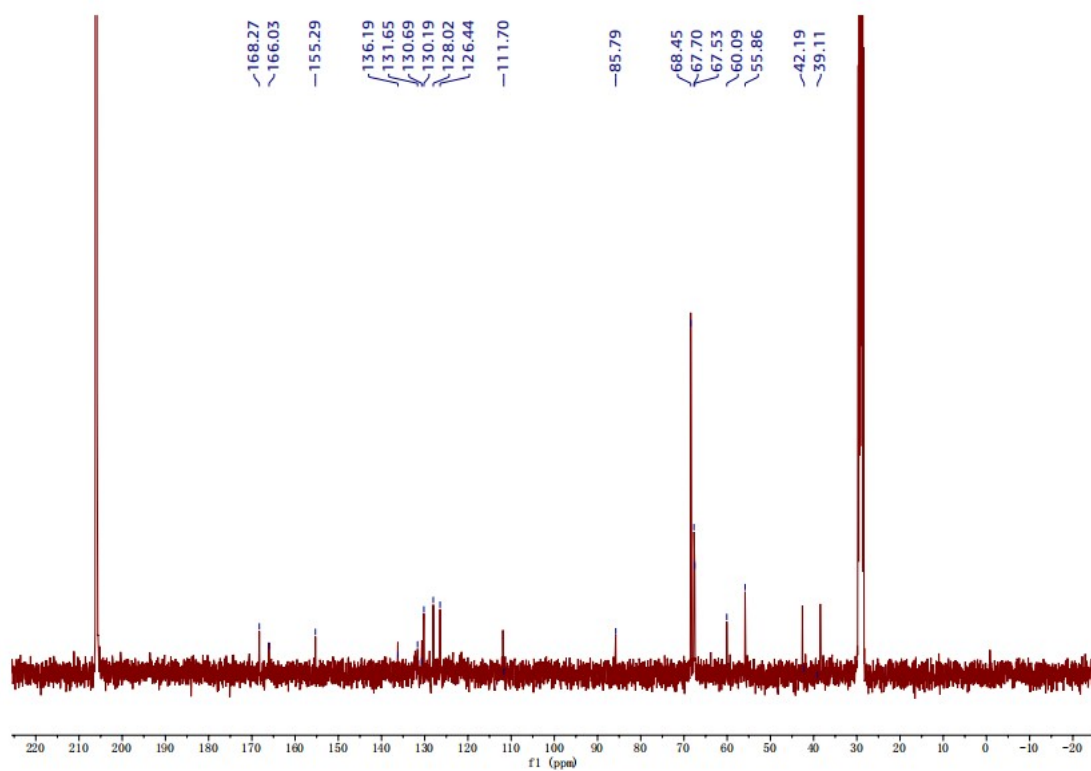
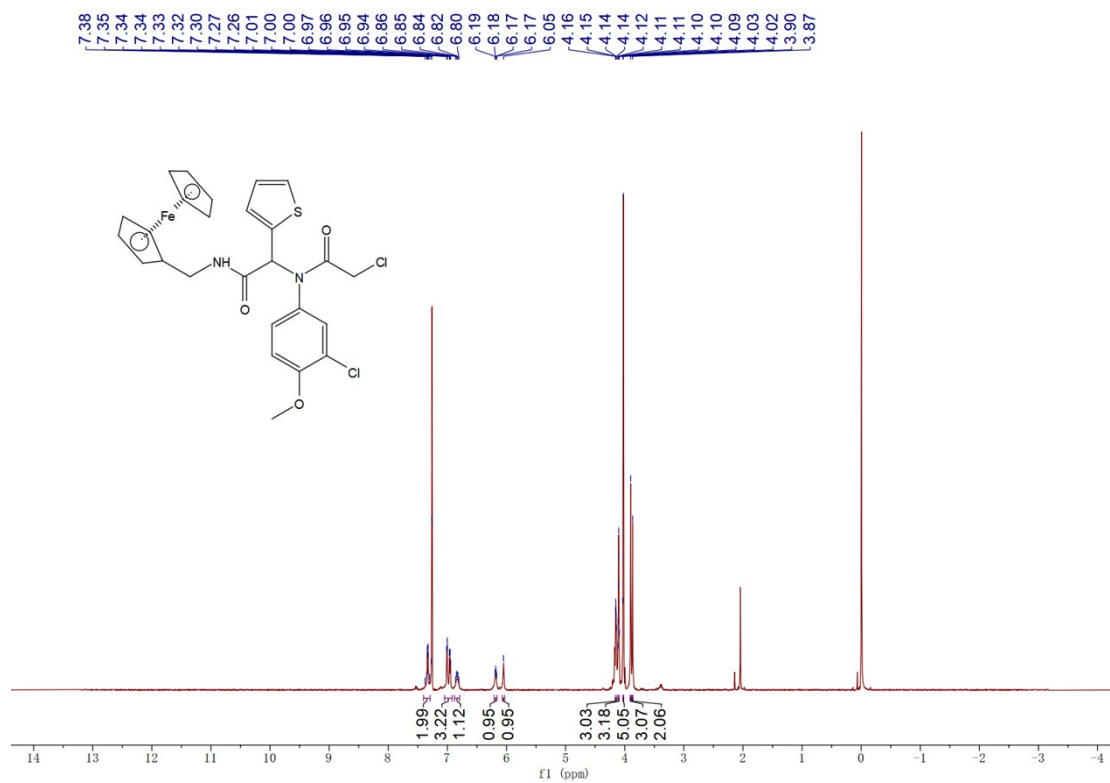
¹H and ¹³C NMR spectrum of compound 10



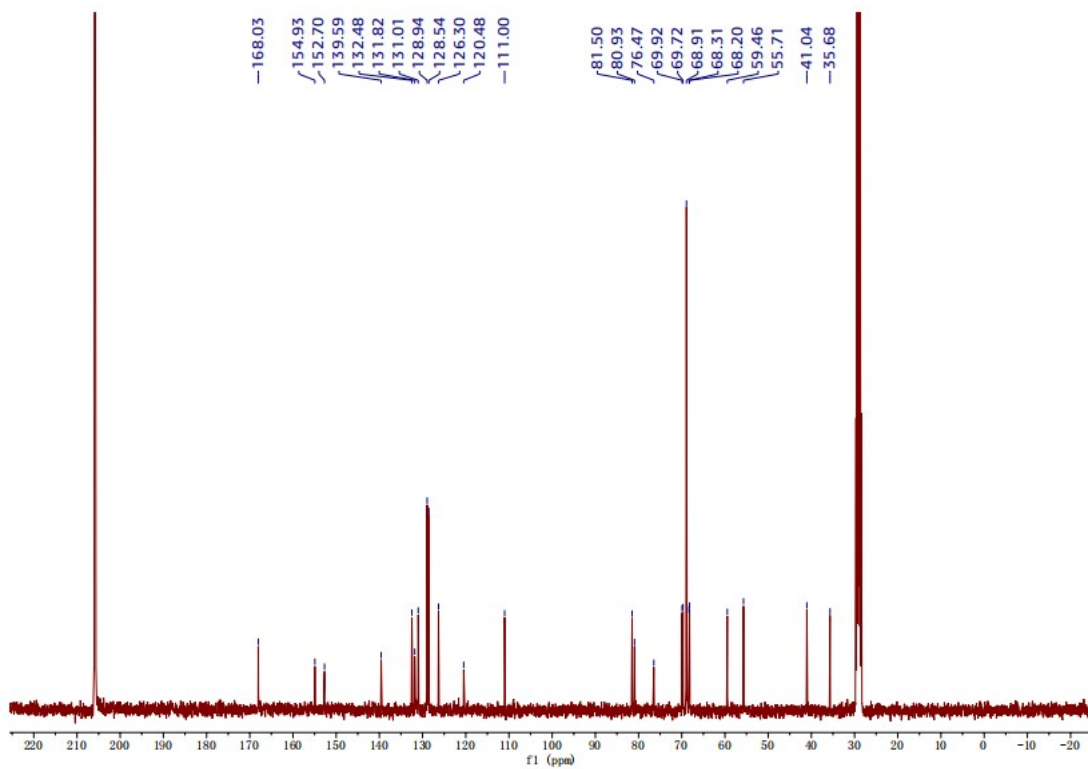
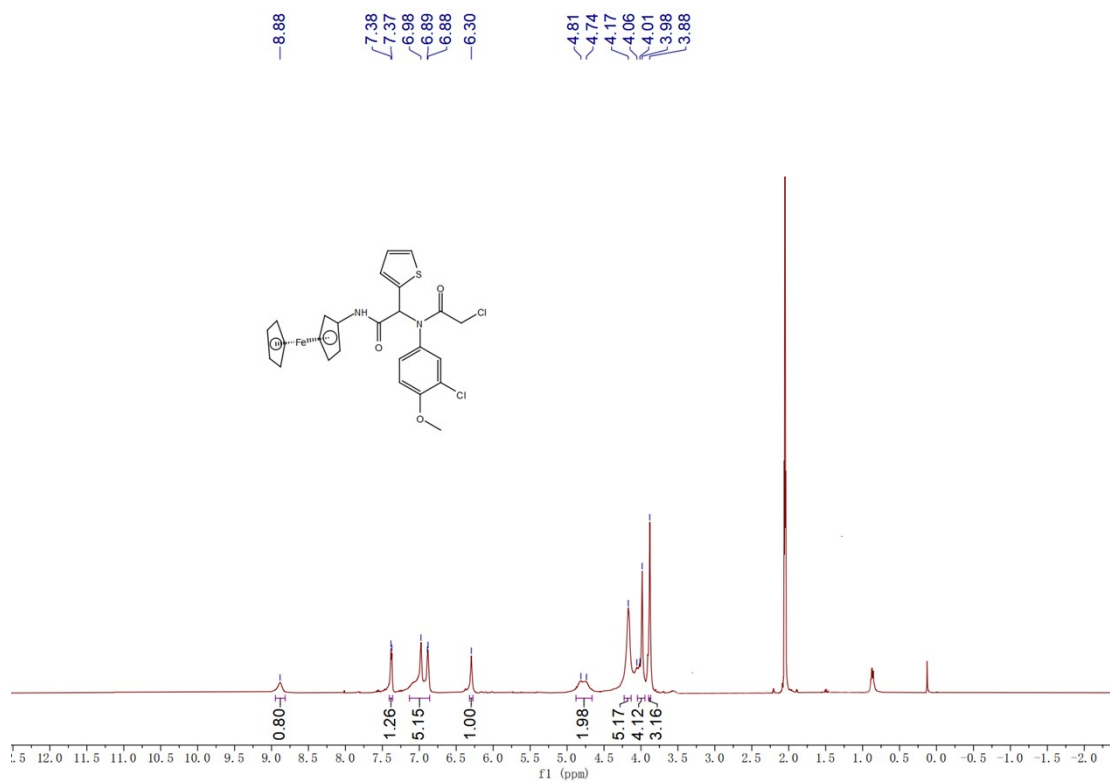
¹H and ¹³C NMR spectrum of compound 11



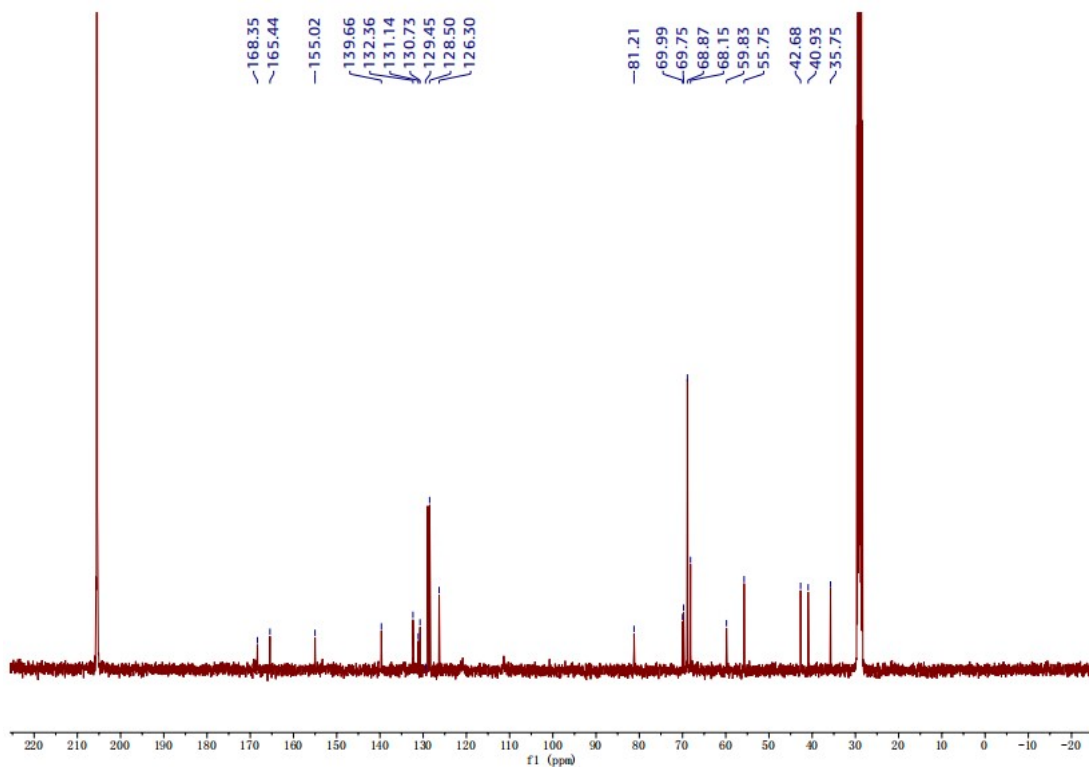
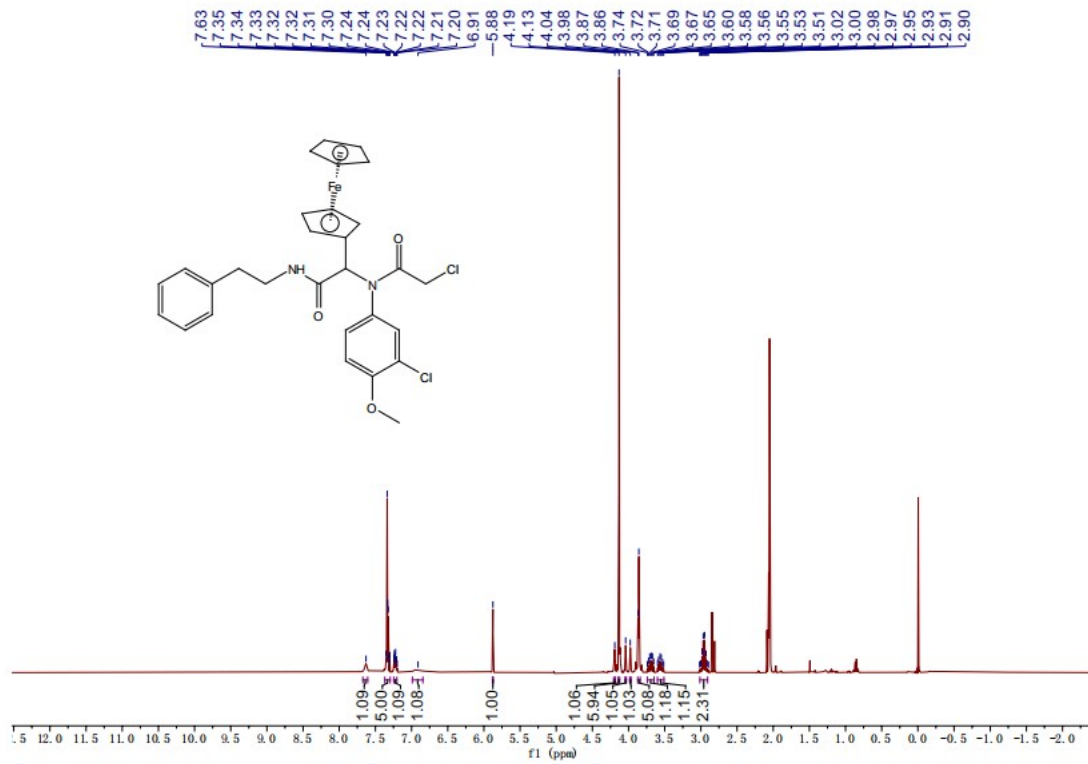
¹H and ¹³C NMR spectrum of compound 12



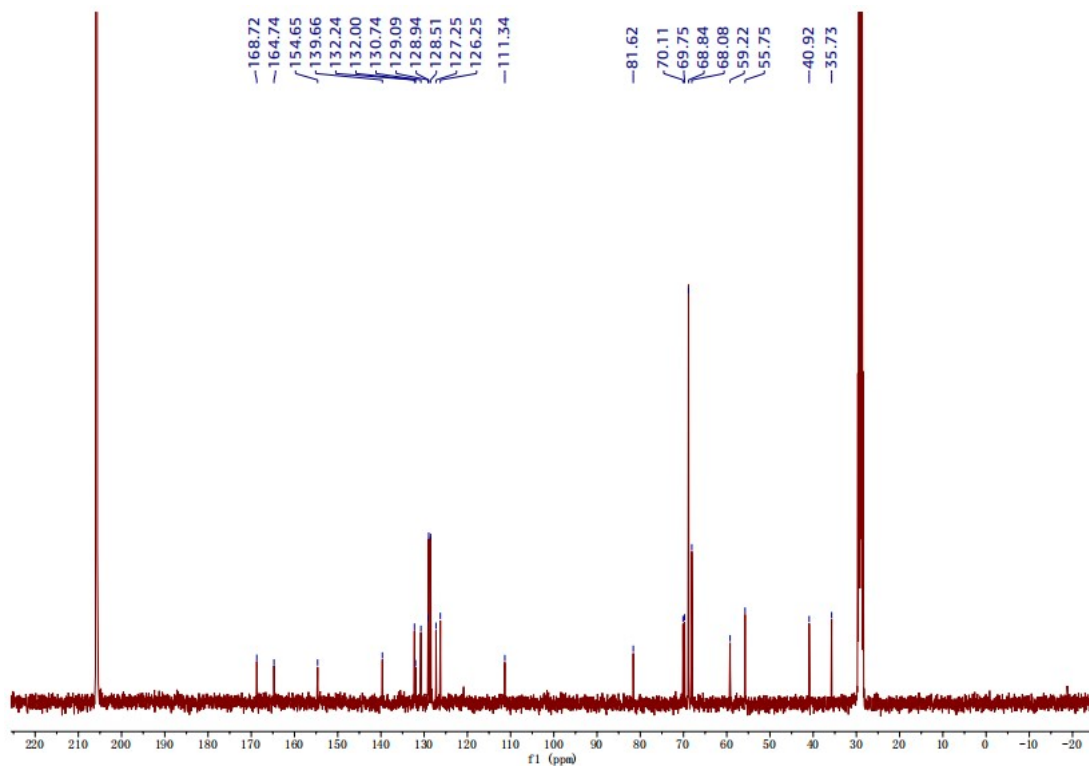
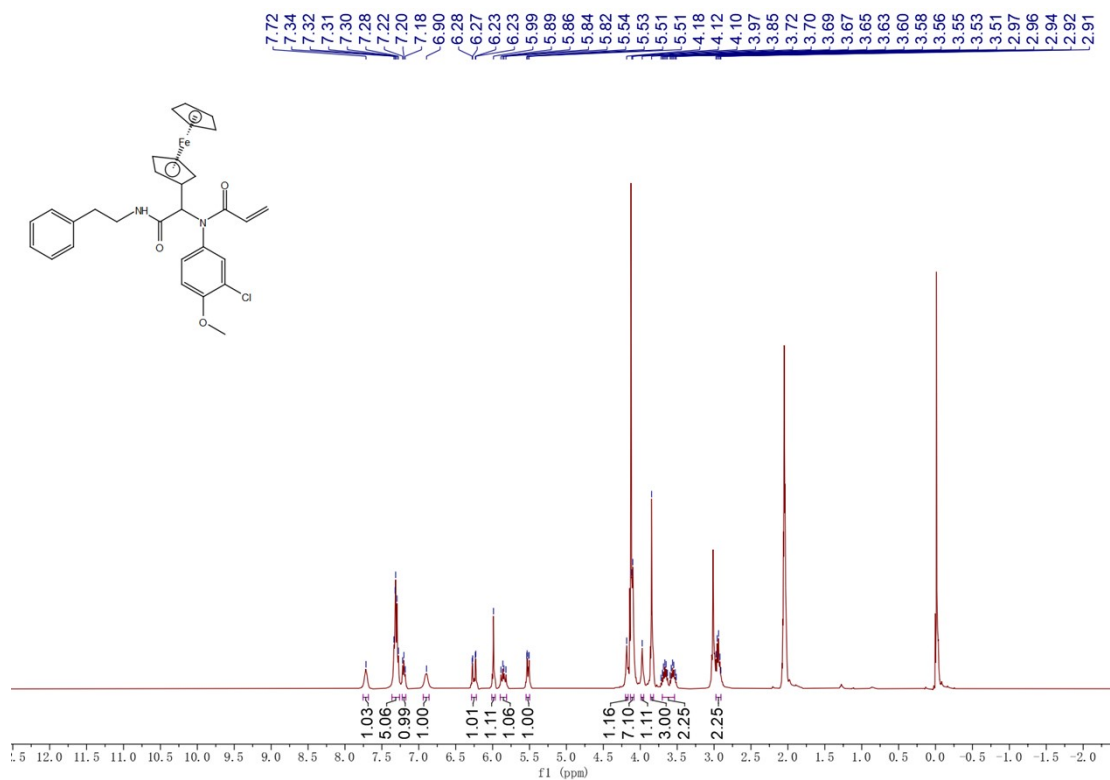
¹H and ¹³C NMR spectrum of compound 13



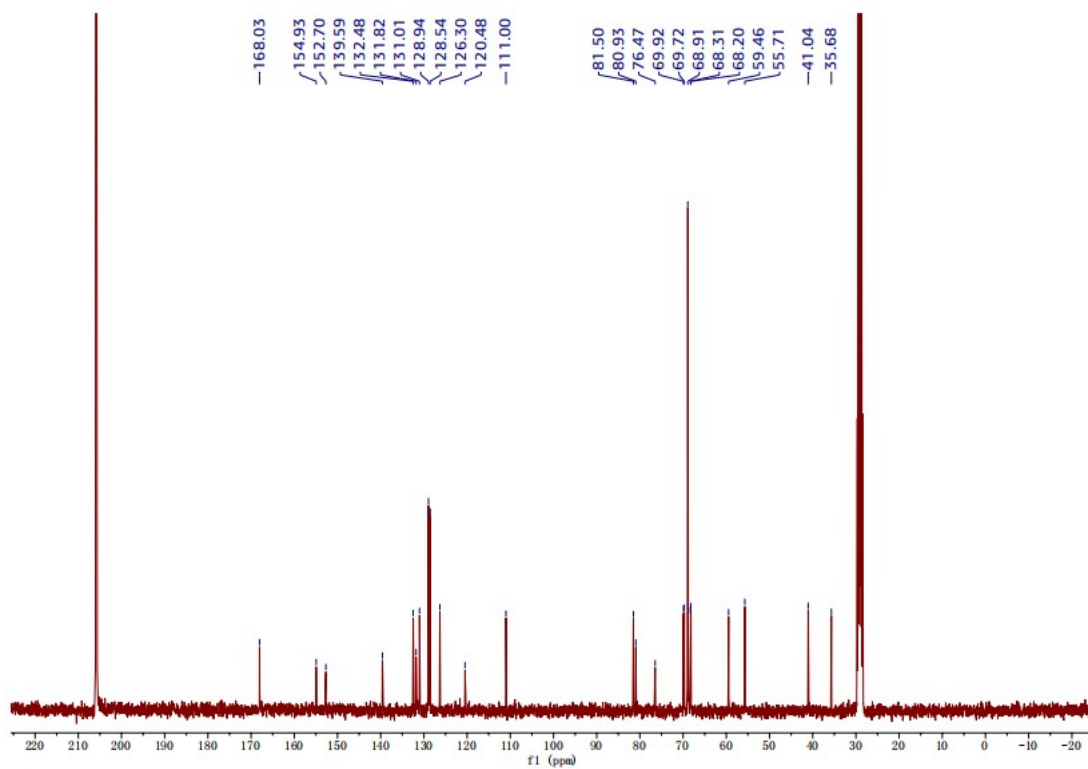
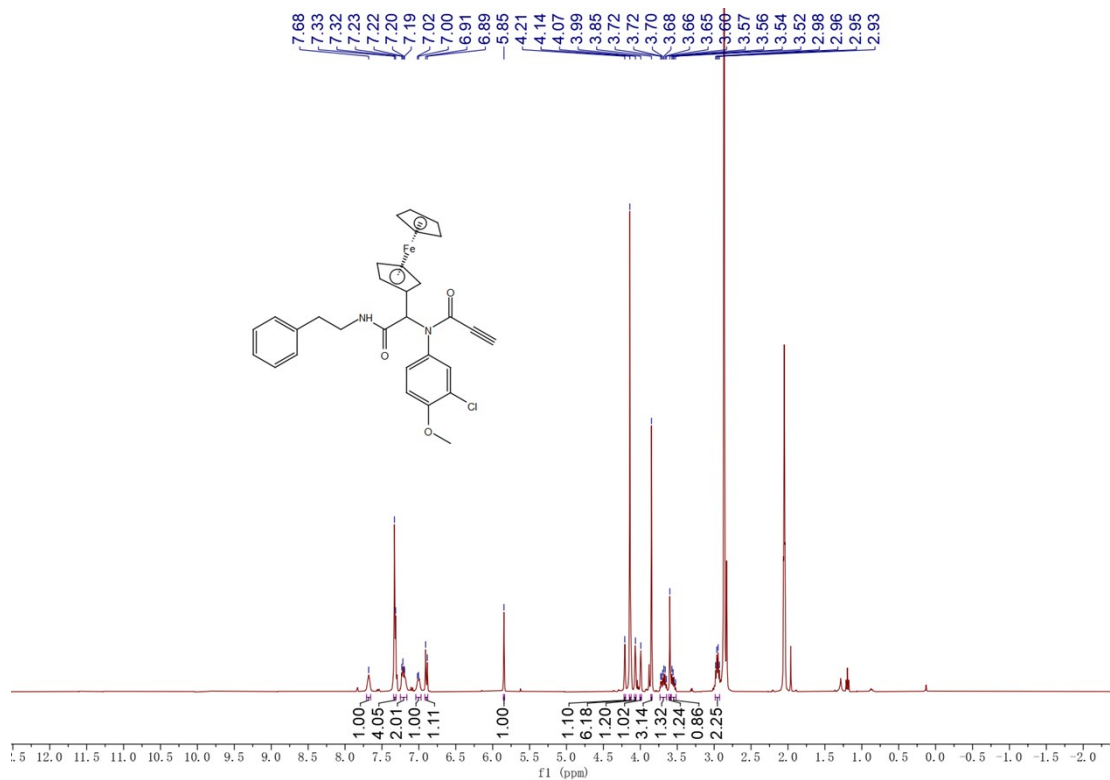
¹H and ¹³C NMR spectrum of compound 14



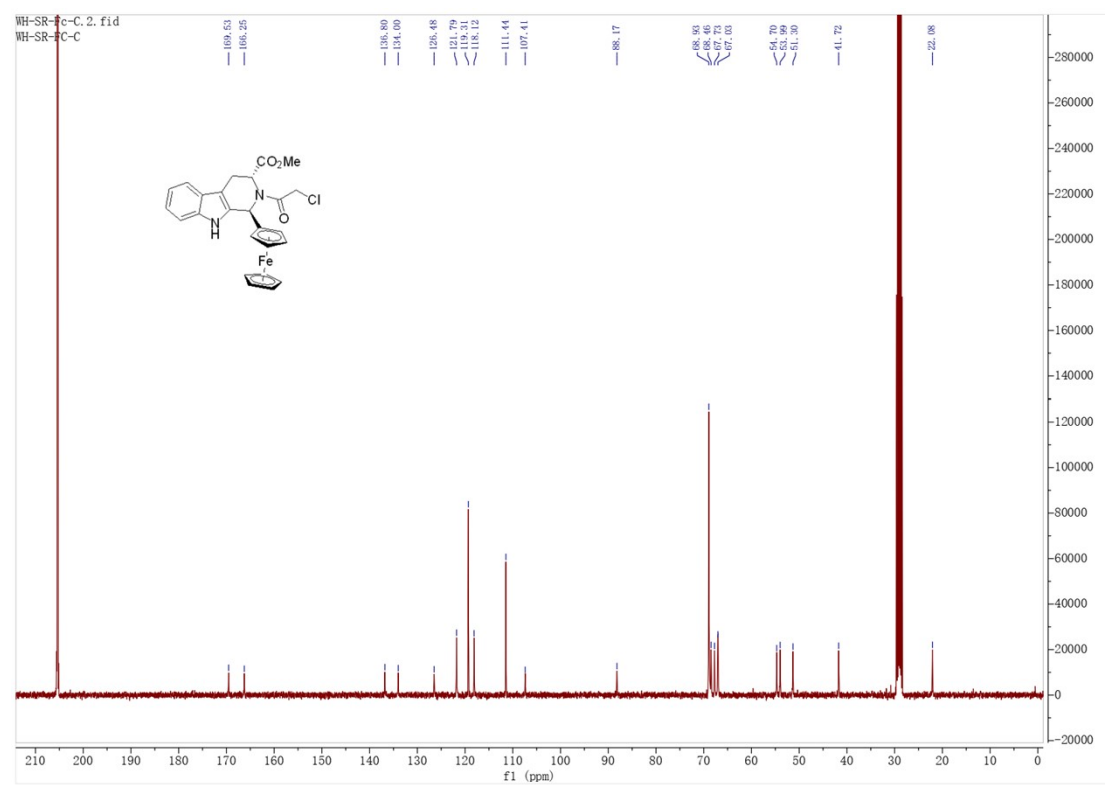
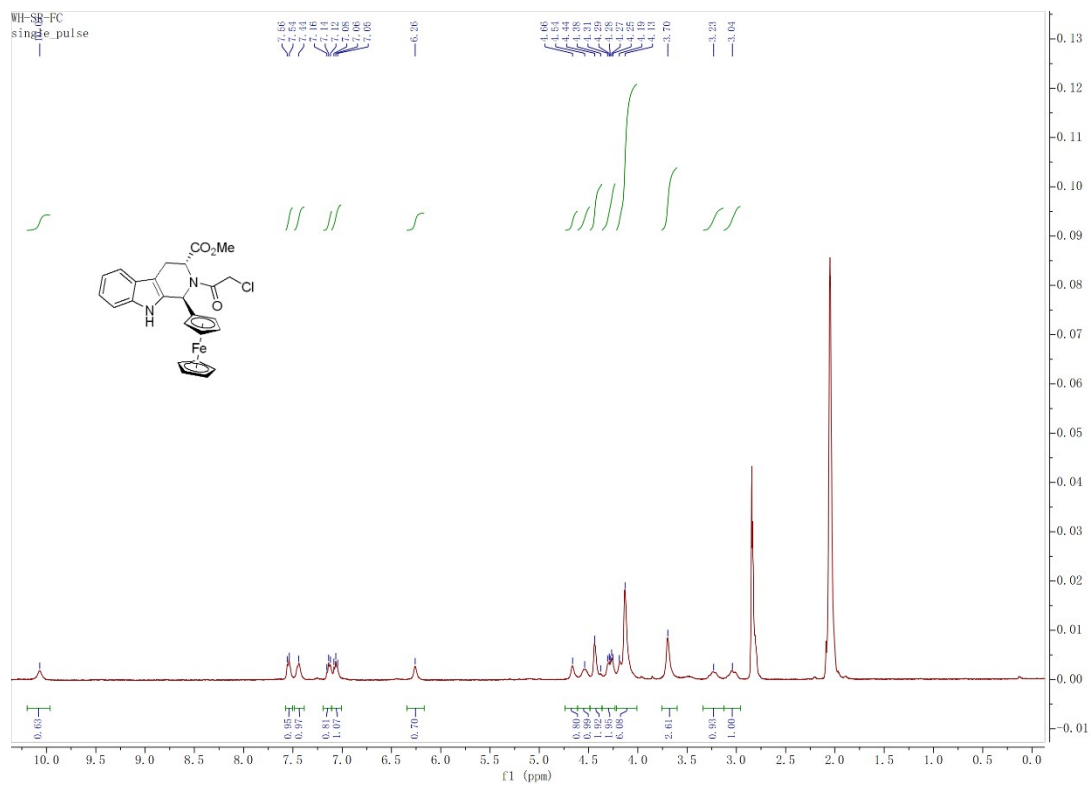
¹H and ¹³C NMR spectrum of compound 15



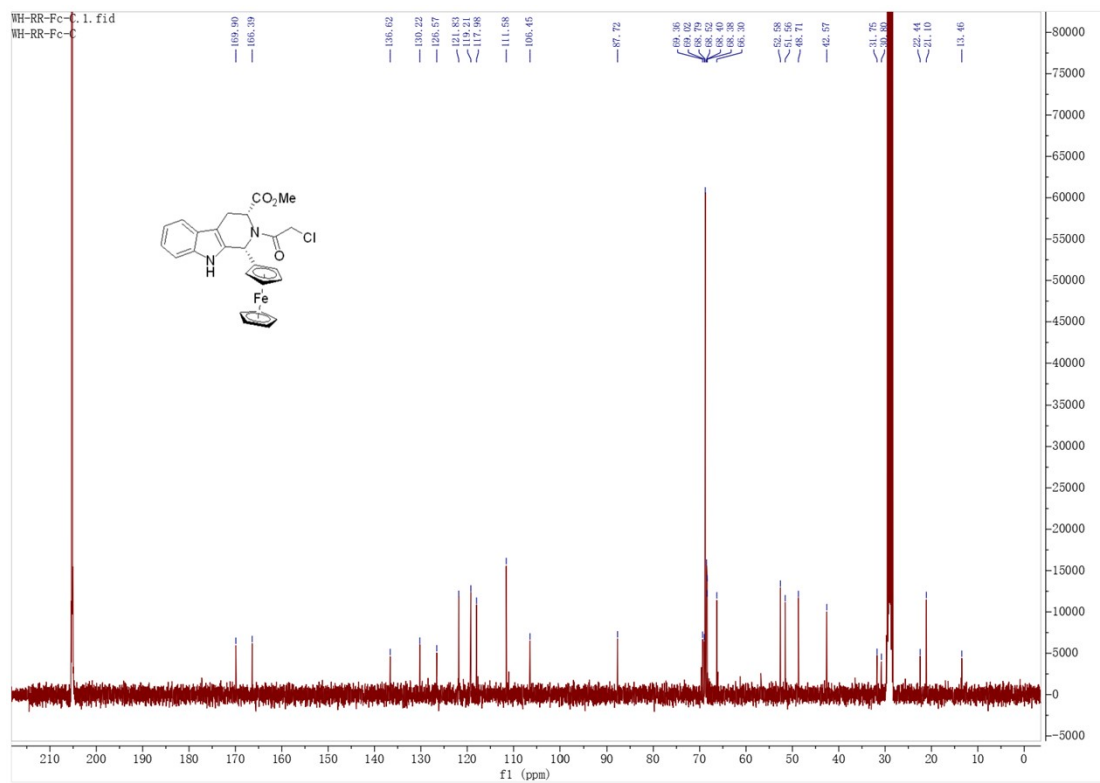
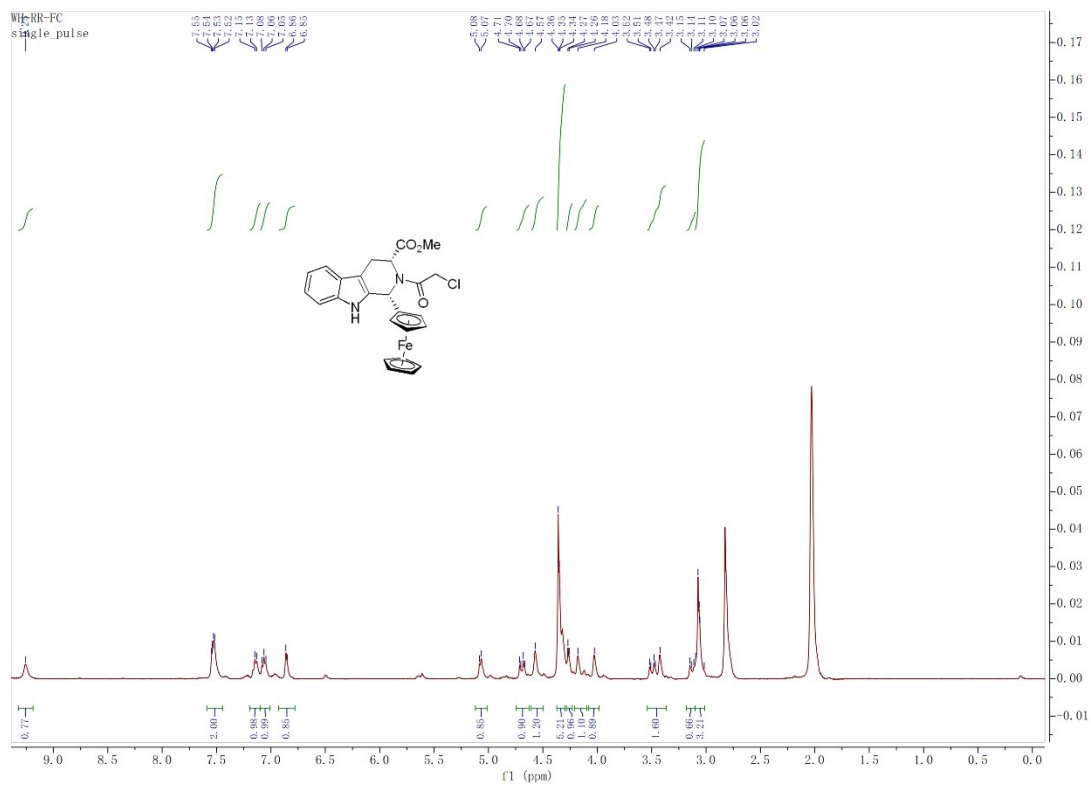
¹H and ¹³C NMR spectrum of compound 16



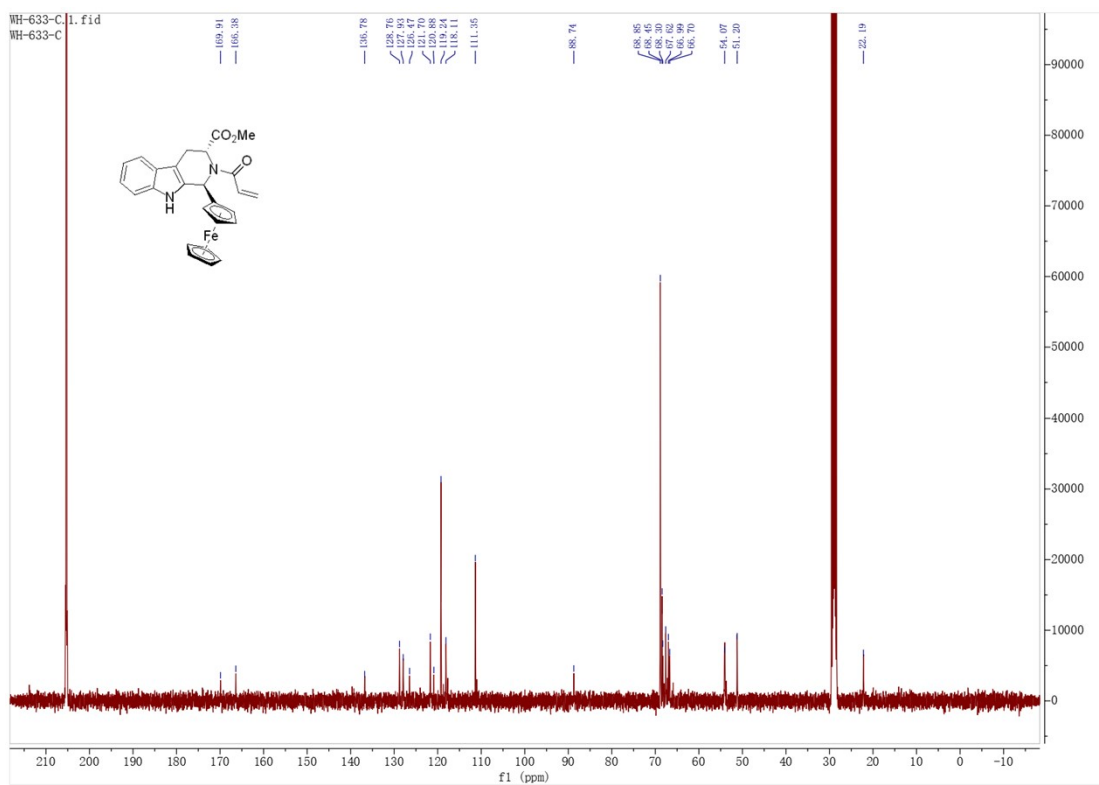
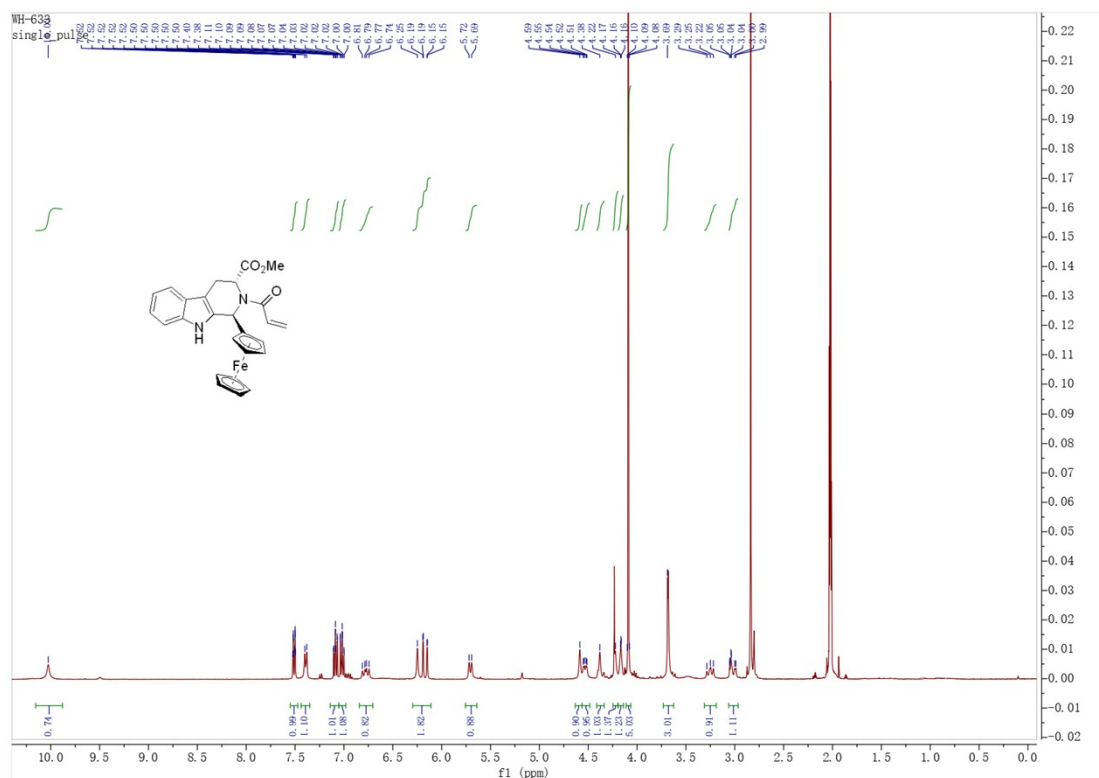
¹H and ¹³C NMR spectrum of compound 17



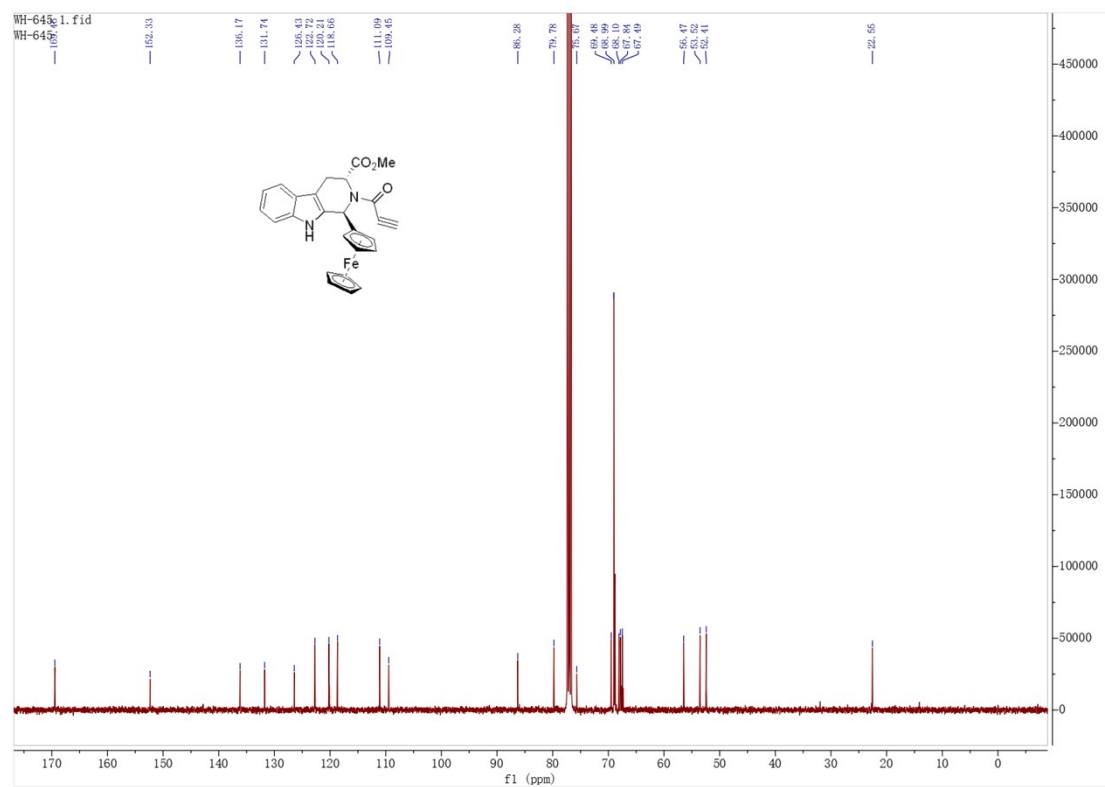
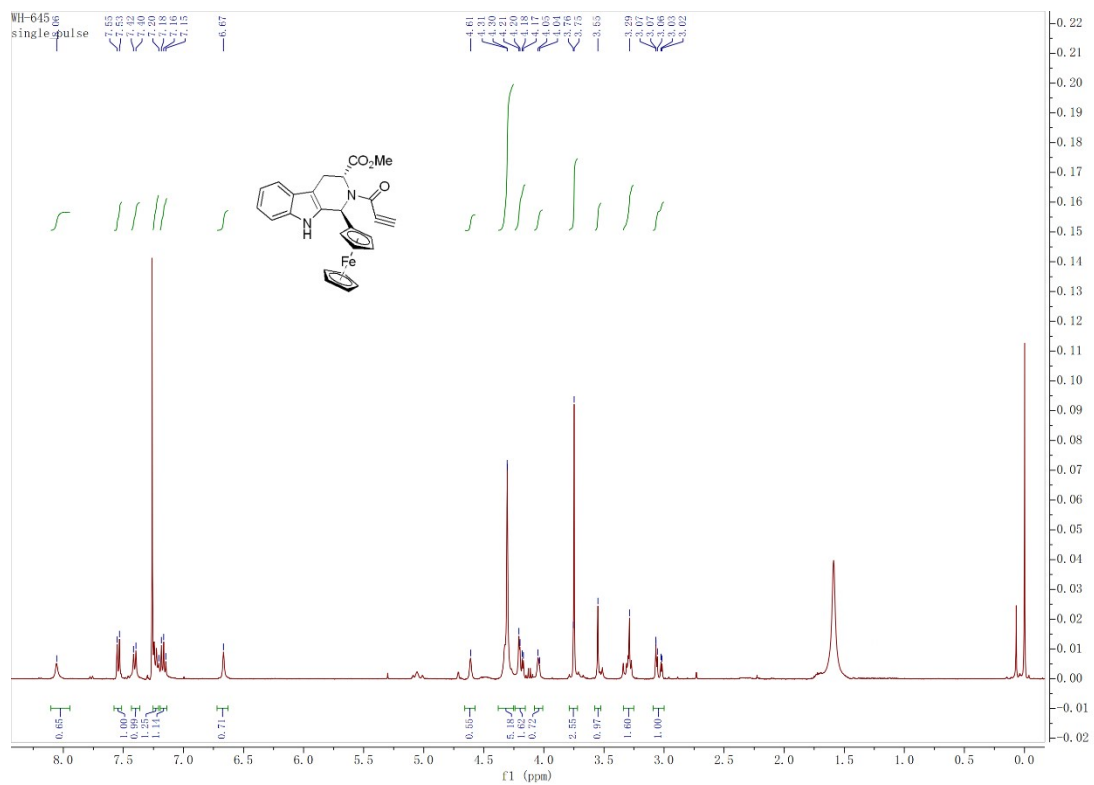
^1H and ^{13}C NMR spectrum of compound 18



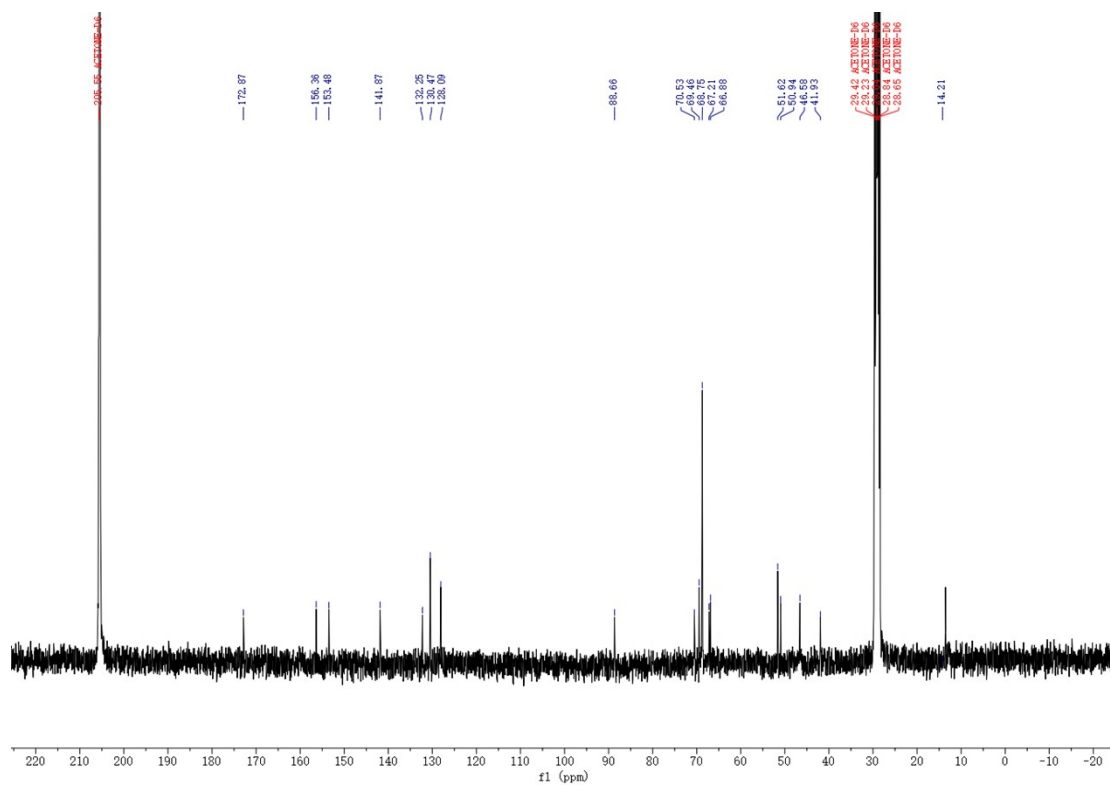
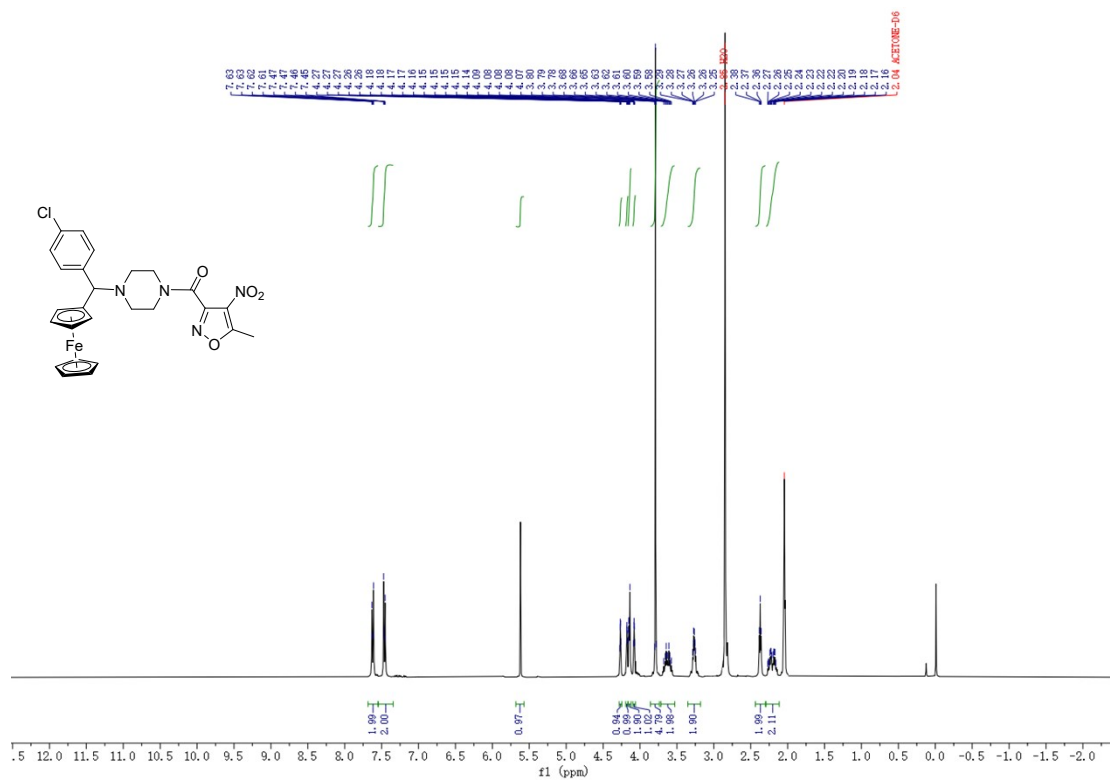
¹H and ¹³C NMR spectrum of compound 19



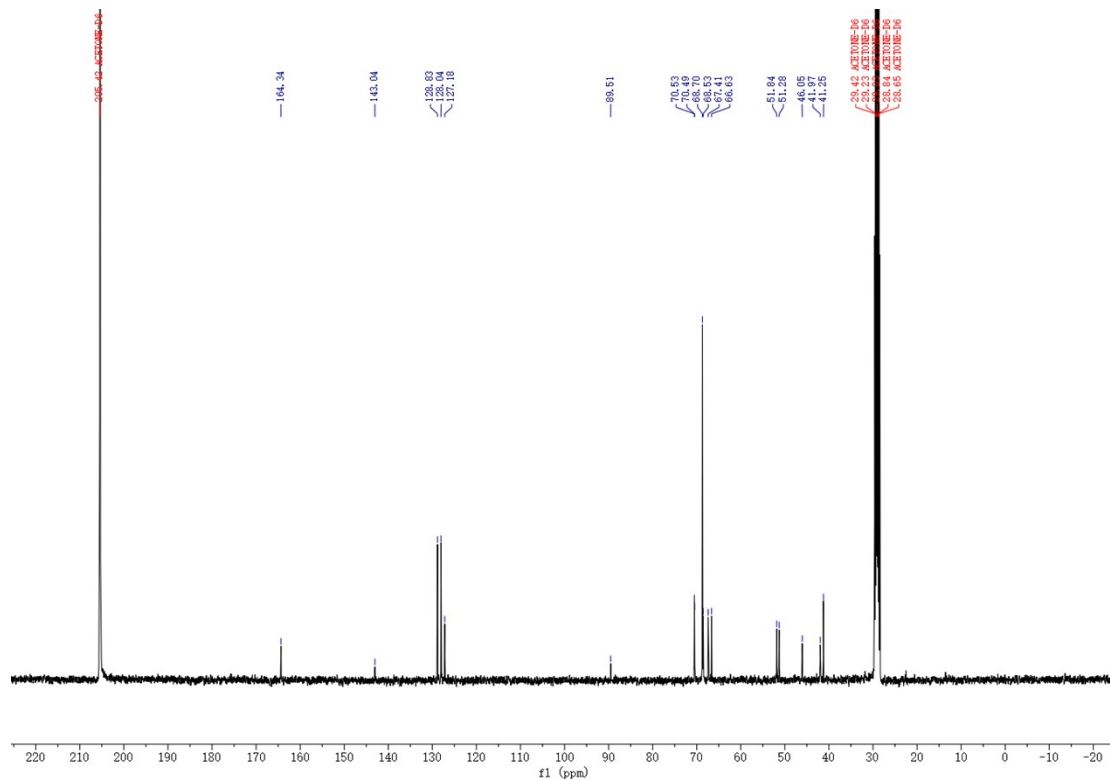
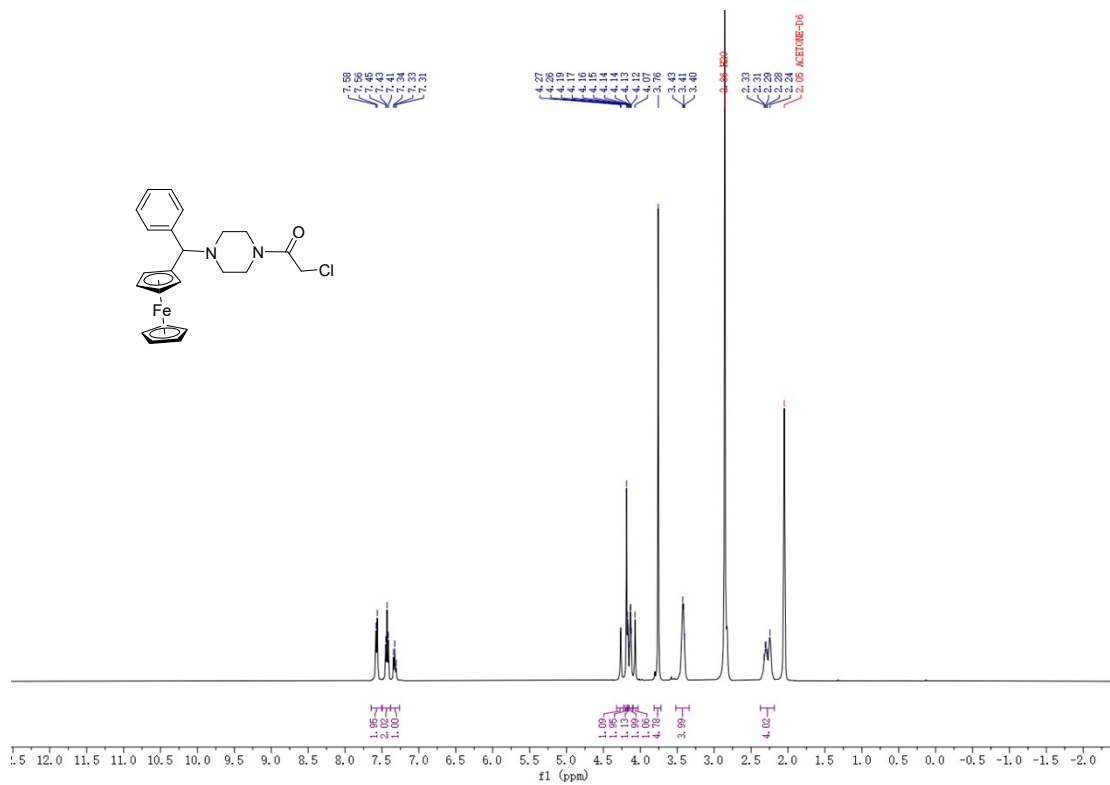
¹H and ¹³C NMR spectrum of compound 20



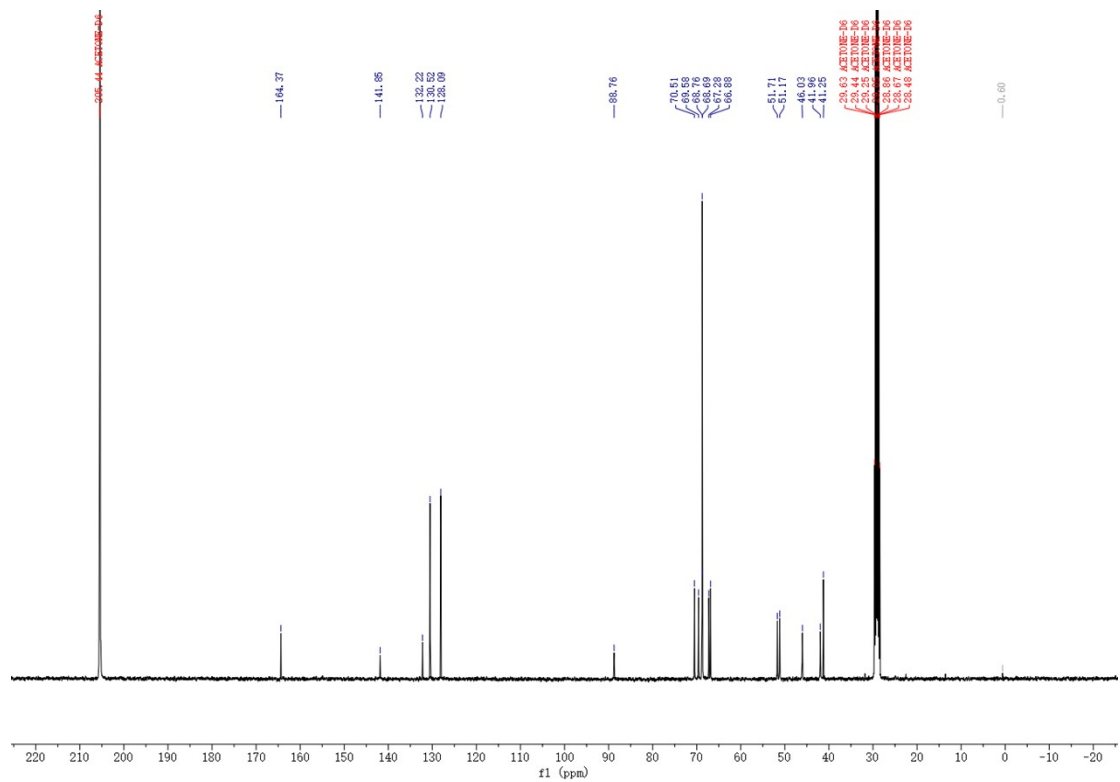
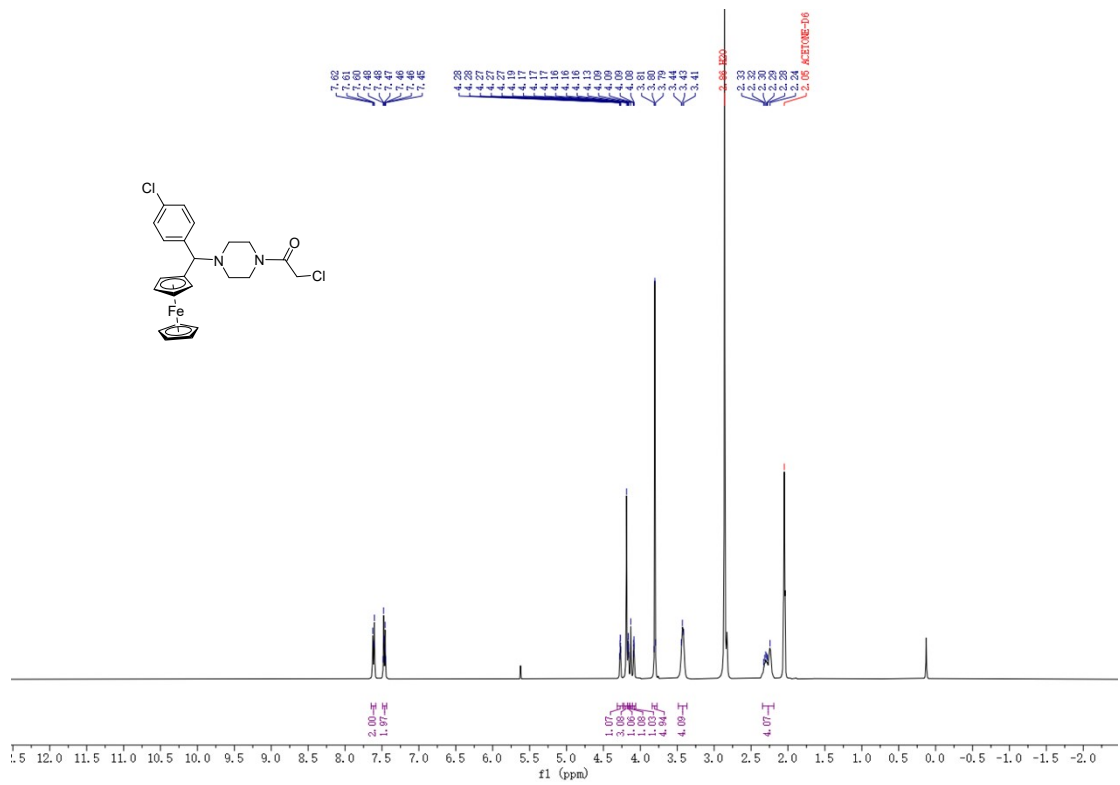
^1H and ^{13}C NMR spectrum of compound 21



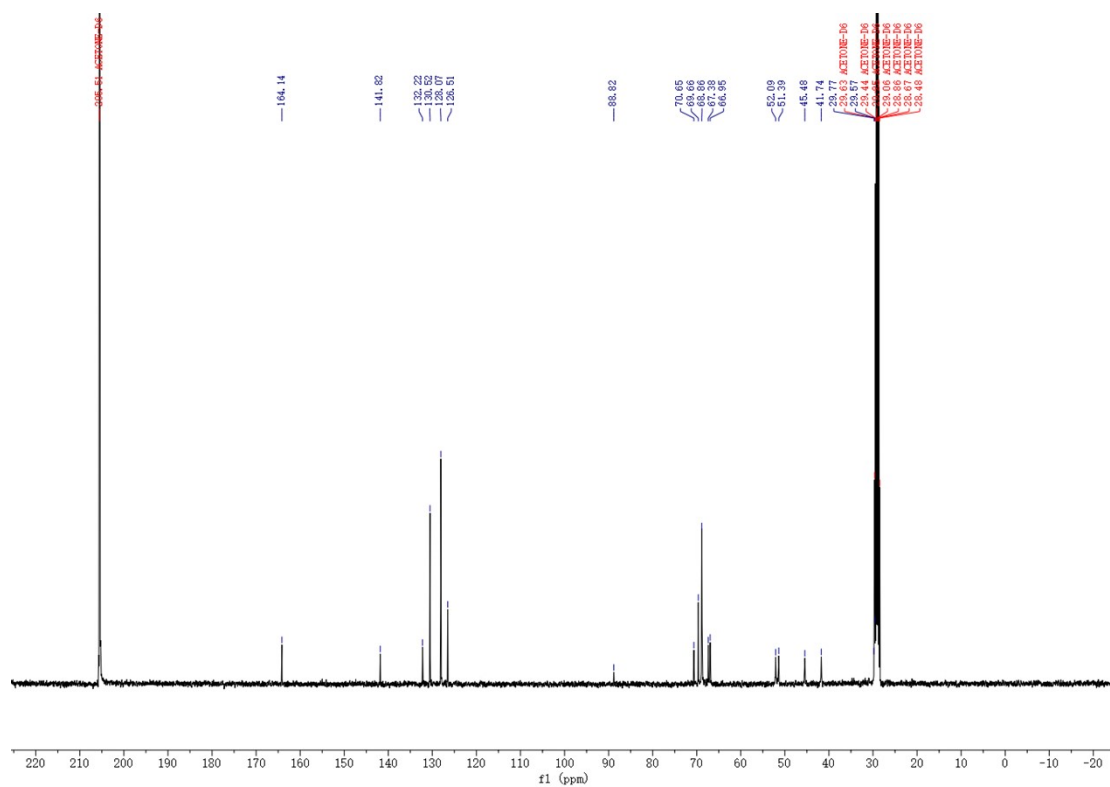
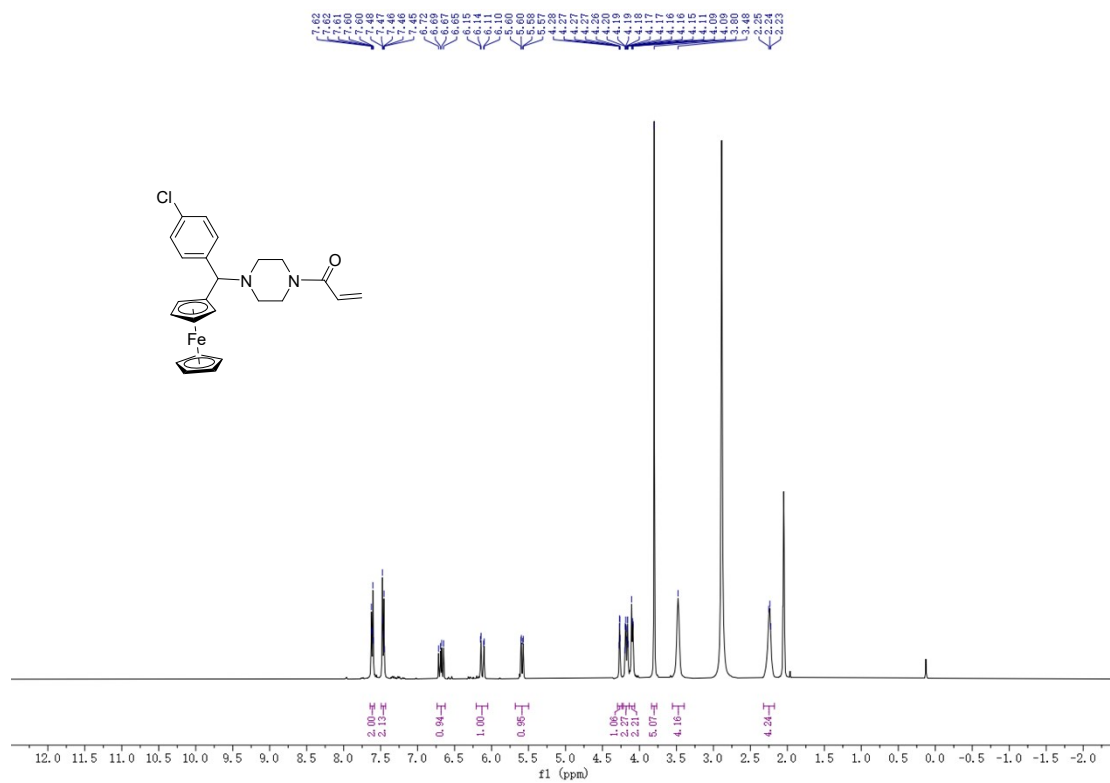
¹H and ¹³C NMR spectrum of compound 22



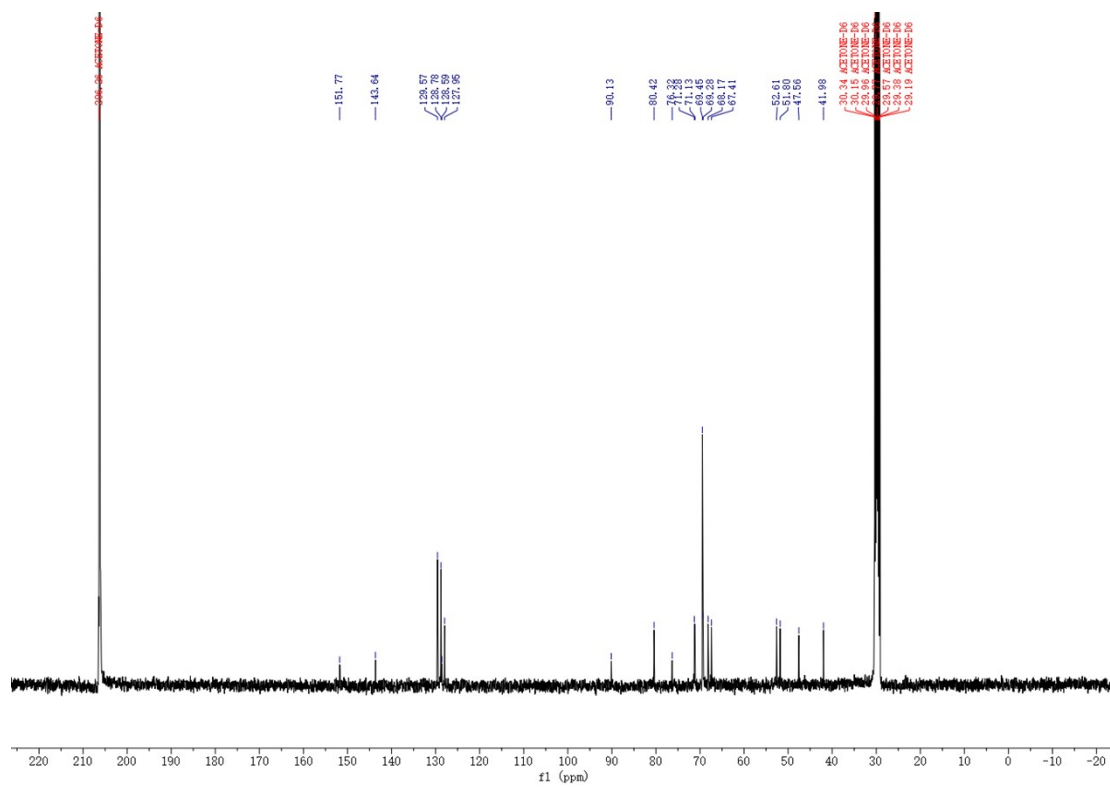
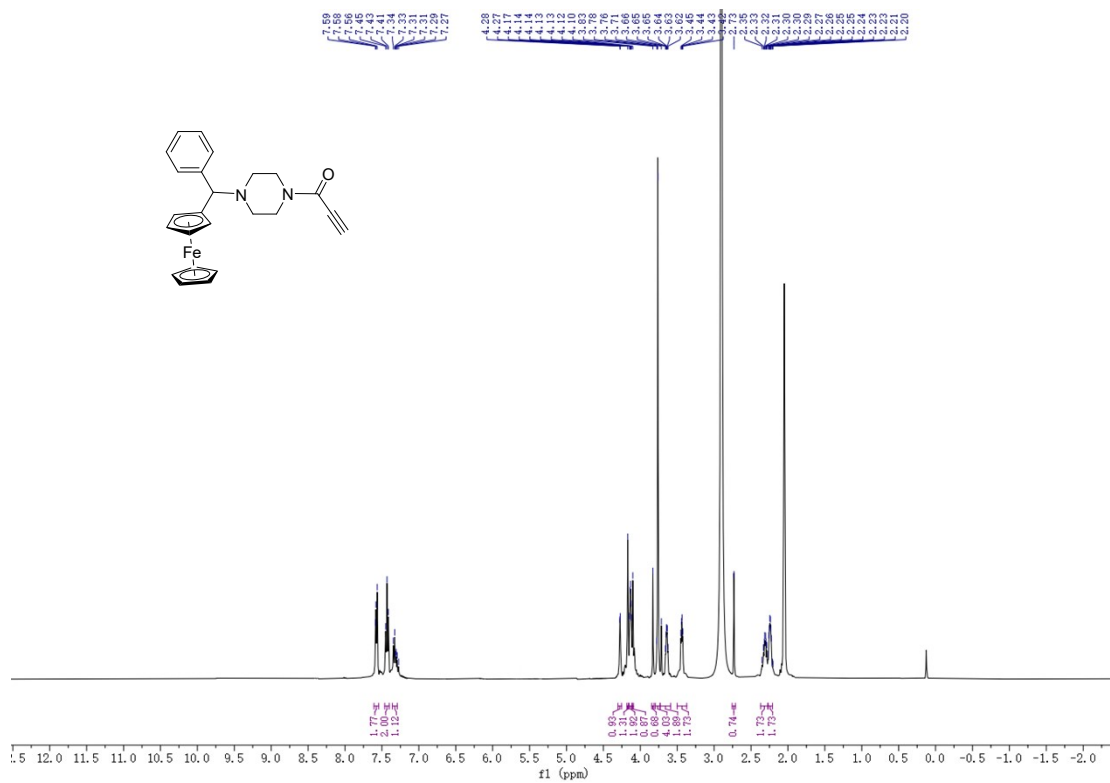
¹H and ¹³C NMR spectrum of compound 23



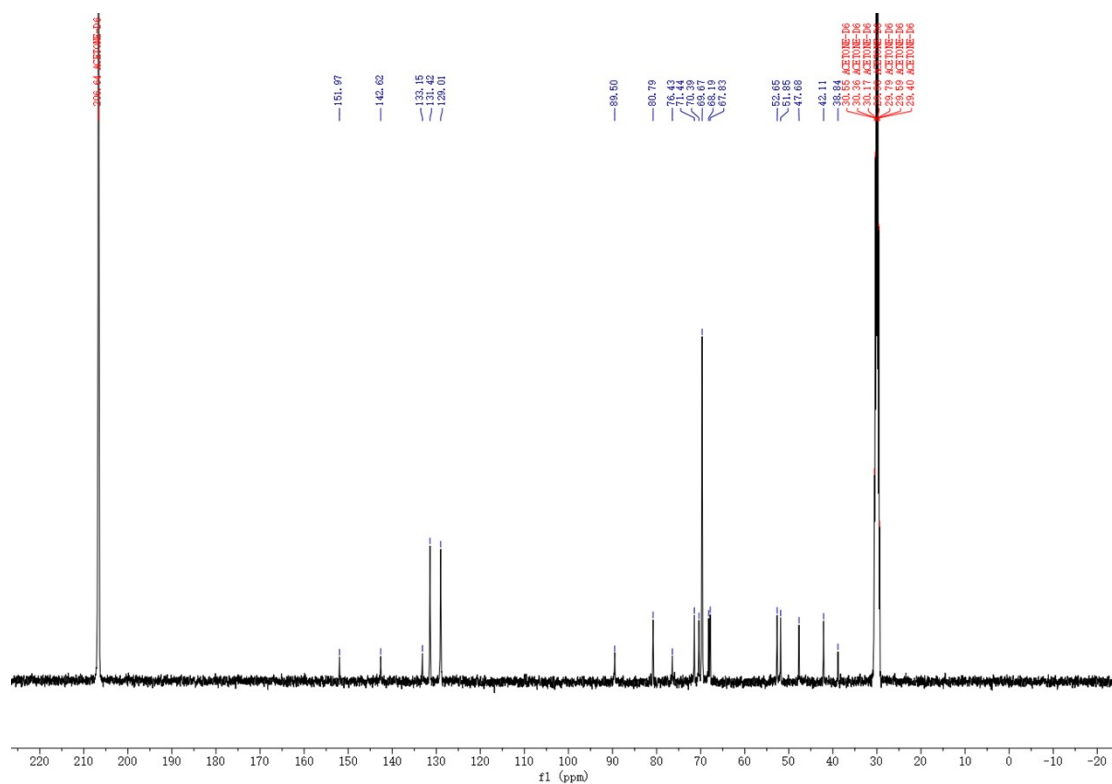
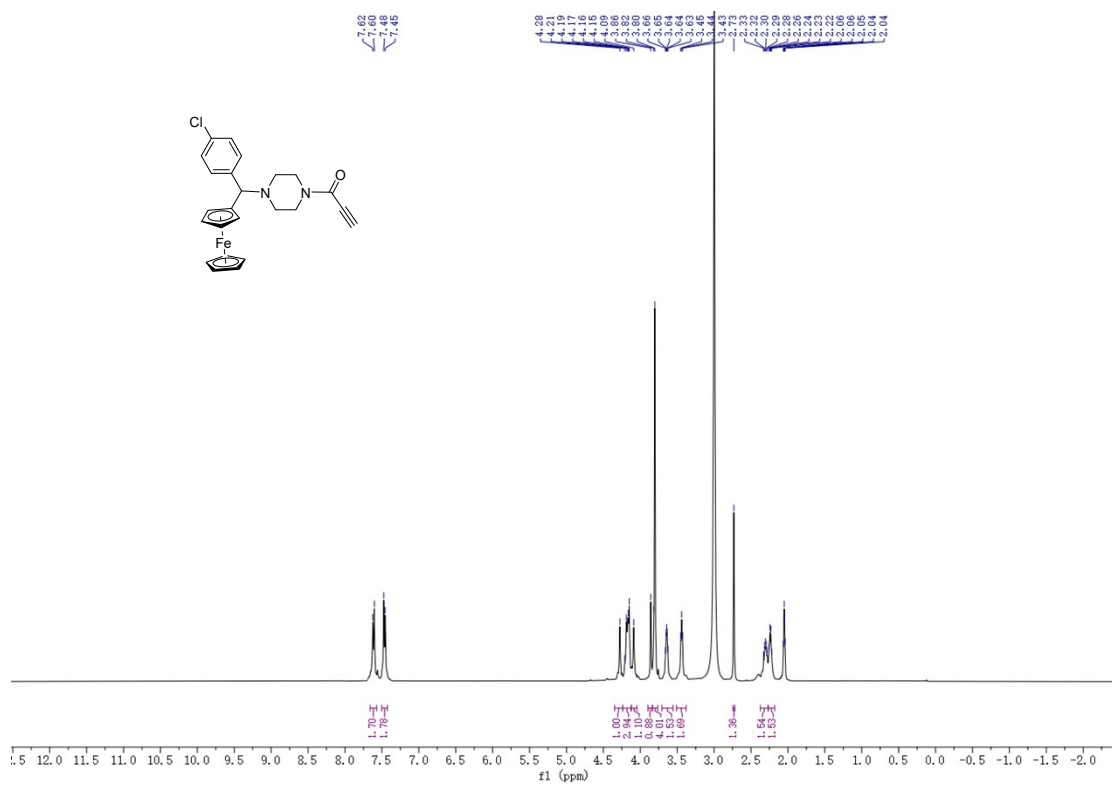
¹H and ¹³C NMR spectrum of compound 24



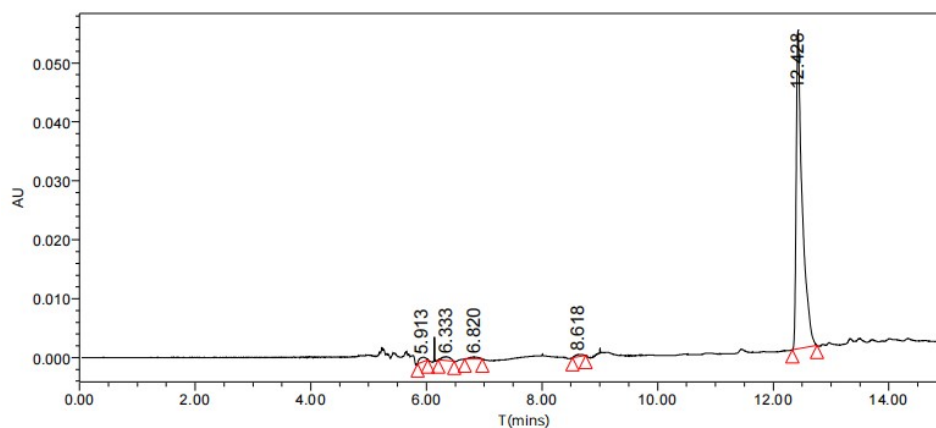
¹H and ¹³C NMR spectrum of compound 25



¹H and ¹³C NMR spectrum of compound 26

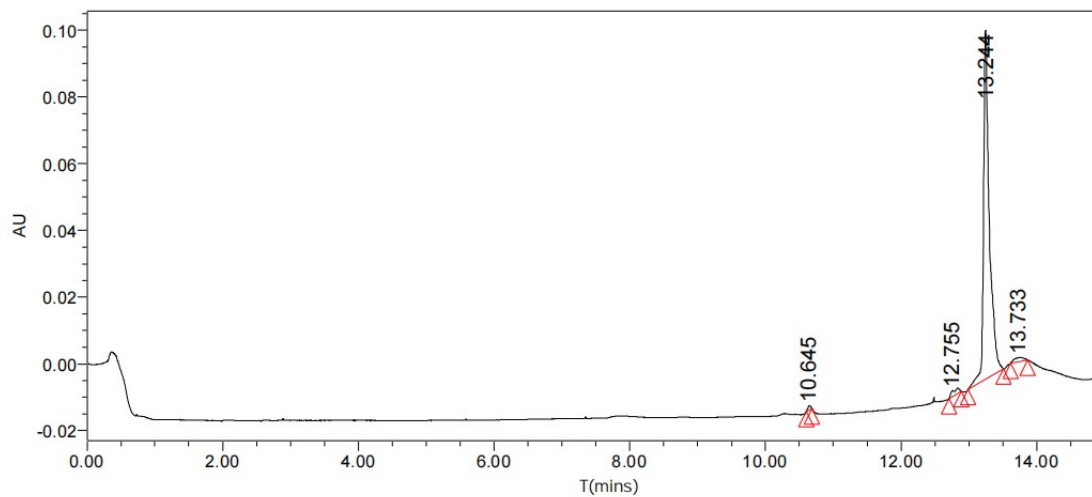


¹H and ¹³C NMR spectrum of compound 27



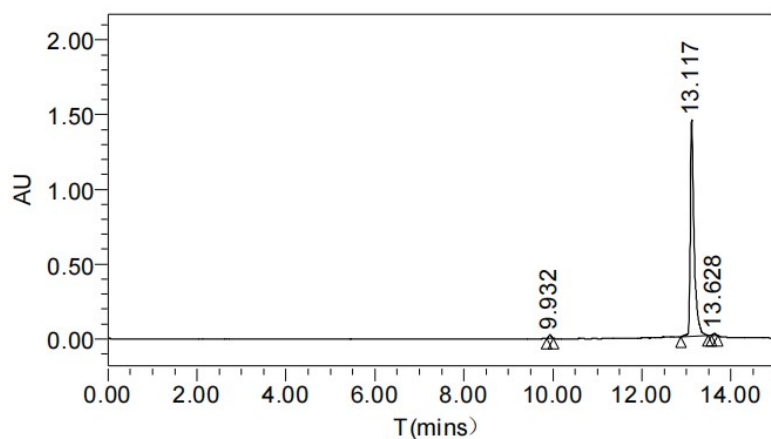
Result			
	Ret.Time	Area	Rel. Area(%)
1	5.913	5882	1.45
2	6.333	6664	1.65
3	6.820	3668	0.91
4	8.618	2919	0.72
5	12.428	385369	95.27

The purity data of the compound **10**



Result			
	Ret.Time	Area	Rel. Area(%)
1	10.645	4082	0.62
2	12.755	12596	1.92
3	13.244	627089	95.52
4	13.733	12725	1.94

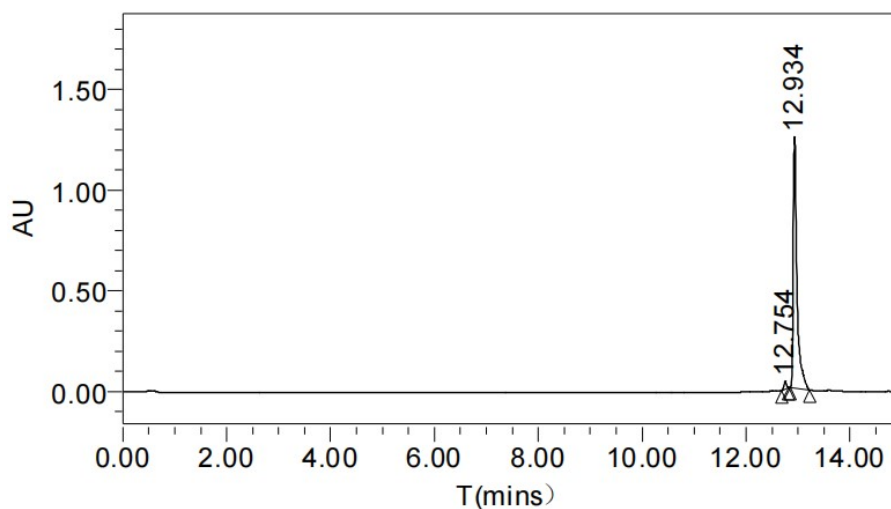
The purity data of the compound **11**



Result

	Ret.Time	Area	Rel.Area(%)
1	9.932	97952	1.13
2	13.117	8495160	98.06
3	13.628	69750	0.81

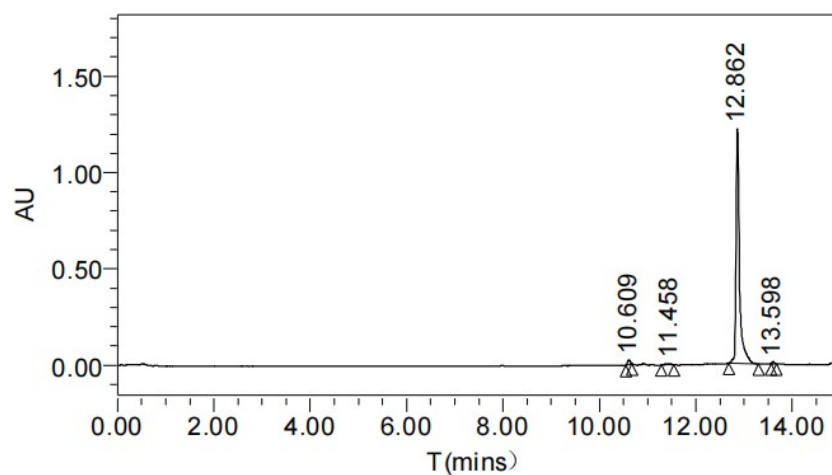
The purity data of the compound **12**



Result

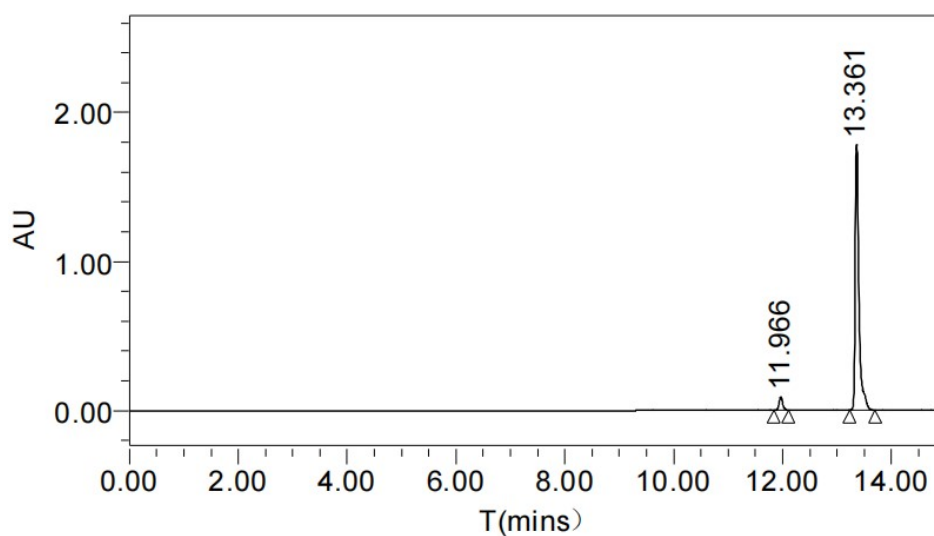
	Ret.Time	Area	Rel.Area(%)
1	12.754	128556	2.02
2	12.934	6232362	97.98

The purity data of the compound **13**



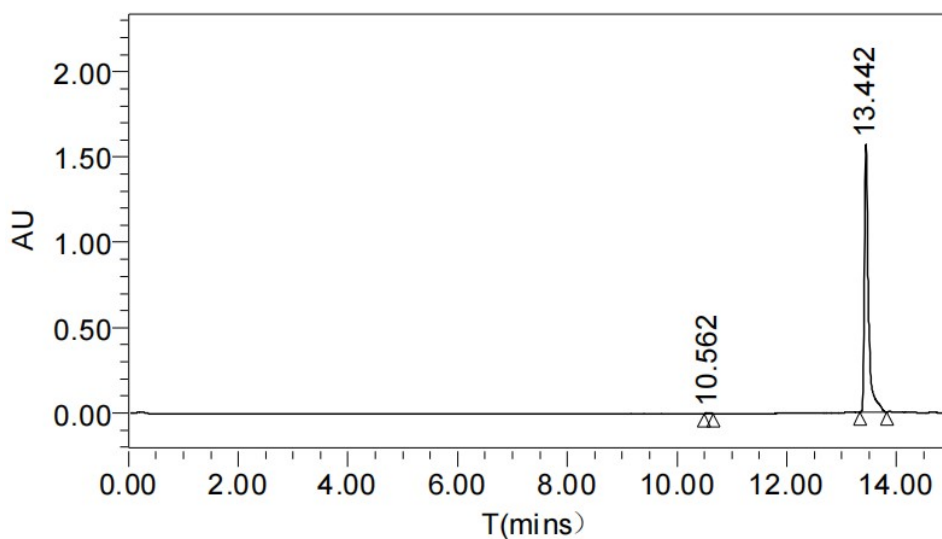
Result			
	Ret.Time	Area	Rel.Area(%)
1	10.609	95878	1.56
2	11.458	49662	0.81
3	12.862	5960249	97.18
4	13.598	27492	0.45

The purity data of the compound **14**



Result			
	Ret.Time	Area	Rel.Area(%)
1	11.966	389872	4.45
2	13.361	8370394	95.55

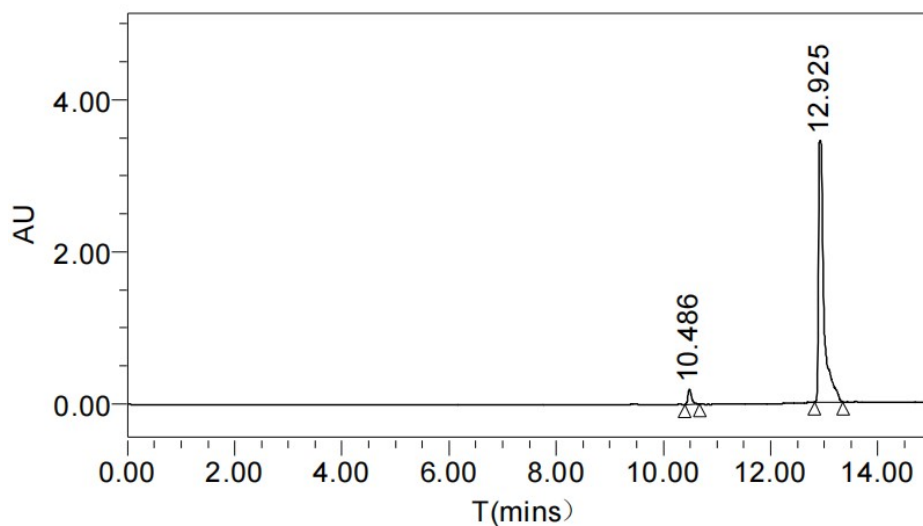
The purity data of the compound **15**



Result

	Ret.Time	Area	Rel.Area(%)
1	10.562	22459	0.28
2	13.442	7928506	99.72

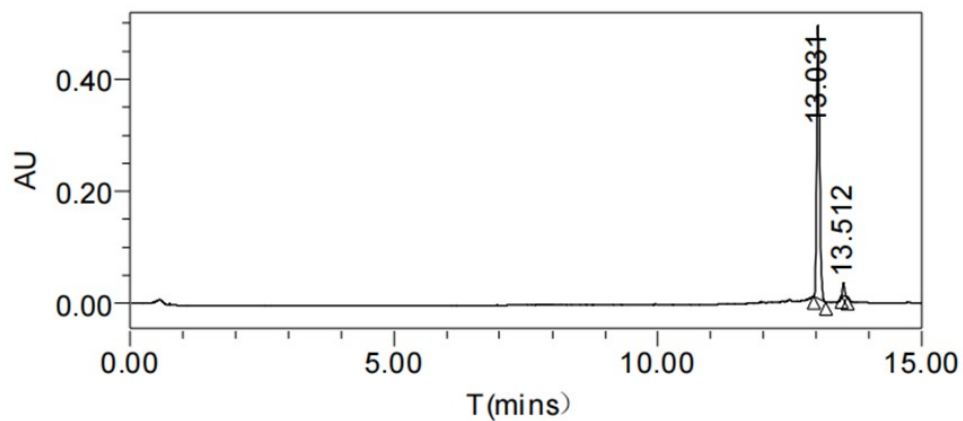
The purity data of the compound **16**



Result

	Ret.Time	Area	Rel.Area(%)
1	10.486	896981	3.50
2	12.925	24717321	96.50

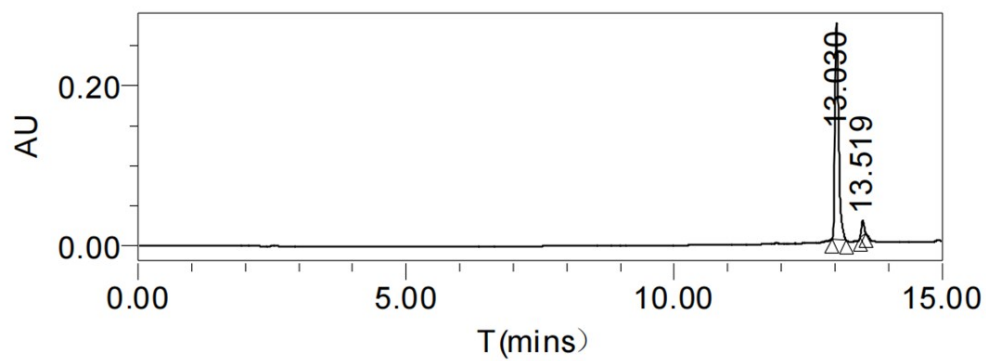
The purity data of the compound **17**



Result

	Ret.Time	Area	Rel.Area(%)
1	13.031	1786725	96.41
2	13.512	66539	3.59

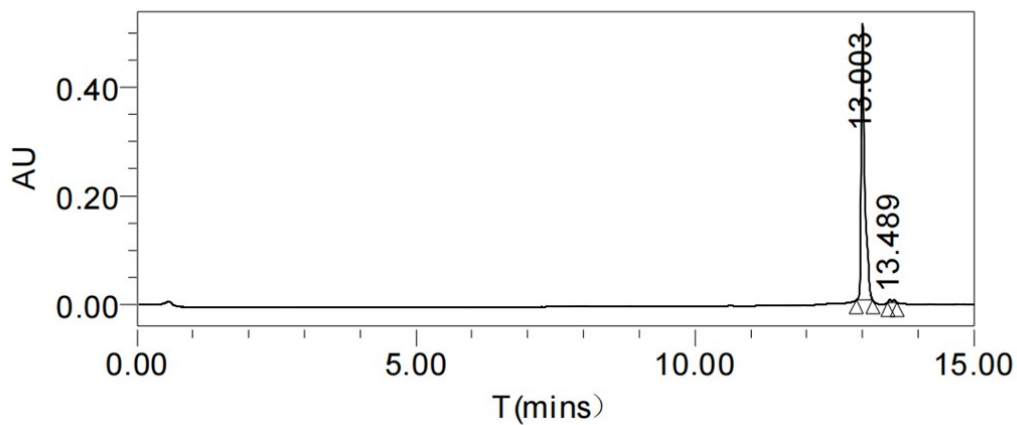
The purity data of the compound **18**



Result

	Ret.Time	Area	Rel.Area(%)
1	13.030	1257529	95.14
2	13.519	64271	4.86

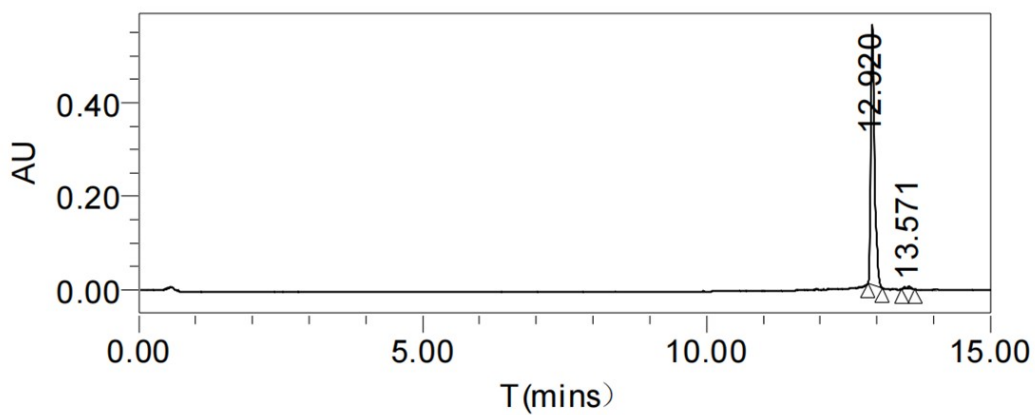
The purity data of the compound **19**



Result

	Ret.Time	Area	Rel.Area(%)
1	13.003	2254595	98.61
2	13.489	31798	1.39

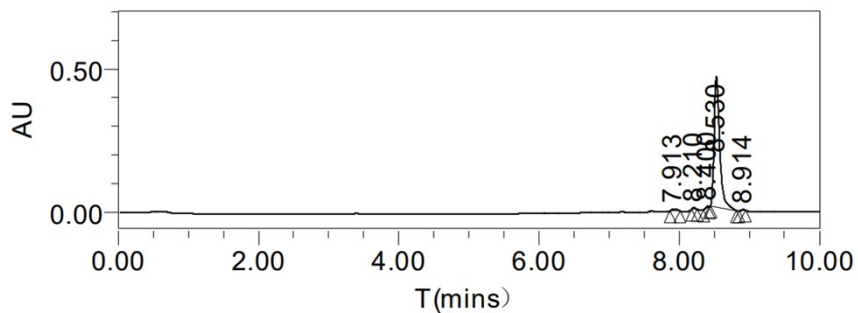
The purity data of the compound **20**



Result

	Ret.Time	Area	Rel.Area(%)
1	12.920	2406383	98.42
2	13.571	38621	1.58

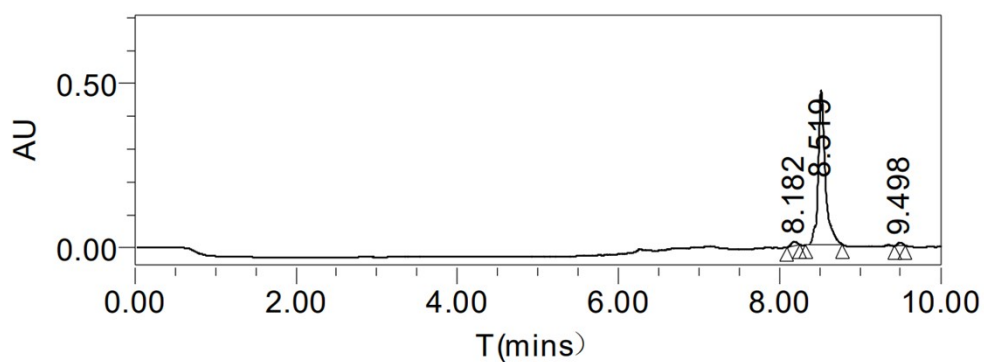
The purity data of the compound **21**



Result

	Ret.Time	Area	Rel.Area(%)
1	7.913	37638	1.46
2	8.210	18147	0.70
3	8.400	11199	0.43
4	8.530	2508737	97.03
5	8.914	9919	0.38

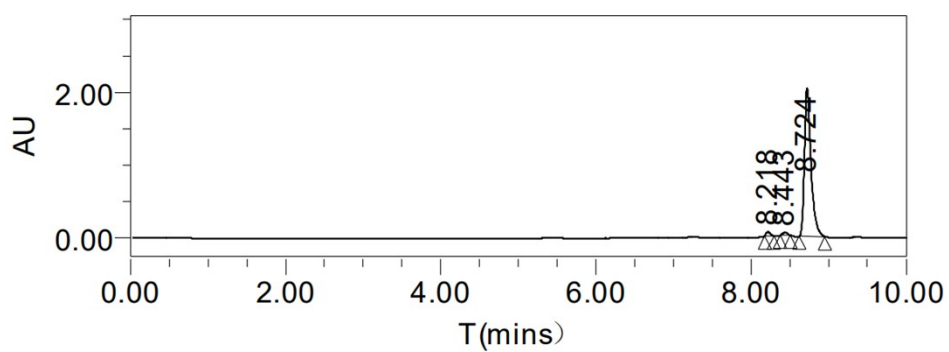
The purity data of the compound **22**



Result

	Ret.Time	Area	Rel.Area(%)
1	8.182	62846	2.02
2	8.519	3008652	96.68
3	9.498	40624	1.31

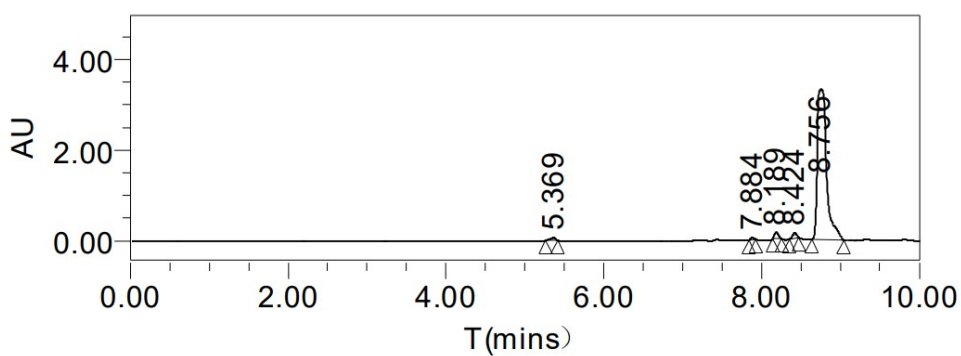
The purity data of the compound **23**



Result

	Ret.Time	Area	Rel.Area(%)
1	8.218	205612	1.69
2	8.443	169392	1.39
3	8.724	11815830	96.92

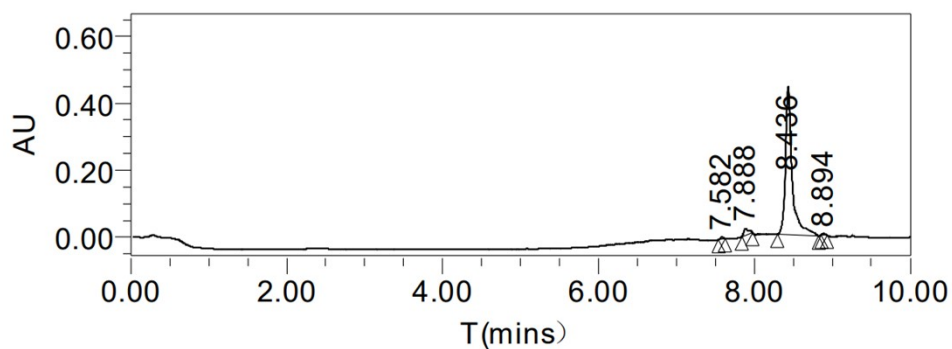
The purity data of the compound **24**



Result

	Ret.Time	Area	Rel.Area(%)
1	5.369	277843	0.91
2	7.884	145296	0.48
3	8.189	498342	1.63
4	8.424	419479	1.37
5	8.756	29170742	95.61

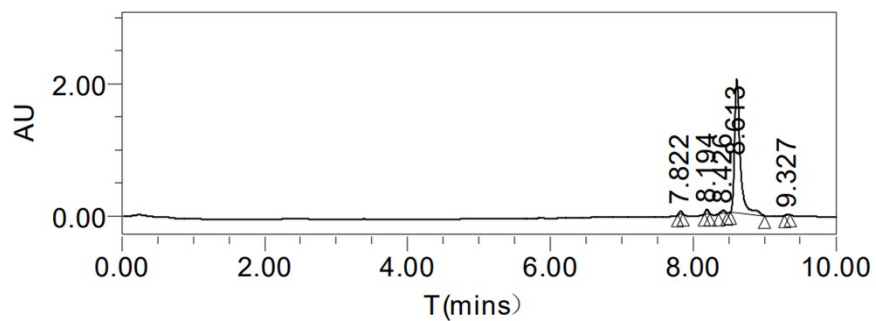
The purity data of the compound **25**



Result

	Ret.Time	Area	Rel.Area(%)
1	7.582	13792	0.48
2	7.888	90665	3.18
3	8.436	2736341	95.93
4	8.894	11533	0.40

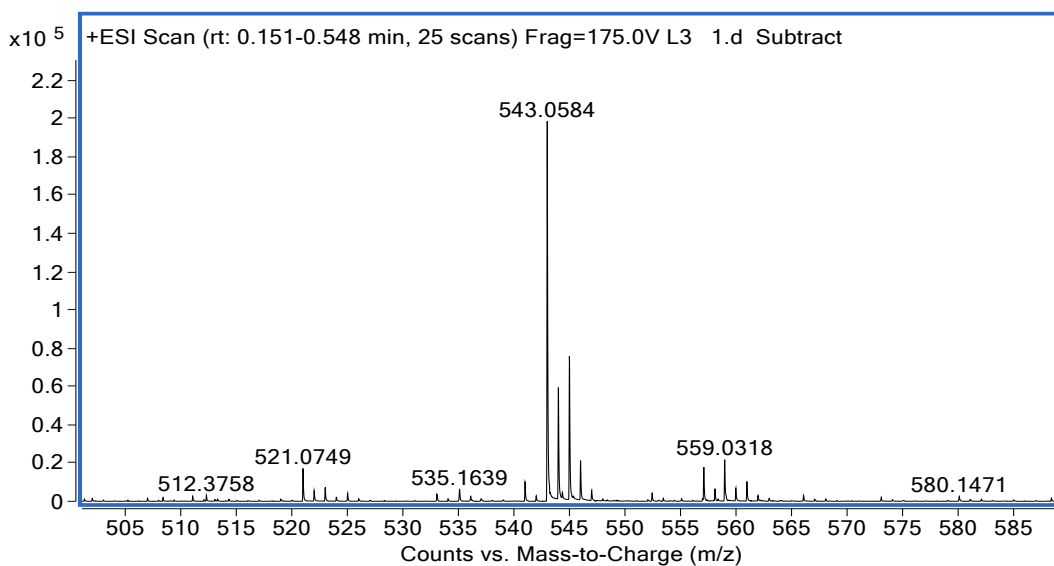
The purity data of the compound **26**



Result

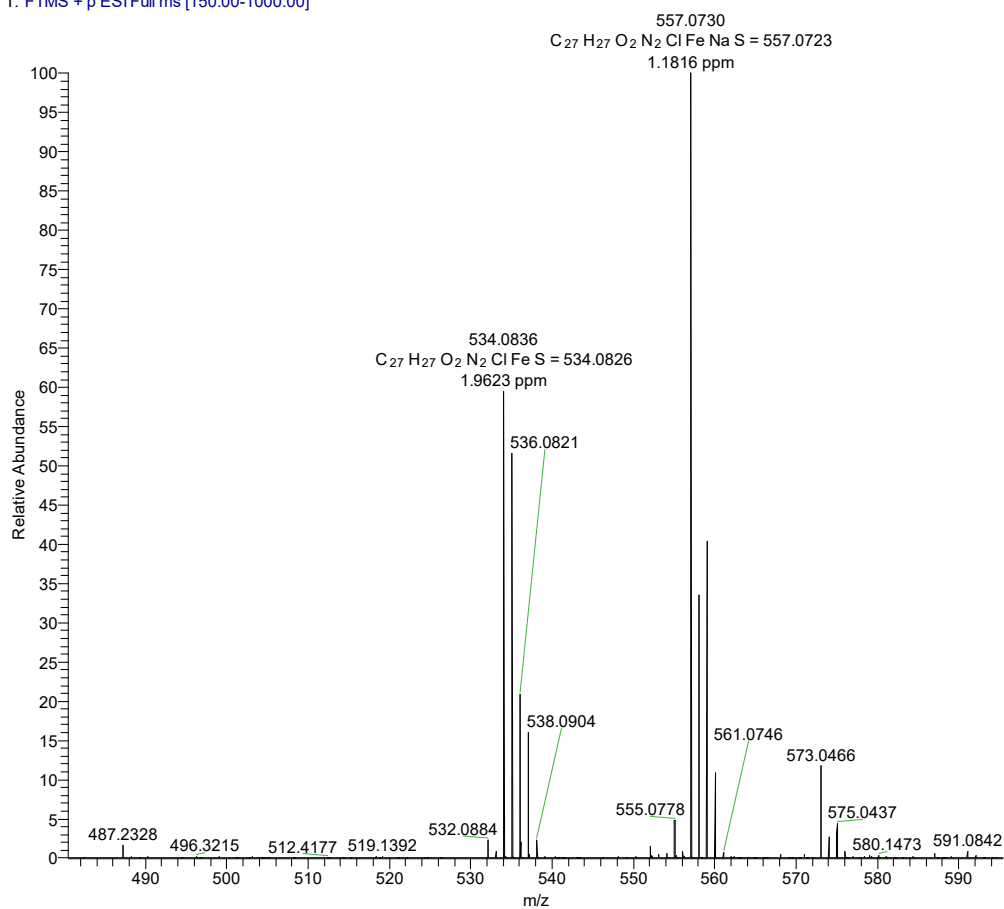
	Ret.Time	Area	Rel.Area(%)
1	7.822	112290	0.96
2	8.194	154619	1.32
3	8.426	159619	1.36
4	8.613	11283033	96.08
5	9.327	34082	0.29

The purity data of the compound **27**

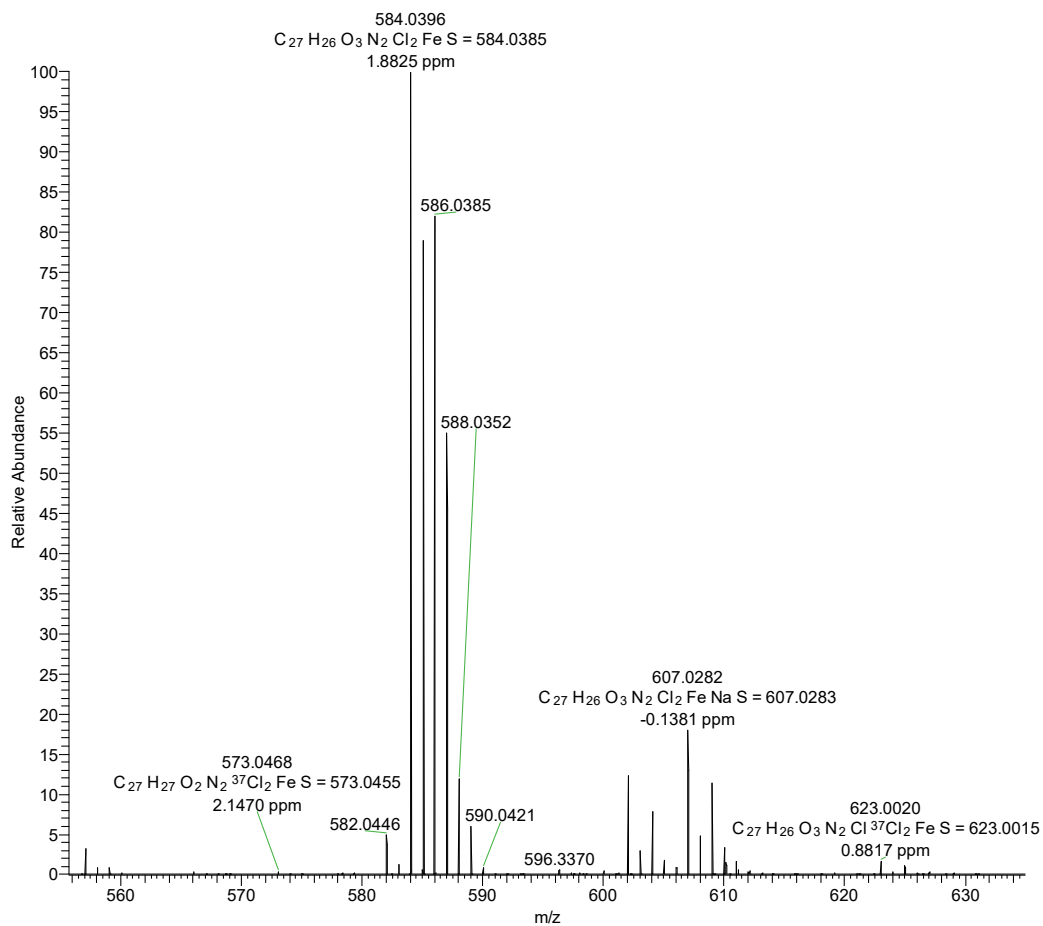


The HRMS (ESI) data of compound **10**

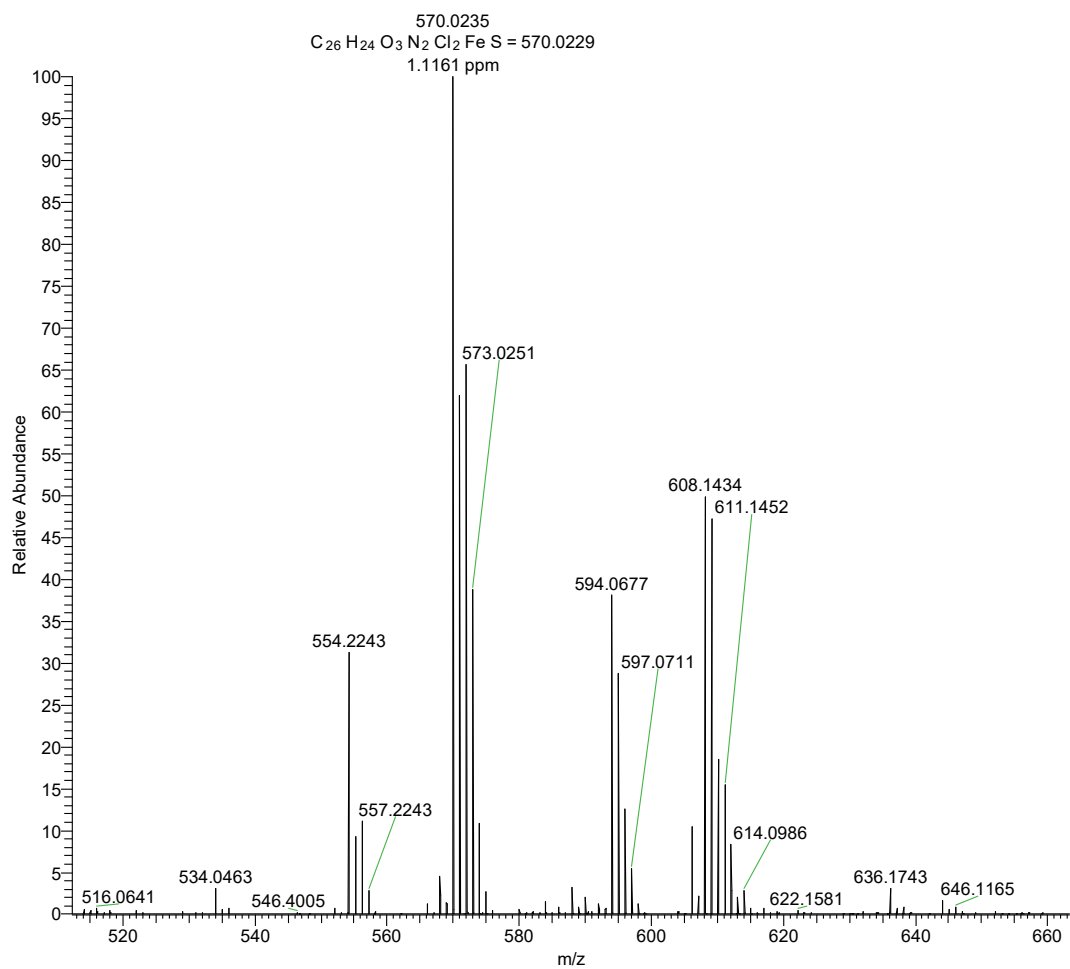
20230911-L4_230911105708 #20 RT: 0.40 AV: 1 NL: 9.79E5
T: FTMS + p ESI Full ms [150.00-1000.00]



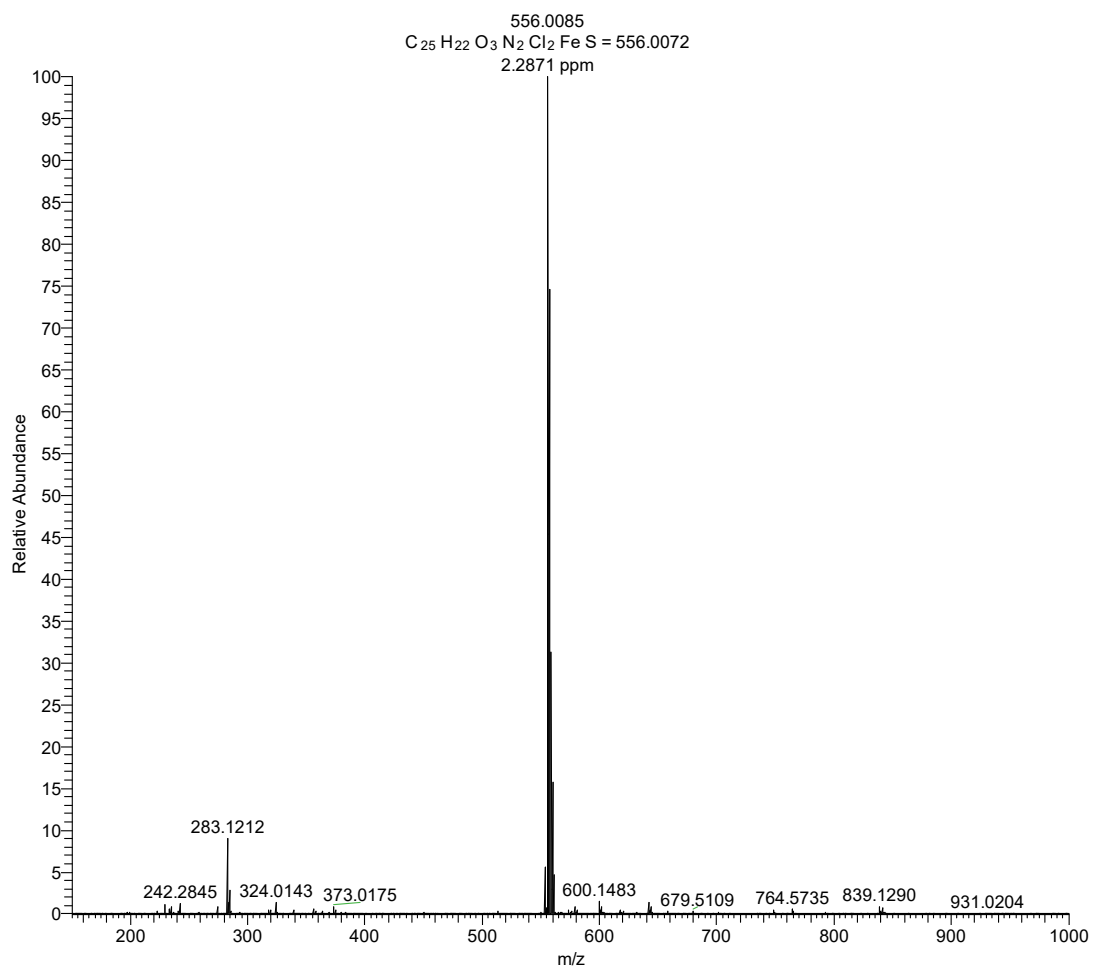
The HRMS (ESI) data of compound 11



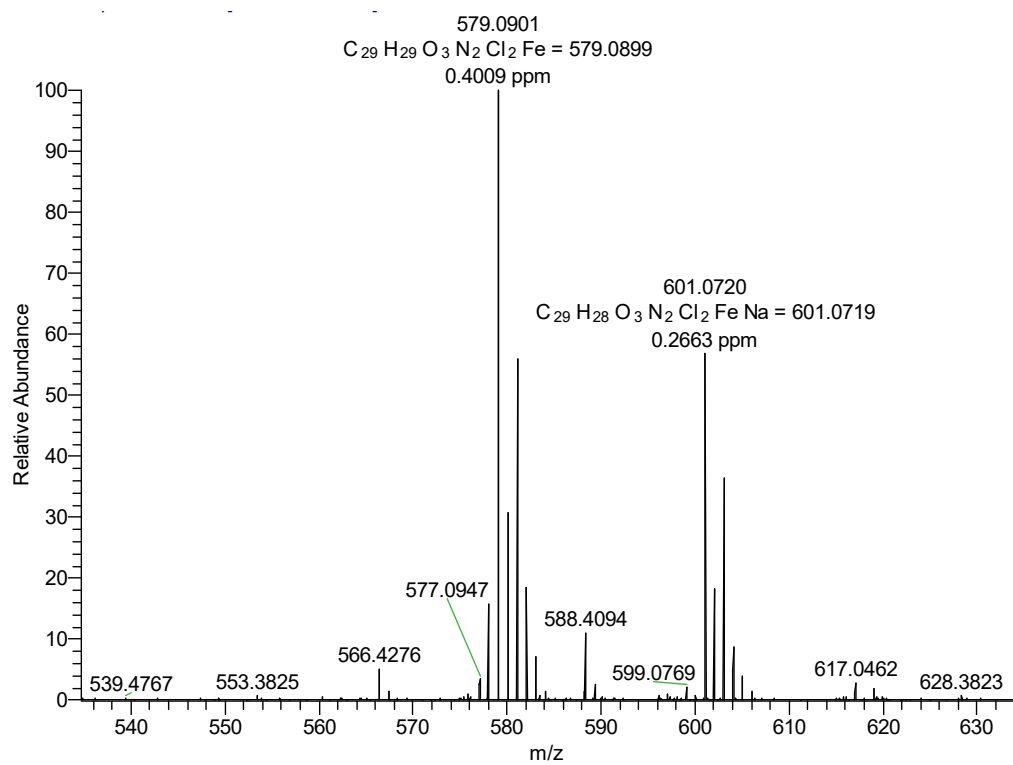
The HRMS (ESI) data of compound 12



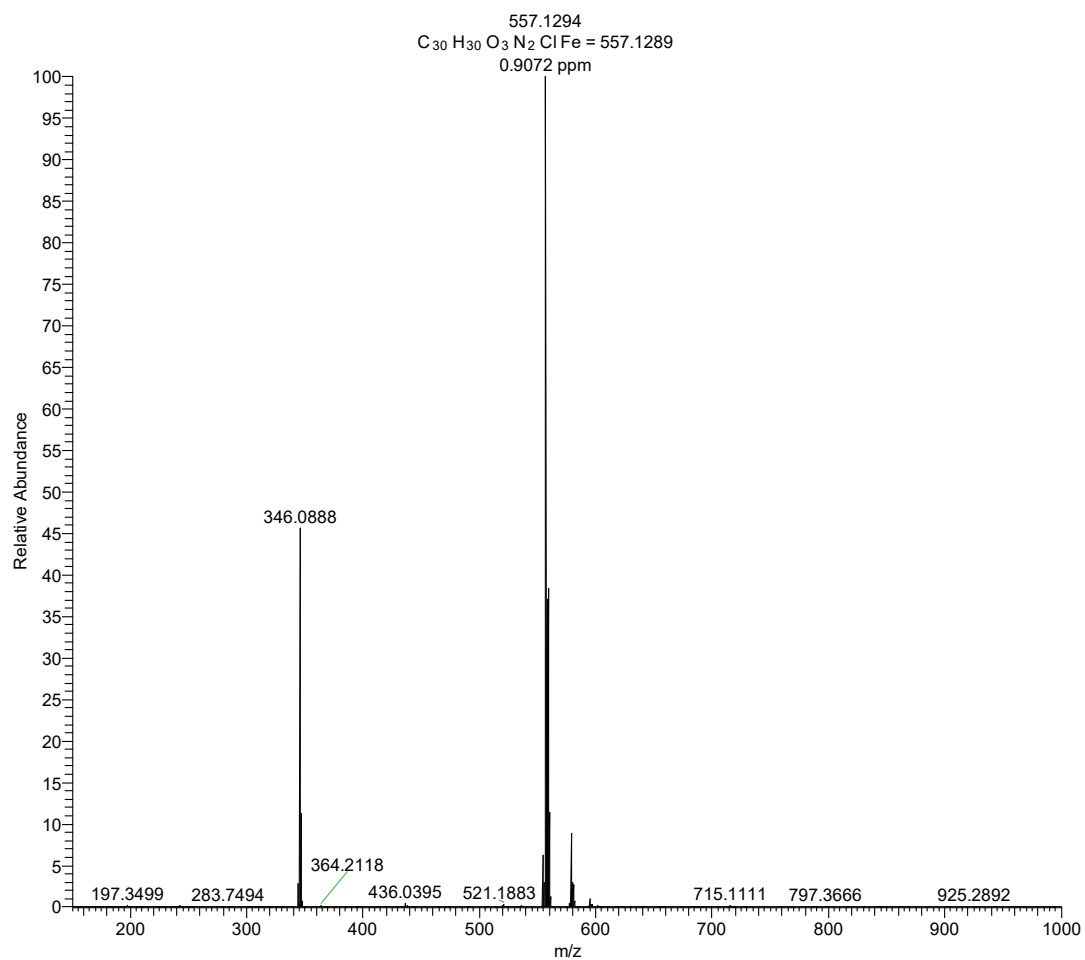
The HRMS (ESI) data of compound **13**



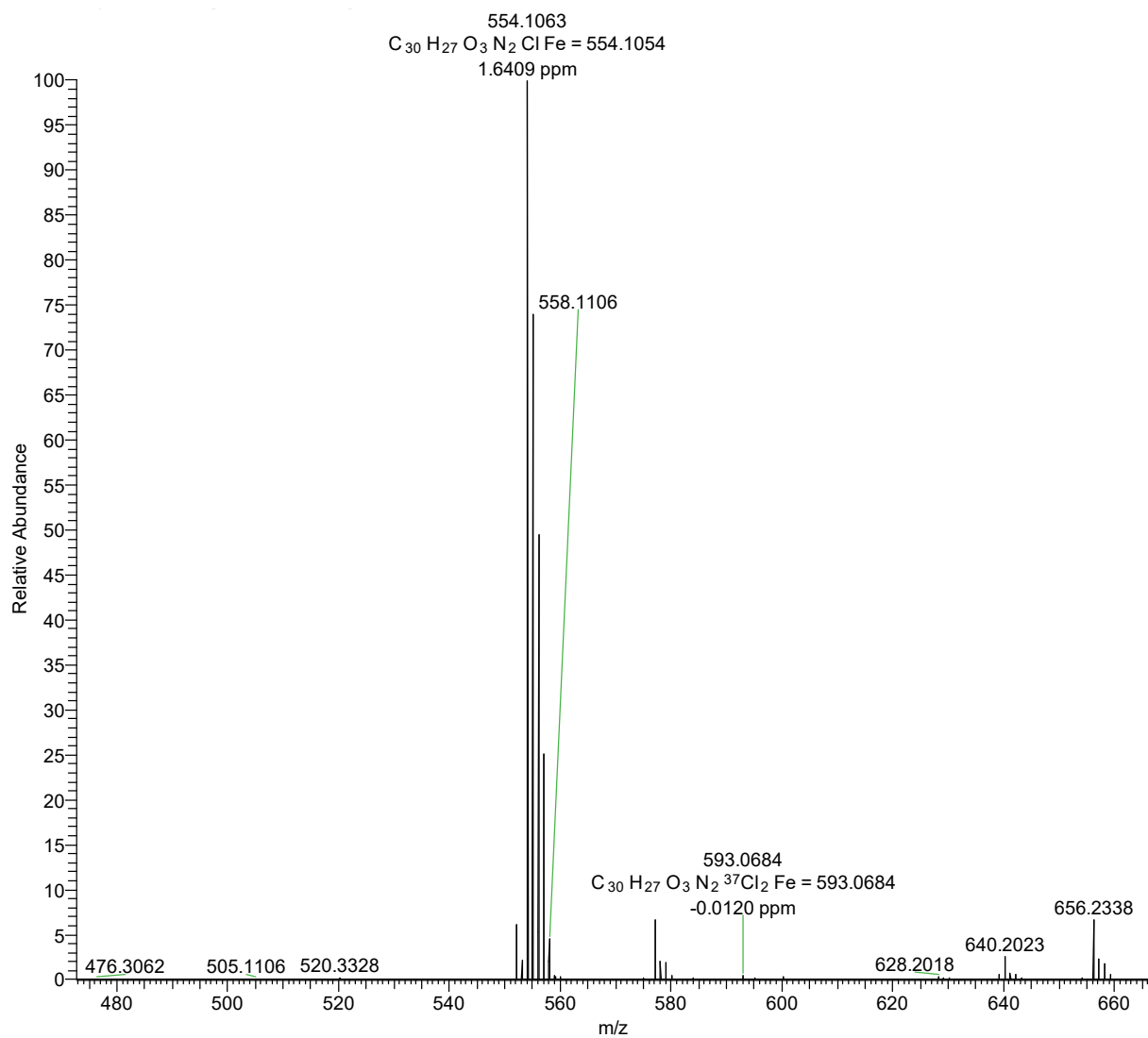
The HRMS (ESI) data of compound **14**



The HRMS (ESI) data of compound **15**

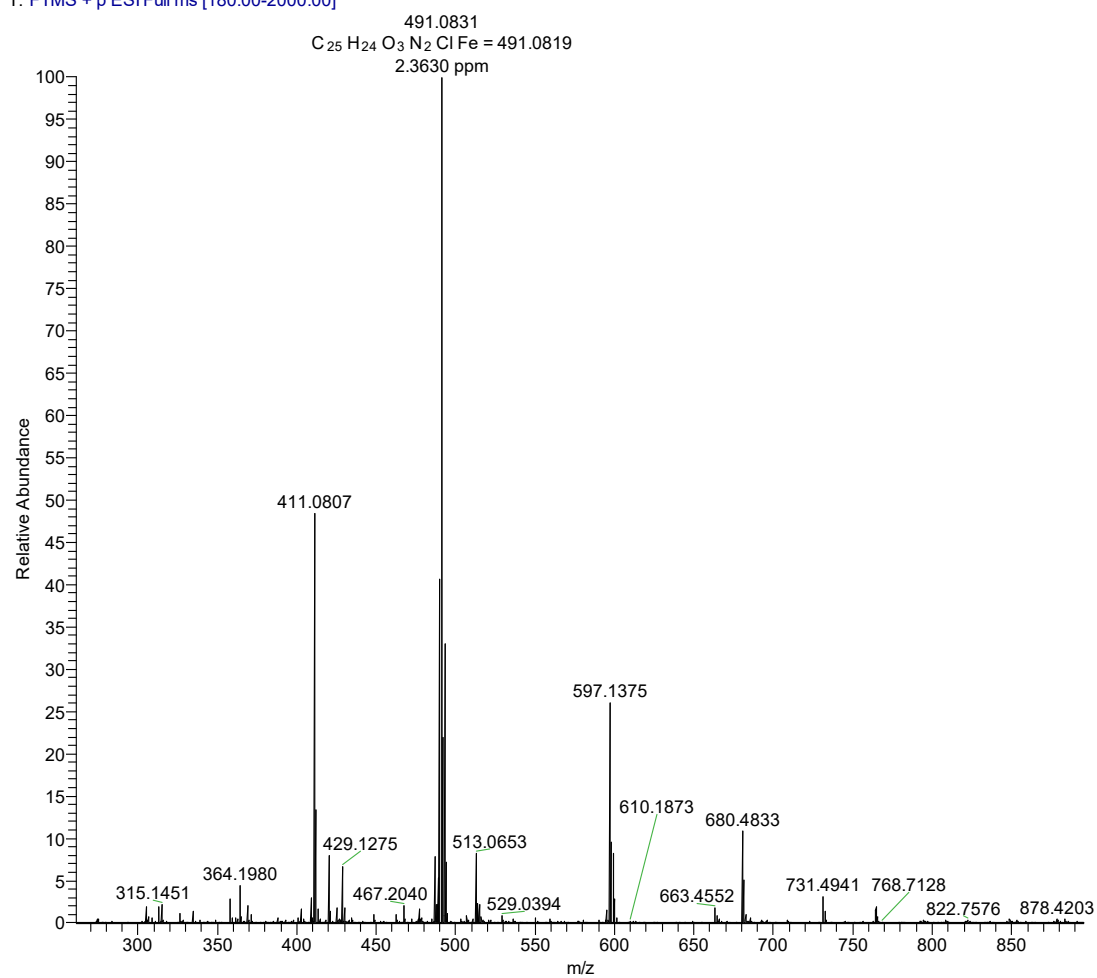


The HRMS (ESI) data of compound **16**



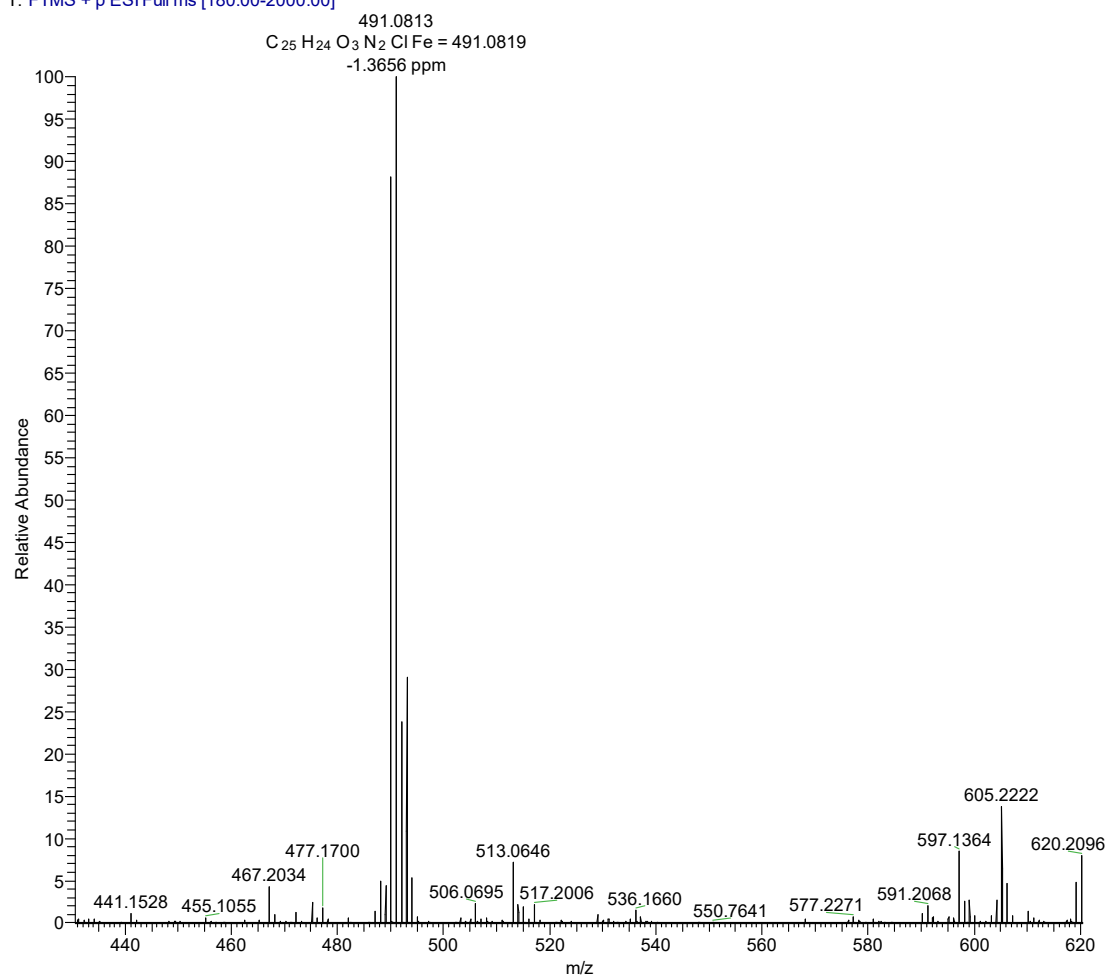
The HRMS (ESI) data of compound 17

20230620-H4-2_230619172329 #42 RT: 0.35 AV: 1 NL: 1.38E7
T: FTMS + p ESI Full ms [180.00-2000.00]



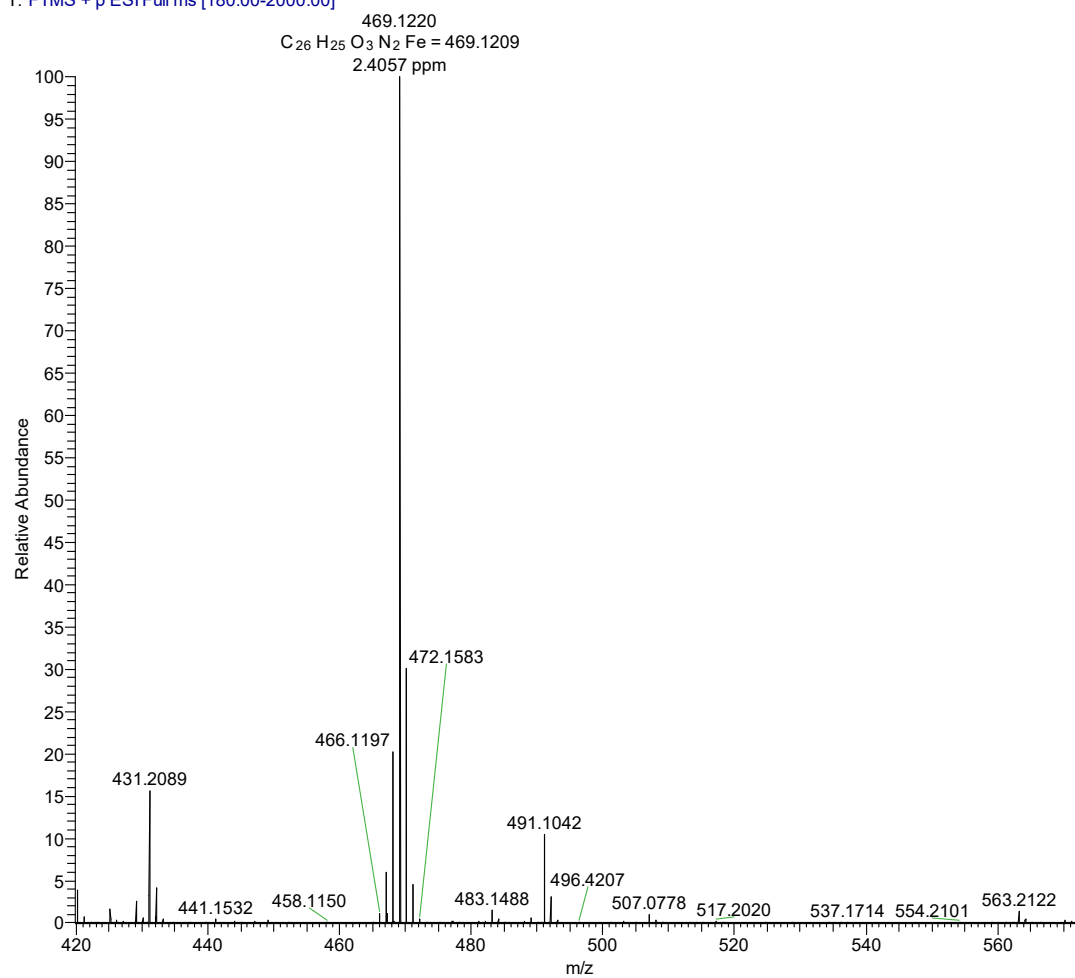
HRMS of the compound **18**

20230620-H8_230619172329 #50 RT: 0.46 AV: 1 NL: 4.13E6
T: FTMS + p ESI Full ms [180.00-2000.00]



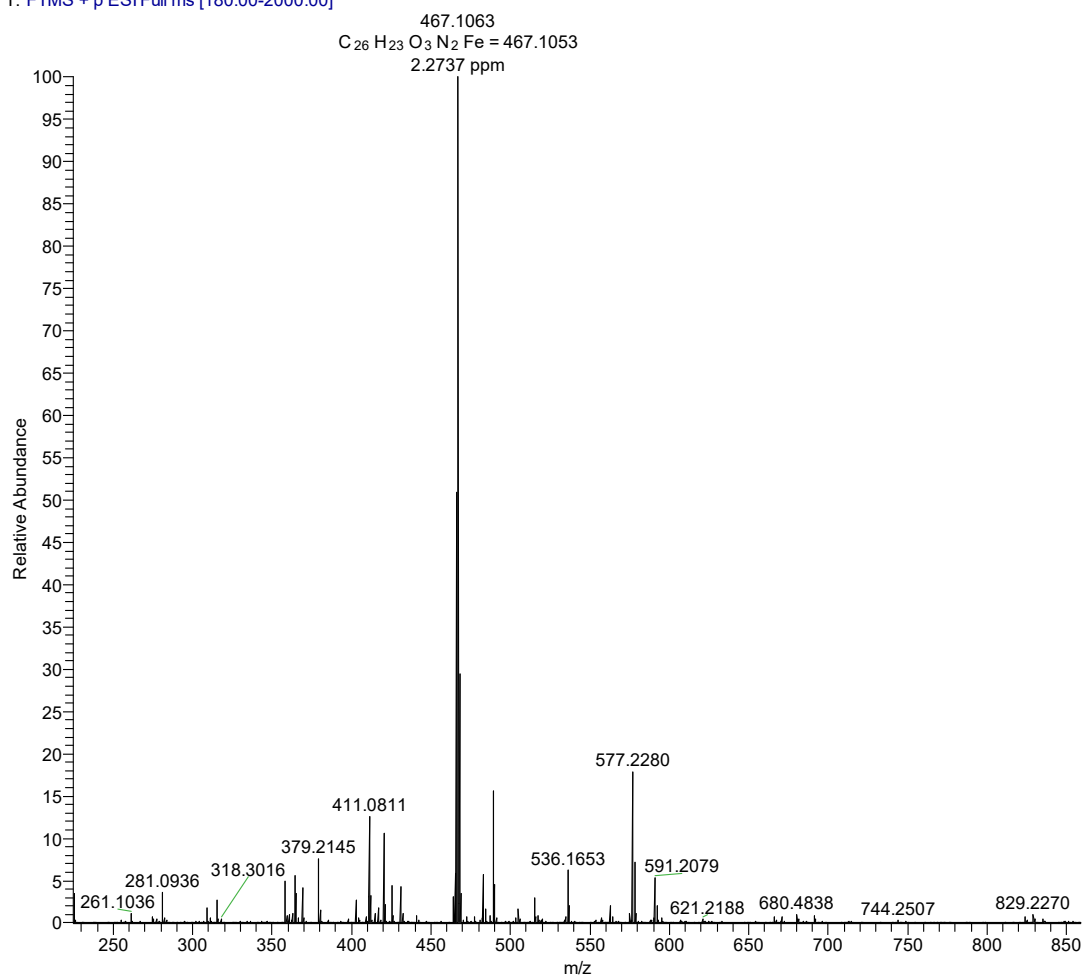
HRMS of the compound **19**

20230620-H42_230619172329 #41 RT: 0.40 AV: 1 NL: 1.17E7
T: FTMS + p ESI Full ms [180.00-2000.00]

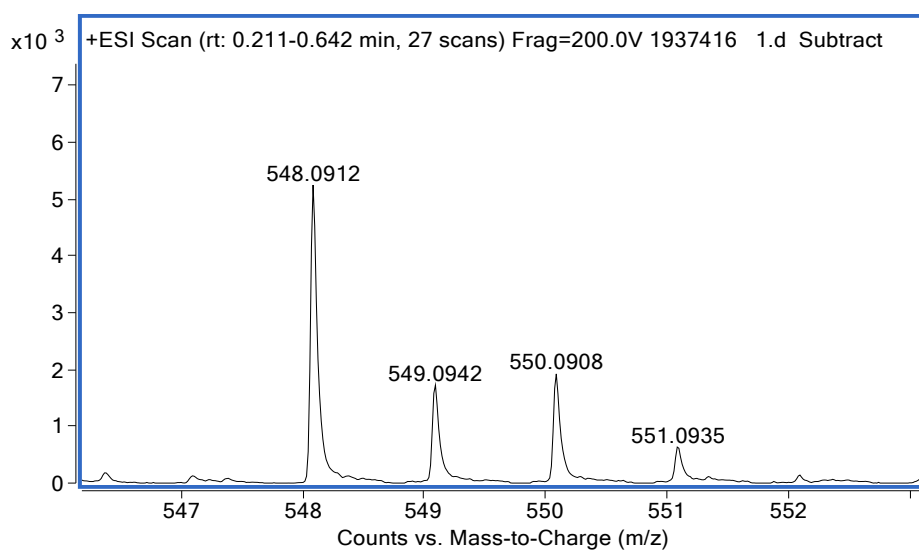


HRMS of the compound **20**

20230620-H70_230619172329 #46 RT: 0.47 AV: 1 NL: 5.10E6
T: FTMS + p ESI Full ms [180.00-2000.00]

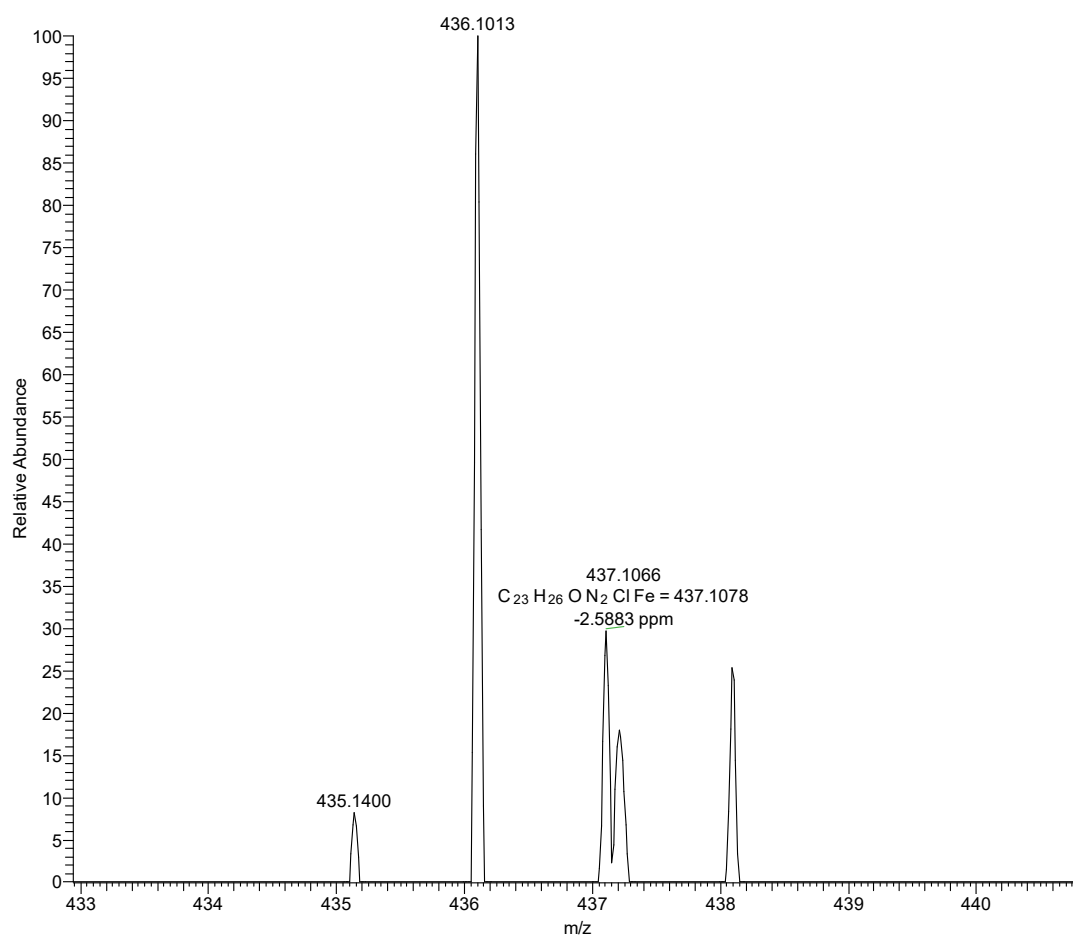


HRMS of the compound **21**



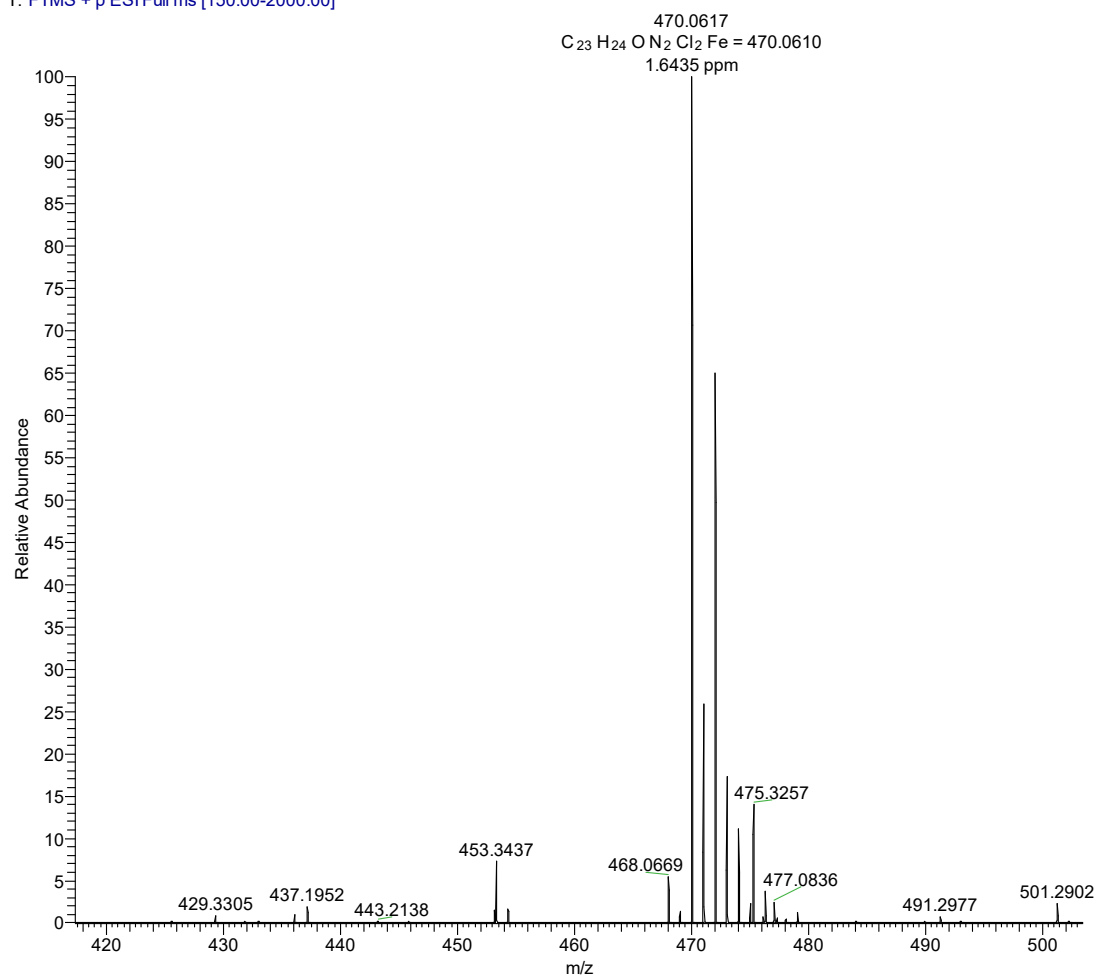
HRMS of the compound 22

20230619-J23_230619084251 #73 RT: 0.38 AV: 1 NL: 2.01E5
T: FTMS + p ESI Full ms [150.00-2000.00]



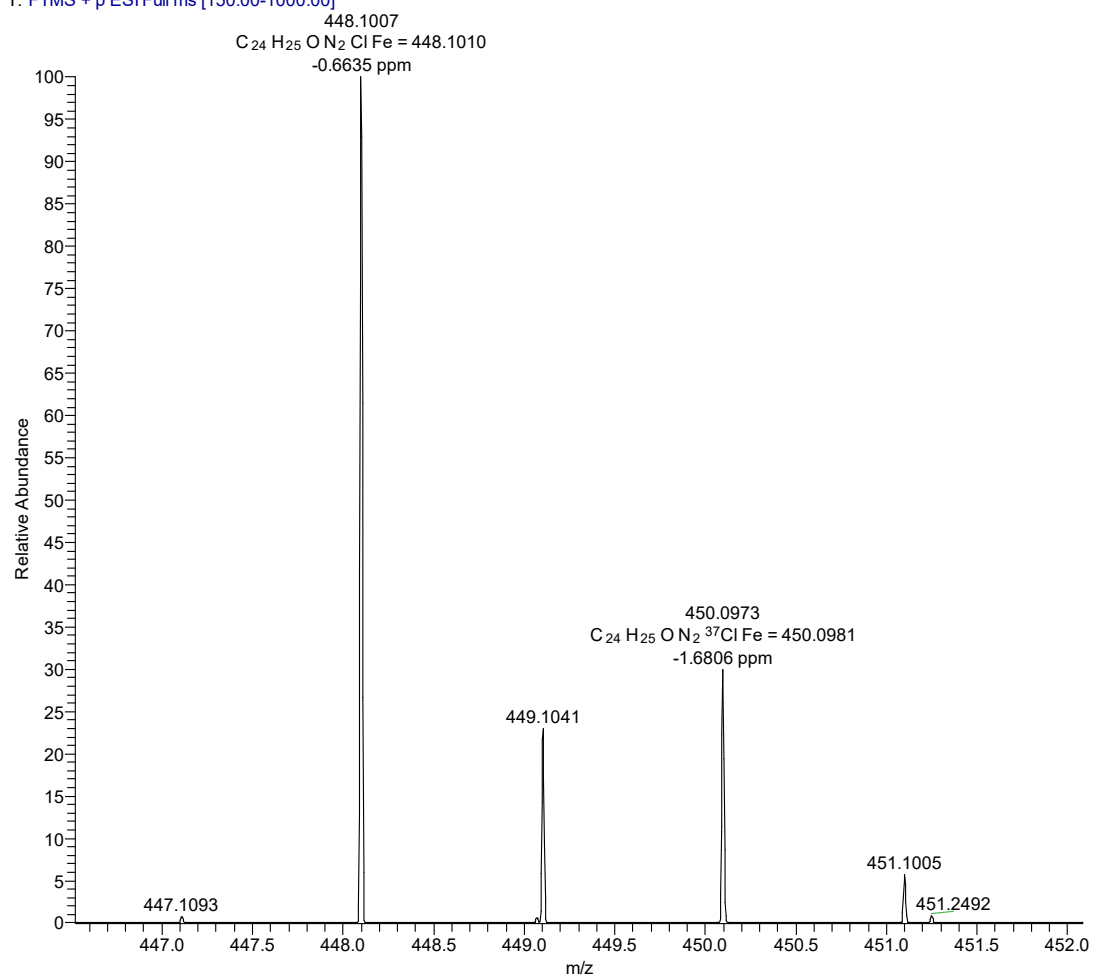
HRMS of the compound 23

20230619-J24_230619084857 #241-245 RT: 0.85-0.86 AV: 5 NL: 1.62E7
T: FTMS + p ESI Full ms [150.00-2000.00]



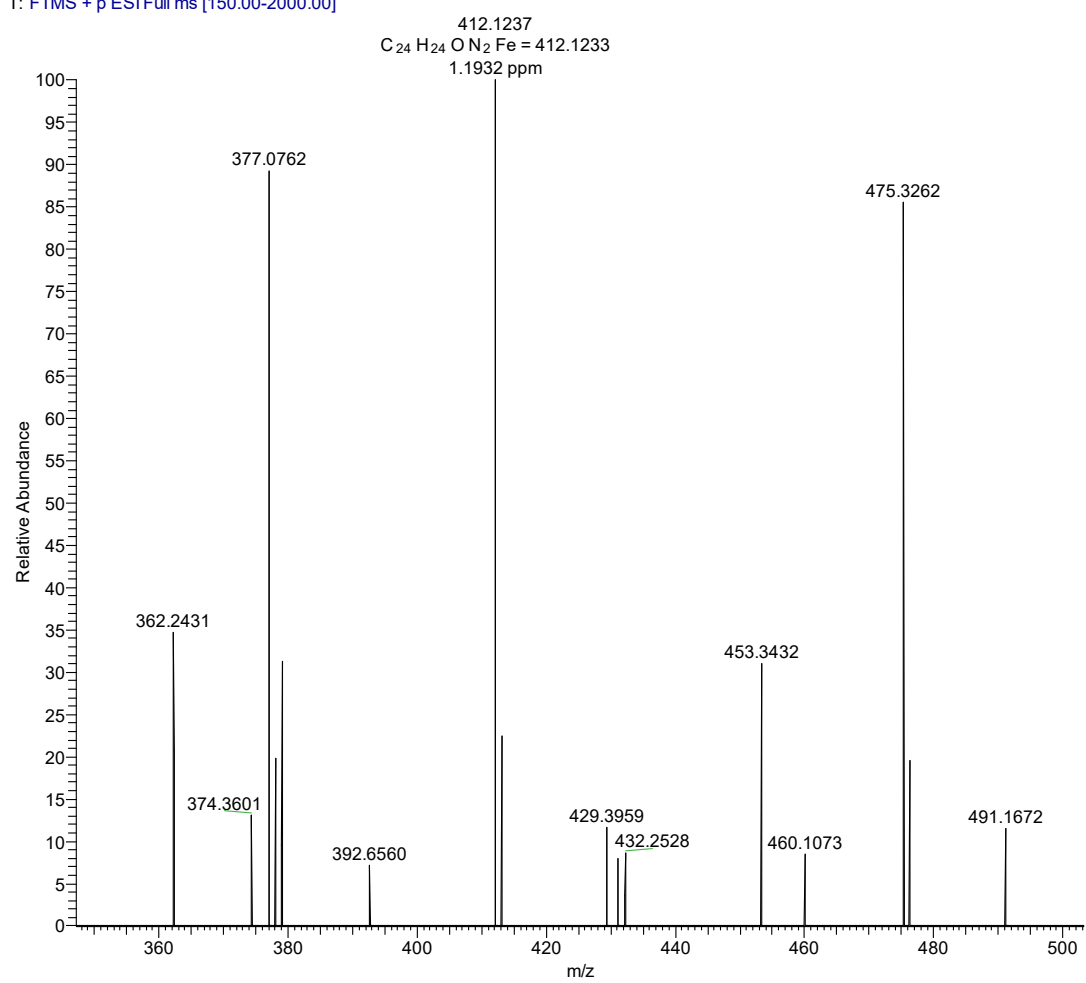
HRMS of the compound **24**

20230616-J27_230616112820 #96-97 RT: 0.75-0.76 AV: 2 NL: 6.63E6
T: FTMS + p ESI Full ms [150.00-1000.00]



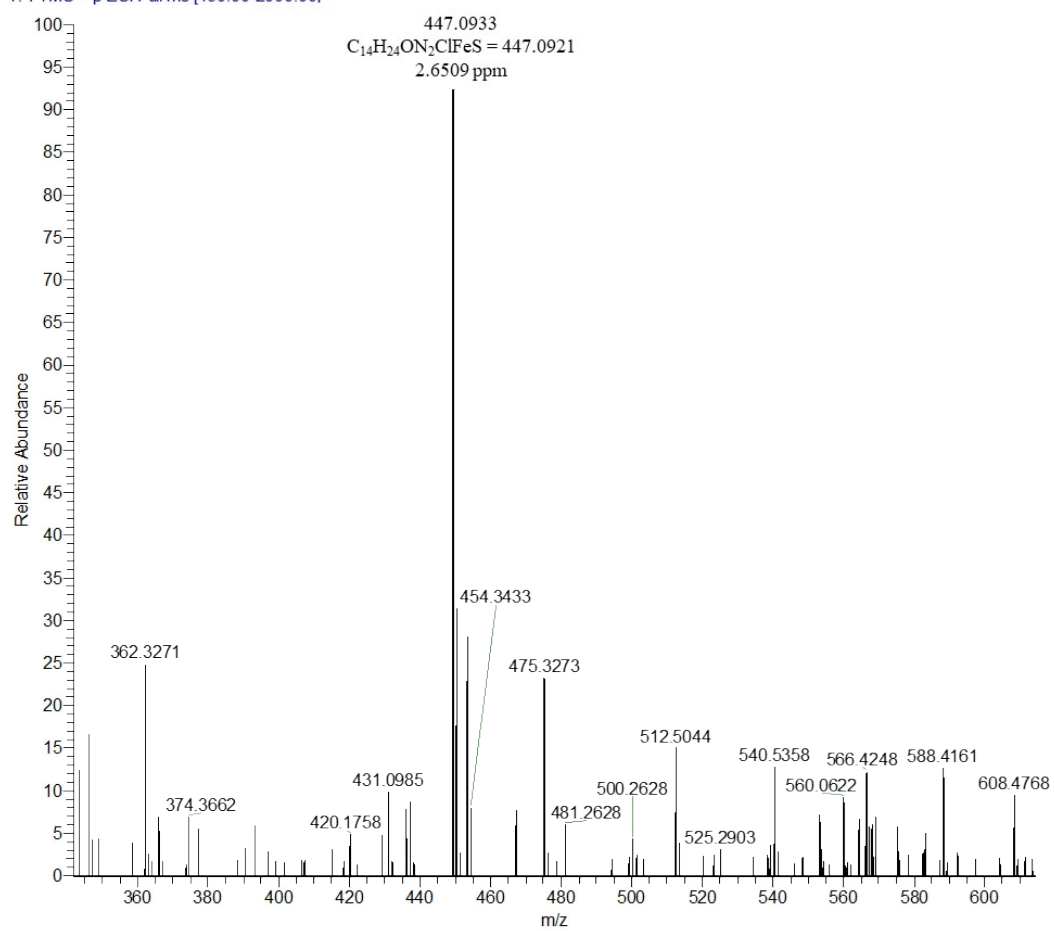
HRMS of the compound 25

20230619-J29_230619084857 #150 RT: 0.55 AV: 1 NL: 2.18E6
T: FTMS + p ESI Full ms [150.00-2000.00]



HRMS of the compound **26**

20230619-J30_230619084251 #103-104 RT: 0.47-0.48 AV: 2 NL: 4.10E6
T: FTMS + p ESI Full ms [150.00-2000.00]



HRMS of the compound 27